Long-term experimental warming increases the efficiency of the methane cycle

School of Biological and Chemical Sciences

Queen Mary University of London

Submitted in partial fulfilment of the requirements of the Degree of Doctor of Philosophy

I, Yizhu Zhu, confirm that the research included within this thesis is my own work or that where it has been carried out in collaboration with, or supported by others, that this is duly acknowledged below and my contribution indicated. Previously published material is also acknowledged below.

I attest that I have exercised reasonable care to ensure that the work is original, and does not to the best of my knowledge break any UK law, infringe any third party's copyright or other Intellectual Property Right, or contain any confidential material.

I accept that the College has the right to use plagiarism detection software to check the electronic version of the thesis.

I confirm that this thesis has not been previously submitted for the award of a degree by this or any other university.

Signature:

Date: 27th September 2019

This research project was supervised by Professor Mark Trimmer and Dr. Kevin Purdy and was supported by Queen Mary Principal's research studentship.

Abstract

Methane is a potent greenhouse gas whose net emission from ecosystems represents the balance between microbial methane production (methanogenesis) and oxidation (methanotrophy), each with different sensitivities to temperature. How this balance will be altered by global warming over the long-term, and especially in freshwaters that are major methane sources, remains unknown. Here I demonstrate, using a well-replicated (n=20), long-term (for 11 years) freshwater warming experiment (+4 °C above ambient), that experimental warming of freshwater ecosystems drives a disproportionate increase in methanogenesis over methanotrophy that increases the warming potential of the gases they emit. After 11 years of warming, an ongoing divergence in methane emission between the warmed and ambient ponds was revealed and the annual methane emissions are now 2.4-fold higher under warming, in far excess of predictions based on temperature alone. Such increase in methane emissions was augmented by shifts in the methanogen community as warming makes hydrogenotrophic methanogenesis more energetically favourable. In contrast, the methanotroph community was conserved. Methanotrophy was able to respond physiologically to higher temperatures and methane, though the overall capacity to oxidise methane was limited to < 95 % of the methane produced but not the 98 % required to prevent methane emission from increasing. This long-term warming experiment provides a mechanistic understanding of a potential positive feedback, where climate warming induces changes at microbial level that stimulate increases in whole-ecosystem methane emissions. Further, the experimentally induced changes to the methane cycle are borne out at global scale as a disproportionate increase in the capacity of naturally warmer ecosystems to emit methane. Together, the findings in this thesis strongly indicate that as Earth continues to warm, natural

ecosystems will emit disproportionately more methane to the atmosphere in a positive feedback warming loop.

Acknowledgements

I would like to express my very great appreciation to my supervisor, Prof. Mark Trimmer, for giving me the opportunity to work on this project and for your guidance during the planning and development of this research work. Thank you for all the time you have been generously given for teaching me statistics, critical thinking and scientific writing.

I would also like to thank Dr. Kevin Purdy, my co-supervisor, for useful suggestions and for patient instructions on molecular work and paper writing.

Thanks to Dr. Ozge Eyice-Broadbent for teaching the molecular work and for sharing your experience in academia.

Thanks to Dr. Liao Ouyang for introducing me the laboratory during my very first days in Queen Mary and to Dr. Lidong Shen and Dr. Sarah Harpenslager for very useful discussions on science.

Thanks to Dr. Ian Sander, Dr. Felicity Shelley and Paul Fletcher for offering technical and fieldwork assistance.

A big thank to Tian Du for your encouragement in the difficult times and for suggestions about surviving a PhD. And to my parents for your unconditional support throughout my study.

Table of Contents

Chapter 1 General Introduction

1.1 Feedback through greater methane emissions in a warmer world

1.1.1 Disproportionate emissions from freshwaters

Methane (CH_4) is the second most important greenhouse gas, with a 28 times greater warming potential than carbon dioxide (CO_2) (IPCC, 2014). The atmospheric concentration of CH_4 has increased by ~2.5 fold since the industrial revolution (Nisbet, Dlugokencky and Bousquet, 2014). A significant proportion (42%) of global CH_4 emissions to the atmosphere comes from freshwaters (wetlands, lakes and rivers) (*see* Table 1.1).

Freshwaters, in spite of their relatively small surface areas, are important CH_4 sources (*see* Table 1.1). Wetlands, being the largest source of CH_4 emissions, cover only 3.8 % of the Earth's land surface area but contribute a quarter of the global CH_4 emissions (Saunois *et al.*, 2016). Other freshwaters, including lakes, rivers, streams, occupy only 2.2 % of the Earth's land surface area. Their CH_4 emissions used to be underestimated due to limited number of measurements; recently, as more CH_4 flux measurements from tropical rivers and streams are being added to the global CH_4 budget, the total emission from lakes, rivers and streams has been updated to 122 Tg CH_4 yr^{-1} (Bastviken *et al.*, 2011; Saunois *et al.*, 2016; Stanley *et al.*, 2016), contributing to 17 % of the global CH_4 emissions.

Through global thermal infrared imagery, water bodies can warm faster than regional air temperature. And worldwide the warming is greater in the high latitudes of the northern hemisphere than in low latitudes (Schneider and Hook, 2010). Climate warming, particularly at high latitudes, may therefore lead to a substantial increase in net CH_4 emissions from freshwaters (Wik *et al.*, 2016). The need to understand how CH_4 emission from the

freshwaters will respond to global warming, especially at a long-term scale (> 10 years), is therefore acute.

Table 1.1 Surface areas and annual CH_4 emissions of freshwaters.

	Surface area (km^2)	**Surface area /Earth's land surface area (%)**	**CH_4 emission (Tg CH_4 yr^{-1})**	**CH_4 emission /global CH_4 emissions[1] (%)**
wetlands	5.7×10^6 (Aselmann and Crutzen, 1989)	3.8	185 (Saunois *et al.*, 2016)	25
lakes	3.6×10^6 (Raymond *et al.*, 2013)	2.2	122 (Saunois *et al.*, 2016)	17
rivers and streams	6.2×10^5 (Raymond *et al.*, 2013)	0.47		
total	**9.92×10^5**	**6.47**	**307**	**42**

[1]Global CH_4 emissions include the natural sources and anthropogenic sources using bottom-up (Saunois *et al.*, 2016).

1.1.2 Temperature sensitivity of methane fluxes

Biogenic CH_4 production is due to a particular type of anaerobic archaeal microorganisms called the methanogens. Their rates of CH_4 production change exponentially with temperature according to the Arrhenius equation – "*a simple exponential dependence of rate constant on the reciprocal of absolute temperature*" (Brown *et al.*, 2004; Hoehler and Alperin, 2014).

The temperature sensitivity of CH_4 fluxes (production and emission) often varies among ecosystems, for a range of activation energy from 0.51 eV to 2.8 eV (Dunfield *et al.*, 1993; Lofton, Whalen and Hershey, 2014; Shelley *et al.*, 2015). Yvon-Durocher et al. (2014) described the average temperature dependence of CH_4 emission among three ecosystem types

– aquatic, wetland and rice-paddy – by Arrhenius equation with an activation energy (E_a) for 0.96 eV, undistinguishable to the 1.10 eV for CH_4 production in pure cultures and laboratory incubations. This finding of a consistent temperature dependence of CH_4 flux from pure cultures to the whole ecosystem level, is very important. The consistency probably simplifies one climate-change problem significantly: can the feedback from CH_4 emission in response to global warming be reduced to a simple mathematical relationship with temperature only (Hoehler and Alperin, 2014)?

Since 1900, almost the entire globe has experienced surface warming. The global average temperature is projected to increase by ~4 °C at the end of the 21st century (IPCC, 2014). This warming potential has a large effect on ecosystems because of the temperature dependence of biological metabolism. Activation energy is a measure of temperature sensitivity; for example, 0.96 eV, an activation energy (E_a) estimated by Yvon-Durocher and his colleagues, corresponds to a 1.70-fold increase in ecosystem-level CH_4 emission under the 4 °C warming scenario (*see Chapter 2* for details). Therefore, warming accelerates CH_4 emissions, which can, in turn, warm the Earth – in a so-called positive climate feedback loop.

But is the climate-change problem for predicting the CH_4 emission feedback to warming as straightforward as this?

1.1.3 Methane emissions are not a simple response to temperature alone

From a meta-analysis comprising 127 studies across the globe, Yvon-Durocher (2014) described the CH_4 emission as a function of temperature, with an apparent activation energy for 0.96 eV, similar to the 1.10 eV for the CH_4 production in pure methanogen culture. Despite this consistency, however, average CH_4 emissions across different wetlands, paddy soils or aquatic ecosystems, for example, are only poorly predicted by differences in their average

temperature alone (Figure 1.1). This inability to predict ecosystem-level CH_4 emissions solely by site-specific temperature, implies that changes in CH_4 emissions in response to climate warming are more complex than a simple exponential response to temperature. If we are to predict any feedback from CH_4 emission to climate warming, we need an overall understanding of any temperature-related response in CH_4 production, CH_4 oxidation and their affiliated microbial communities (Dean *et al.*, 2018).

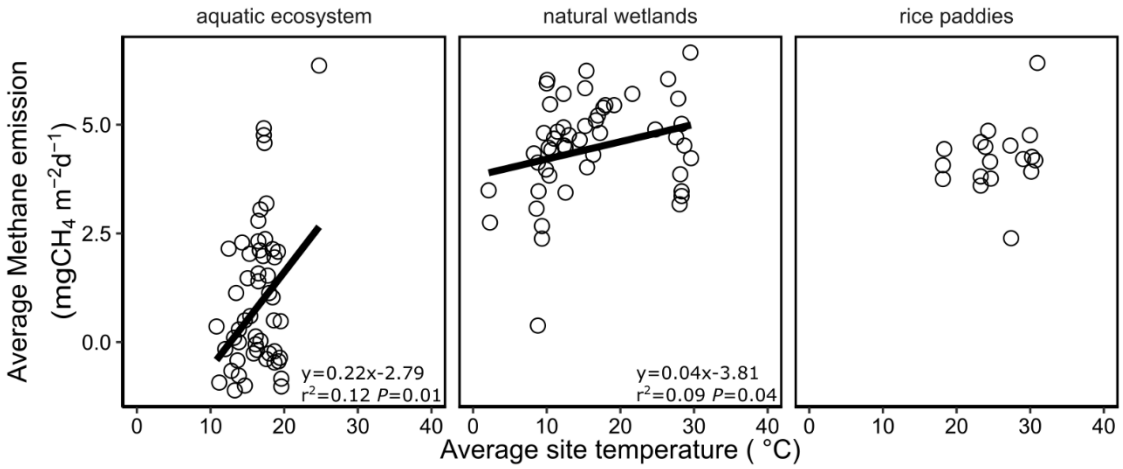

Figure 1.1 Correlations of average site temperatures with average CH_4 emissions (data from Yvon-Durocher (2014)). Average site temperature is positively correlated with average CH_4 emission for aquatic ecosystems and natural wetlands, but temperature explain 12% and 9% of variance only.

1.2 Net CH_4 emission: the balance between production (methanogenesis) and oxidation (methanotrophy)

Methane is produced in deeper anoxic sediments by strictly anaerobic archaeal methanogens where oxygen is limited by diffusion and quickly depleted by aerobic respiration (Reim *et al.*, 2012). The CH_4 produced diffuses through the sediment column to the upper more oxidized zone where aerobic bacterial methanotrophs oxidize CH_4 to CO_2. Methanogenesis and methanotrophy therefore drive the biological CH_4 cycle, with the balance

between the two regulating the net CH_4 emissions (Bridgham *et al.*, 2013) (Figure 1.2). To fully understand the response of the CH_4 emissions to global warming, knowledge about both the production and oxidation is essential.

1.2.1 Methanogenesis and its response to warming

Methanogenesis is highly sensitive to temperature. Its activation energy is well-characterized at 0.96 eV, higher than photosynthesis (0.65 eV) and respiration (0.3 eV) (Gillooly *et al.*, 2001; Yvon-Durocher *et al.*, 2014). This high activation energy predicts a substantial increase of methanogenesis by 4-fold based on an increase from 5 °C to 15 °C as well as a greater proportion of deposited organic carbon released as CH_4 (Gudasz *et al.*, 2010; IPCC, 2014; Marotta *et al.*, 2014).

In freshwaters, a methanogenic response to warming is further complicated by there being two dominant methanogenic pathways – acetoclastic producing 50 % CH_4 and 50% CO_2 ($CH_3COOH \rightarrow CH_4+CO_2$) and hydrogenotrophic producing CH_4 only ($4H_2+CO_2 \rightarrow CH_4+2H_2O$) (Liu and Whitman, 2008; Thauer *et al.*, 2008). As CH_4 is a more potent greenhouse gas than CO_2, the pathway of CH_4 production is important. In lake sediments and paddy soils, acetoclastic methanogenesis dominates at lower temperatures and the relative contribution of hydrogenotrophic methanogenesis to the total CH_4 production has been shown to increase with temperature (Fey and Conrad, 2000; Glissmann *et al.*, 2004). A shift in the dominant methanogenic pathways with temperature can have important implications for CH_4 production under current warming scenarios.

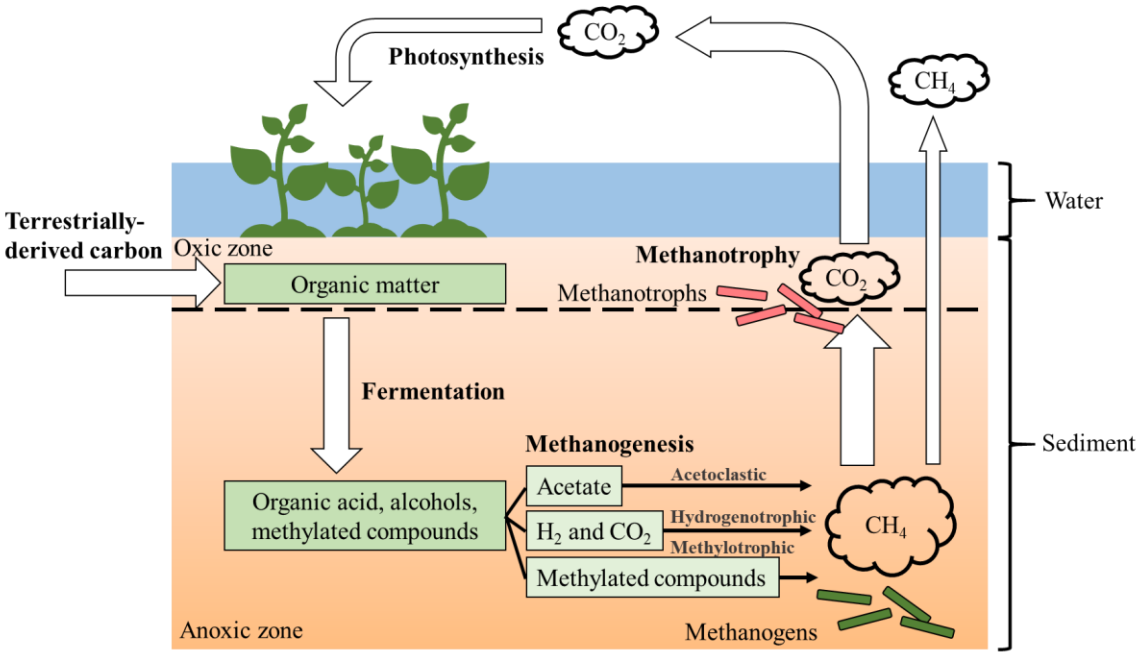

Figure 1.2 Methane production and oxidation in freshwaters. Methane is produced in deeper anoxic sediments by methanogens that convert substrates from organic carbon fermentation. Methane diffuses through the sediment towards the upper more oxic zone. The majority (~90% to 95%) of the produced CH_4 is oxidized to CO_2 by aerobic methanotrophs before escaping into the atmosphere. The net CH_4 emission is therefore the balance between methanogenesis and methanotrophy.

1.2.2 Methanotrophy responses to temperature and greater methane availability

Methanotrophy (microbial CH_4 oxidation) is the sole biological sink for CH_4 which in total, oxidizes some 30 Tg CH_4 per year (Saunois *et al.*, 2016). Aerobic methanotrophy can consume the majority (~90 to 95 %) of CH_4 produced in freshwaters, allowing only a small fraction of CH_4 to escape into atmosphere (Frenzel, Thebrath and Conrad, 1990). Methanotrophy is therefore important in regulating the net CH_4 emission because CH_4 escapes into atmosphere when it is not oxidized by methanotrophs (Hanson and Hanson, 1996).

Temperature is known to increase CH_4 oxidation, suggesting that this sole biological CH_4 sink will continue to consume CH_4 as the climate warms (Mohanty, Bodelier and Conrad, 2007; Kip *et al.*, 2010); however, the temperature dependence of CH_4 oxidation is often

suppressed by substrate availability (Duc, Crill and Bastviken, 2010; Lofton, Whalen and Hershey, 2014; Shelley *et al.*, 2015). At low CH_4 concentrations, CH_4 oxidation showed no response to temperature. Even at higher CH_4 concentrations, the activation energy of CH_4 oxidation is ~ 0.45 to 0.55 eV, predicting an increase of methanotrophy by ~1.3-fold based on an increase from 5 °C to 15 °C lower than the predicted 4-fold increase of CH_4 production for an activation energy of 0.96 eV (Whalen, Reeburgh and Sandbeck, 1990; King and Adamsen, 1992; Knoblauch *et al.*, 2008; Yvon-Durocher *et al.*, 2014).

Despite the fact that methanotrophy is less temperature sensitive than methanogenesis, methanotrophy responds rapidly to increasing CH_4 production as there is a strong kinetic response too (Bender and Conrad, 1992). Shelly et al. (2015) measured the CH_4 oxidation capacity in contrasting riverbed sediments and calculated that the CH_4 oxidation capacity in the largely anoxic fine sediments under the macrophytes stands was 2000 times greater than in coarse-gravel sediments using the kinetic response to different pore water CH_4 concentrations. This kinetics of methanotrophy may enable it to potentially counteract warming-induced increase in CH_4 production (Duc, Crill and Bastviken, 2010; Shelley *et al.*, 2015).

1.2.3 Coupled processes between methane production and oxidation

Methane emissions result from the coupled process as methanogens provide "food" for methanotrophs by transforming simple organic carbon substrates into gaseous CH_4. Despite the fact that methanogens are spatially separated from methanotrophs (Figure 1.2), it is difficult to detect the relationship between CH_4 emissions and either of the microbial processes solely, as neither the *mcrA* gene or the *pmoA* gene abundances are significantly related to CH_4 fluxes in a meta-analysis (Rocca *et al.*, 2015).

Furthermore, the effect of warming has been limited to changes in temperature only in most of the experiments conducted so far (Mohanty, Bodelier and Conrad, 2007; Knoblauch *et al.*, 2008; Ho and Frenzel, 2012). But, in fact, warming not only increases temperature in freshwaters, but also stimulates CH_4 production (Gudasz *et al.*, 2010; Marotta *et al.*, 2014), which alleviates the substrate limitation faced by methanotrophs and potentially shifts methanotroph community compositions. For example, by incubating sediments under a range of temperatures, experiments demonstrated that increasing temperature increased the relative abundance of type II methanotrophs (Knoblauch *et al.*, 2008; Ho and Frenzel, 2012). Unlike continuous increase in CH_4 concentrations due to warming, these experiments provided the sediments with a one-shot injection of CH_4 at the same initial concentrations only. The design of the previous experiment therefore misses the simultaneous higher temperature and higher CH_4 concentrations, i.e., the exact conditions induced by warming, and underscores an important problem for CH_4 cycling studies: How do methanogens and methanotrophs interact with each other under current warming scenarios?

1.2.4 Long-term effects: can methanotrophy counterbalance methanogenesis in a warmer world?

Biogeochemical processes, for example, photosynthesis and respiration, require decades or even centuries to equilibrate after perturbations like climate warming (Thornley and Cannell, 2000; Luo *et al.*, 2001). Transient responses observed in the short-term experiments may not reflect the long-term, equilibrium response (Melillo, 2002; Morgan, 2002). For example, in terrestrial ecosystems, warming stimulated organic carbon degradation and CO_2 emissions in short term. But this stimulation declines over time and diminishes the warming effect on soil because of thermal acclimation or soil nutrient limitation (Melillo, 2002; Bradford, 2013). Therefore, the response of biogeochemical cycles to global warming

over a long-term scale is more complex than a simple exponential effect of temperature alone (Yvon-Durocher *et al.*, 2017).

Warming has been shown to enhance methanogenesis and methanotrophy promptly in freshwaters (Fey and Conrad, 2000; Gudasz *et al.*, 2010; Marotta *et al.*, 2014; Shelley *et al.*, 2015) but current studies have been restricted to relatively short-term experiments of less than one year. How these two processes evolve over time under warming, whether their responses would be balanced and how it might affect net CH_4 emissions are unclear (Singh *et al.*, 2010) (Figure 1.3). The unclear effect of warming on CH_4 cycling over a longer term (for example, >10 years) severely limits our ability to predict any feedback from CH_4 emissions to climate warming.

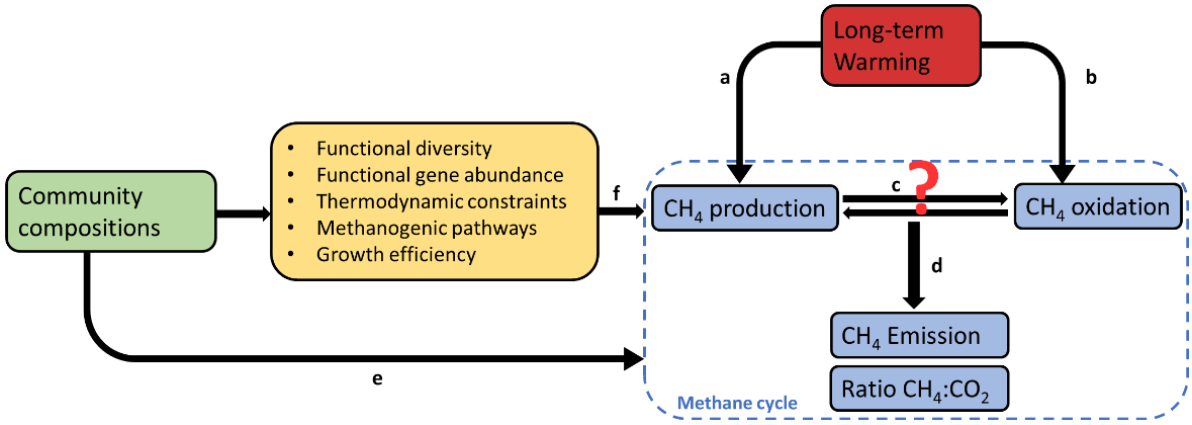

Figure 1.3 Warming enhances CH_4 production (**a**) and CH_4 oxidation (**b**) which together regulate the net CH_4 emissions (**d**) and ratio CH_4 to CO_2 emission. Whether methanogenesis and methanotrophy balance under warming is nevertheless unclear (**c**). Linking the methane-related community compositions to the ecosystem-level methanogenesis and methanotrophy is difficult (**e**). Therefore, elucidating the measurable microbial community characteristics and subsequently, linking these characteristics to ecosystem-level processes is essential (**f**).

1.3 Linking microbial communities to ecosystem-level processes

Microorganisms drive biogeochemical cycles and play an important role determining atmospheric CH_4 concentrations (Singh *et al.*, 2010). The communities of archaeal

methanogens and bacterial methanotrophs are therefore fundamental in determining CH_4 emissions. The taxonomic compositions of methanogens and methanotrophs of microbial community vary between environments (Louca, Parfrey and Doebeli, 2016), and changes in environmental conditions can potentially alter their communities leading to altered CH_4 emissions (Chin, Lukow and Conrad, 1999; Fey and Conrad, 2000; Ho, Lüke and Frenzel, 2011; Ho and Frenzel, 2012). Therefore, understanding the mechanisms under which methanogen and methanotroph communities control the ecosystem-level CH_4 emission – whether the methanogen and methanotroph community would alter under warming and how the community structure relates to net CH_4 emission, is essential (Konopka, 2009; Singh *et al.*, 2010).

1.3.1 Limitation in microbial community ecology

Microbial community ecology studies the mechanisms in the interactions between microbial community and their environments; however, the application of ecological theory in microbial community is currently limited as existing ecological theories usually have only been shown to apply to higher organisation levels (Prosser *et al.*, 2007).

One of the central issues in ecology is the relationship between diversity and ecosystem functioning. Diversity is often measured as richness (the number of unique species) and evenness (the equitability among species) (Cardinale *et al.*, 2012). For higher organisms, such as plants, insects and animals, diversity governs ecosystem function (Cardinale *et al.*, 2012), but this diversity-function relationship may be more complex for microbes given their immense richness, high abundances and physiological diversities (Prosser *et al.*, 2007; Peter *et al.*, 2011). For example, bacteria have higher multifunctional redundancy than plants and a change in diversity is unlikely to have a substantial effect on ecosystem functions (Bell *et al.*, 2005; Gamfeldt, Hillebrand and Jonsson, 2008).

Diversity is ultimately shaped by constituent taxa, that is microbial membership (Hall *et al.*, 2018). Linking microbial membership to ecosystem processes may be more important in understanding, modelling and predicting changes in the ecosystem processes that microbes perform (Griffiths *et al.*, 2004; Girvan *et al.*, 2005; Peter *et al.*, 2011). The community membership is particularly important for methanogenesis and methanotrophy. Unlike broadly distributed functions such as respiration, these two metabolisms are narrowly distributed among archaea and bacterial taxa and are therefore more likely to be constrained by microbial community membership and less resistant to changes in taxonomic compositions (Louca *et al.*, 2018). In this case, describing how methanogenic and methanotrophic microbial memberships alter under warming should lead to a better understanding and prediction of CH_4 emissions in a warmer world.

1.3.2 Archaeal methanogens and bacterial methanotrophs

Sequencing phylogenetically conserved protein sequences, for example, the *mcrA* (encoding methyl coenzyme-M reductase alpha unit) for methanogens and the *pmoA* (encoding particulate methane monooxygenase) for methanotrophs, can identify the community members, however, the difficulty in linking microbial community membership to ecosystem-level processes directly is well recognized (Bier *et al.*, 2015; Hall *et al.*, 2018). Therefore, elucidating the intermediary – the measurable community characteristics (for example, functional diversity (Høj, Olsen and Torsvik, 2008; Ho, Lüke and Frenzel, 2011), functional gene abundance (Rocca *et al.*, 2015), growth efficiency (Trimmer *et al.*, 2015), thermodynamic constraints (Fey and Conrad, 2000), *etc.*) - and subsequently, linking to microbial process that contribute to the ecosystem-level process of interest is essential (Hall *et al.*, 2018) (Figure 1.3).

1.3.3 Temporal scales in linking microbial community to ecosystem-level processes

Unlike animals and plants, microorganisms have the potential to grow rapidly; yet, in nature, this potential is often constrained by environmental factors like substrate availability (Gómez and Buckling, 2013). Growth rates can vary over several orders of magnitudes depending on environmental conditions. Therefore, temporal scales need to be taken into account while linking microbial community to ecosystem-level processes (Prosser *et al.*, 2007).

Favourable conditions, such as warming and increases in substrate availability, can serve as selective pressures and leads to shifts in microbial community compositions. Nevertheless, physiological responses precede changes in community compositions (Bier *et al.*, 2015). Microorganisms can withstand changes in environmental conditions by temporarily changing their physiological states or metabolism while the community compositions remain unchanged. An example is that warming enhances methanogenesis and methanotrophy immediately before changes in composition could happen (Gudasz *et al.*, 2010; Shelley *et al.*, 2015). Allison *et al*., (2008) and Bier *et al*., (2015) reviewed recent experiments and assessed whether the length of time affected the detection of any changes in community compositions. They found that the studies in which microbial community changed were significantly longer than those that did not detect any changes, implying a lag in the response of microbial community to disturbance (Allison and Martiny, 2008; Bier *et al.*, 2015). Therefore, short-term measurements may not be able to capture the link between physiological processes and community compositions.

Furthermore, microbial community structure may continue to change over time (Shade *et al.*, 2013). Linkage between microbial community and ecological process that is significant in the short-term can be irrelevant or even opposite at a longer time-span (Frey *et al.*, 2008).

Community analysis after short-term disturbance provide a "snapshot" of the community characteristics; however, if we are to predict the effect of long-term warming on methane-related microbial communities, the knowledge about their changes over time is needed (Faust and Raes, 2012).

Recently, community analysis has been included in the experiments of temperature effect on methanogenesis and methanotrophy in rice field soils (Chin, Lukow and Conrad, 1999; Conrad, Klose and Noll, 2009), lake sediments (Nozhevnikova *et al.*, 2007) and arctic soils (Knoblauch *et al.*, 2008; Tveit *et al.*, 2015), *etc*. All these experiments have been restricted with relatively short-term incubations (< 1 year). Although these measurements have detected shifts in community compositions, how the microbial communities would continue to change over the longer scale under current warming scenarios remains unknown.

1.3.4 A long-term warming mesocosm experiment

Feedback of CH_4 emission in freshwaters to global warming can be difficult to predict due to the large spatial scale of freshwaters. Mesocosm experiments are a useful tool for predicting ecosystem-level processes under global warming scenarios because mesocosms provide replication on model systems where the statistical approaches can be tested (Benton *et al.*, 2007; Yvon-Durocher, 2010). To understand how the CH_4 cycle responds to the predicted climate warming of + 4 °C by the end of this century in the long-term (> 10 years) and how the methane-related microbial communities will alter over time, a replicated artificial-pond experiment, which simulated the potential effect of moderate warming on freshwater ecosystems, was used in this study. The experiment consists of 20 freshwater mesocosms (artificial ponds) of which 10 replicates have been heated by 4 °C above the ambient temperature since September, 2006, while the other 10 remained at ambient

temperature (Yvon-Durocher, Montoya, Trimmer, *et al.*, 2011). The experimental set-up is described in detail in *Chapter 2*.

1.4 Goals and structural outline of the thesis

This thesis aims at understanding the key unanswered questions under current climate warming scenarios: 1, does the balance between methanogenesis and methanotrophy alter over long-term warming and 2, how do changes in the methane-related microbial communities influence net CH_4 emissions?

To target this knowledge gap, the research is divided into four main sections, outlined below:

Chapter 2. Long-term warming continuously amplifies methane emissions

Warming is expected to increase CH_4 emissions but to what extent can long-term warming enhances CH_4 emissions is unclear. This chapter concerns the high-frequency (three times a day) measurements of CH_4 emissions in a year-long monitoring programme to characterize CH_4 emission patterns and yield better annual carbon fluxes values from our long-term warming of the experimental mesocosm ponds described above (section 1.3.4). A meta-analysis for global CH_4 and CO_2 emissions was performed to test if mesocosm predictions applied to natural ecosystems.

Chapter 3. Long-term warming enhances methanogenesis and alters the methanogen community composition

Amplified CH_4 emissions after 11 years of warming are expected to be driven by increased CH_4 production capacity in the sediments. Using slurry microcosm incubations, I estimated the CH_4 production capacity and the cell-specific methanogen activity in the experimental ponds. Further experiments with a range of methanogenic substrates were

performed to investigate whether increased CH_4 production was associated with specific methanogenic pathways. The methanogen community composition was analysed using molecular techniques, targeting the critical functional gene for CH_4 production (*mcrA*).

Chapter 4. Methanotrophy responds physiologically to warming with a conserved methanotroph community

Methanotrophy is the sole biological CH_4 sink and is expected to increase with both temperature and greater CH_4 availability. Using slurry microcosm incubations, the temperature dependence and kinetics of CH_4 oxidation in experimental ponds was calculated. As the activity of methanotrophs is confined to a thin oxic zone at the sediment surface (Reim *et al.*, 2012), oxygen penetration profiles were measured and used as proxy for the methanotroph-active depth. Furthermore, the methanotroph community composition was investigated using the key functional gene for CH_4 oxidation (*pmoA*). To further investigate how warming may affect the growth of methanotrophs, the fraction of CH_4 oxidized assimilated into biomass (carbon conversion efficiency (CCE)) was calculated.

Chapter 5. Summary: Warming increases the efficiency of the methane cycle

In this chapter, the effect of long-term warming on the net CH_4 emissions and ratio CH_4 to CO_2 production (*Chapter 2*) were rationalized by summarizing the functional and structural changes in both methanogenic (*Chapter 3*) and methanotrophic (*Chapter 4*) components of the CH_4 cycle. Furthermore, the annual CH_4 budget was calculated using the CH_4 emissions, the measured increase in CH_4 production capacity and CH_4 oxidation capacity in the slurry microcosms. We are currently preparing this chapter for publication.

Chapter 2 Long-term warming continuously amplifies methane emissions

2.1 Abstract

Methane (CH_4) and carbon dioxide (CO_2) are the most abundant carbon greenhouse gases in the atmosphere (Hartmann *et al.*, 2013; Ciais *et al.*, 2014). Freshwaters, despite of their comparatively small surface areas, emit disproportionately large amounts of CH_4 and CO_2 (Bastviken *et al.*, 2004; Tranvik *et al.*, 2009; Wik *et al.*, 2016). Methane is not only more potent than CO_2 as greenhouse gas but its emission is also more sensitive to temperature than CO_2 flux related processes (e.g., respiration and primary production) (Gillooly *et al.*, 2001; Yvon-Durocher, Montoya, Woodward, *et al.*, 2011; Yvon-Durocher *et al.*, 2014, 2017), understanding how CH_4 and CO_2 emissions from freshwaters will respond to current warming scenarios is therefore essential for predicting carbon greenhouse gas feedbacks. The need is particularly acute at the long-term time-scale as the effect of warming may be continuously amplified over the long term (Yvon-Durocher *et al.*, 2017). Here, I investigated the effect of long-term warming of +4 °C above ambient since 2006 on whole-ecosystem CH_4 and CO_2 emissions using high-frequency (three times per day) chambers. After 11 years of warming, CH_4 and CO_2 emissions have responded to warming in two distinct ways - the CH_4 emission capacity, here represented by emission standardized to 15°C, has enhanced in the warmed ponds relative to their ambient controls while, nevertheless, the CO_2 emission capacity stayed the same. The distinct responses between CH_4 and CO_2 to warming was further vindicated by a meta-analysis of global CH_4 and CO_2 emission as the CH_4 emission at each site standardized to 15 °C was positively correlated to average annual temperature but the CO_2 emission was consistent. In line with the increased capacity of CH_4 emission under warming, the average

annual CH_4 emission was 2.4-fold greater from the warmed ponds relative to their ambient controls, exceeding the 1.6-fold increase predicted by temperature alone. Furthermore, the CH_4:CO_2 emission ratio has increased, due to the distinct responses between CH_4 and CO_2 to warming, by 1.6-fold, increasing the total carbon greenhouse gas emission (expressed as CO_{2eq}) by 3 % to 15 %. These findings clearly show that, as the Earth continues to warm, freshwaters will emit increasingly more CH_4 to the atmosphere in a positive feedback warming loop.

2.2 Introduction

In a recent meta-analysis, the average temperature dependence of CH_4 emissions has been shown to be consistent across a range of levels of organization, with a well-characterized temperature dependence (expressed as apparent activation energy) of 0.96 eV (Yvon-Durocher *et al.*, 2014). The apparent activation energy predicts a 1.7-fold increase in the ecosystem-level CH_4 emissions under the 4 °C warming scenario (the most severe climate projection by IPCC, *see* equation (2.13)). Methane emissions from freshwaters are therefore sensitive to temperature and very likely to increase with future global warming (Holgerson and Raymond, 2016; Wik *et al.*, 2016; Davidson *et al.*, 2018).

Warming has been shown to increase CH_4 emission in mesocosm ponds (Wik *et al.*, 2014). However, the response of CH_4 emission to warming may be complicated as the elevated emissions of CH_4 observed after short-term experimental warming can be amplified by the continuous warming later (Yvon-Durocher *et al.*, 2017). Yvon-Durocher *et al*. (2017) demonstrated, using long-term warmed freshwater mesocosm ponds, that warming increased the CH_4 emission by 1.4-fold after 1 year warming but amplified to 2.2-fold after 7 years of warming. Therefore, an important unanswered question for understanding how CH_4 emission

will respond to global warming is: will warming continuously enhance CH_4 emission over the long term (> 10 years)?

Methane and CO_2 are major carbon greenhouse gases. A freshwater ecosystem may represent a source of CH_4 but a sink for CO_2, in terms of annual net uptake (Whiting and Chanton, 2001). The balance between CH_4 emission and CO_2 exchange determines the function of a freshwater, i.e., whether the freshwater acts as a source or sink for carbon greenhouse gases (Whiting and Chanton, 2001; Frolking, Roulet and Fuglestvedt, 2006). The balance between CH_4 emission and CO_2 exchange would very probably alter as the Earth continues to warm because the CH_4 emissions appear to be more sensitive to temperatures than CO_2 flux related processes (e.g., respiration and primary production) (Gillooly *et al.*, 2001; Yvon-Durocher, Montoya, Woodward, *et al.*, 2011; Yvon-Durocher *et al.*, 2017). Given that CH_4 has a greater global warming potential than CO_2 (IPCC, 2014; Balcombe *et al.*, 2018), the positive radiative forcing of emitted CH_4 under warming may offset the negative radiative forcing of CO_2 uptake and ultimately alter the function of freshwaters from sink to source for carbon greenhouse gases (Battin *et al.*, 2009). Yet very few studies have performed direct comparison of the balance of CH_4 and CO_2 exchange and the response of the balance to warming remains unknown (Whiting and Chanton, 2001; Friborg *et al.*, 2003; Pohlman *et al.*, 2017).

In this Chapter, I measured the ecosystem level quantification of simultaneous CO_2 and CH_4 fluxes using high-resolution dynamic chambers, which would reveal subtle changes in gas dynamics missed by monthly sampling, to determine the effect of long-term warming on CH_4 and CO_2 emission as well as on carbon greenhouse gas balance. Furthermore, I completed a meta-analysis of global CH_4 and CO_2 emissions to investigate whether the

mesocosm ponds predict the CH_4 and CO_2 emissions from natural ecosystems across a wide temperature gradient.

2.3 Materials and Methods

2.3.1 Mesocosm pond facility

The 20 artificial pond mesocosms were installed in 2005 at the Freshwater Biological Association's River Laboratory in East Stoke, Dorset, UK (2°10'W, 50°30'N) (Figure 2.1 a). The ponds hold ~1 m^3 of water of 50 cm in depth and were designed to mimic shallow lakes (Yvon-Durocher, Montoya, Woodward, *et al.*, 2011). Half of the ponds have been warmed by 3 to 5 °C (average 4 °C, Figure 2.1 b) above the ambient temperature since 2006 by way of an electrical heating element connected to a thermocouple which monitors a pair of warmed and ambient ponds to maintain a consistent temperature differential between them (Figure 2.1 c).

2.3.2 Sediment characteristics

Sediment samples were collected monthly from April, 2016, to August, 2016, by hand using a small corer (Ø 34 mm, polycarbonate). Oven-dried sediments were acidified to remove inorganic carbon (1 M HCl) (Hedges and Stern, 1984) and their carbon and nitrogen content measured with an elemental analyser as per (Hedges and Stern, 1984) (Sercon Integra2 Stable Isotope Analyser).

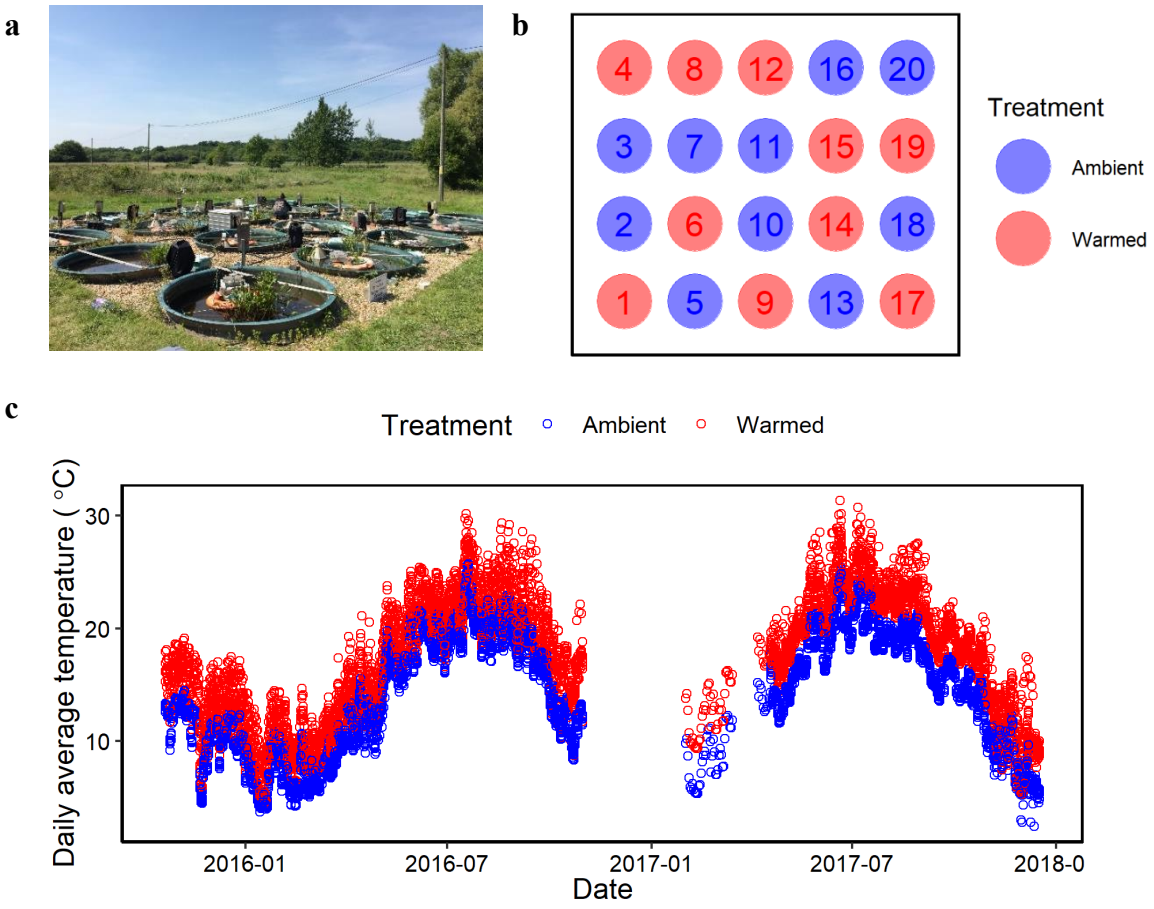

Figure 2.1. a, Mesocosm ponds with floating chambers in place. **b**, Schematic illustration demonstrating warming mesocosm experiment consisting 20 ponds: 10 warmed by 4ºC above the 10 ambient ponds. **c**, Daily average temperature of experimental warmed (red) and ambient (blue) ponds. The mesocosm ponds were designed to simulate the potential effects of predicted climate warming on aquatic ecosystems. The warmed ponds were heated at 3 to 5 °C (averaged at 4 °C) above the ambient controls, in line with the A1B warming scenarios predicted for an increase in temperature by the end of 21st century.

2.3.3 Dissolved methane concentrations

Dissolved CH_4 in the overlying water was quantified by taking water samples (n=3 for each pond) using Tygon tubing attached to a 50 mL gas-tight syringe. Water was gently discharged into a 12 mL gas-tight vials (Labco Exetainer®) until filled. Zinc Chloride ($ZnCl_2$, 3.7M, 200 µL) was injected to inhibit any microbial activity and the vials sealed. Upon return to the laboratory, a 2 mL headspace was generated by replacing the water with nitrogen (N_2,

BOC). The vials were then shaken vigorously to equilibrate. The CH_4 concentrations in the headspace were quantified using a gas chromatograph (*see Chapter 3* for details). The amount of CH_4 in the original pond water was calculated using Bunsen coefficients (Wiesenburg and Guinasso, 1979).

2.3.4 Methane and carbon dioxide fluxes measurements via high-frequency chambers

Fluxes of CH_4 and CO_2 were measured at high frequency over the annual cycle of 2017 using an Ultra-Portable Greenhouse Gas Analyzer (915-0011, LGR, Los Gatos Research) and a customised, Multi-port Inlet Unit (MIU, LGR), as a steady-state, multiplexed automatic open chamber system. Each chamber (Ø 20 cm, 0.43 L, 8100-101, Licor) was mounted on a floating ring, fixed at the centre of each pond. A Campbell data logger was used to operate the chambers in sequence and the chambers were open between each sampling phase (Figure 2.2 a).

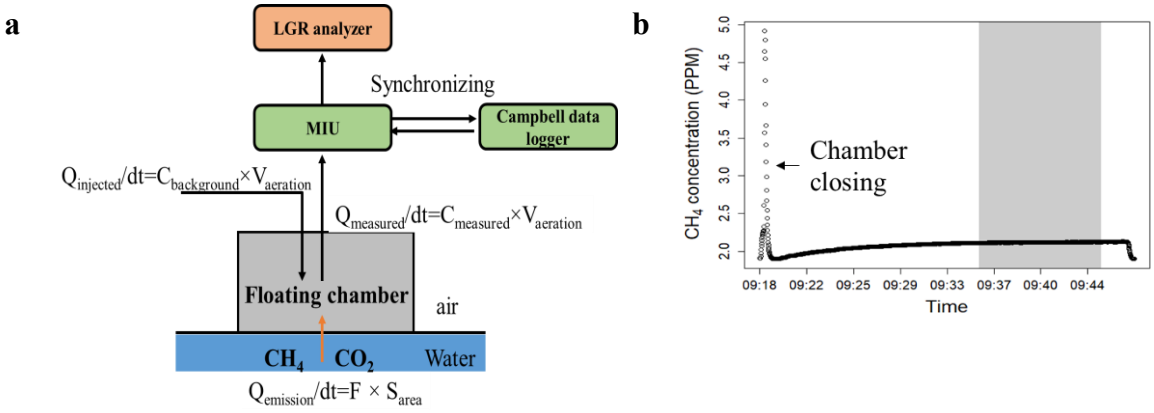

Figure 2.2 High-frequency measurements of CH_4 and CO_2 fluxes from experimental mesocosm ponds using floating chambers. a, Schematic showing flow-through open chamber. **b,** Example data set during a 30-minute measurement of CH_4 emissions from a single pond (Pond 4 from 09:18 to 09:48 in 23rd July, 2017). The shaded area represents the steady-state period used to estimate CH_4 emissions by averaging CH_4 concentrations during that time and comparing them to injected air concentrations for CH_4.

Every chamber was closed for gas measurement for the same length of time: from February, 2017 to April, 2017, every chamber was closed for 20 minutes and from April, 2017 to February, 2018, every chamber was closed for 30 minutes to guarantee a steady-state. MIU was synchronized with Campbell data logger and was used to switch the LGR automatically between each chamber. Fourteen parallel chambers on 7 of the 10 warmed and 7 of the 10 ambient replicate ponds were used. One inlet port was for atmospheric CH_4 measurement as background.

2.3.5 Characterization of ebullition in methane emission measurements

Floating LI-COR dynamic chambers in an open-loop configuration was used to quantify CH_4 emissions from our experimental ponds. In total, 16504 chamber measurements were made. Diffusional CH_4 emissions were characterised from steady-state differences in CH_4 concentrations between ambient air and air circulating through a closed chamber (Figure 2.3 a). In contrast, ebullition events lead to sudden increases in CH_4 concentrations over short periods of time that would bias the flux estimates. For example, during strong ebullition events, CH_4 concentrations in a chamber could increase up to 30 ppm at a rate of 4000 ppb per second (Figure 2.3 b), while, in gentler ebullition events, CH_4 concentrations could increase at 90 ppb per second and to a maximum of only 5 ppm (Figure 2.3 c). In either case, after reaching post-ebullition, maximum CH_4 concentrations, concentrations subsequently decreased at a gentler rate than their initial rates of increase.

Ebullition events were, therefore, identified according to two criteria: **1**, CH_4 concentrations increased consistently for 5 seconds at a rate greater than 50 ppb per second to reach the maximum concentration during the measurement windows; or **2**, CH_4 concentrations decreased consistently for 5 seconds at a rate greater than 10 ppb per second after the maximum concentration during the measurement windows. I acknowledge that these criteria

may also identify other non-steady flux events besides ebullition but excluding these other non-steady flux events made it possible to calculate the CH_4 emissions by averaging CH_4 concentrations at steady-state. Of the 16504 total chamber measurements, 205, i.e., 1.2%, were identified as either ebullition or other non-steady-state events and excluded from further methane emission calculations.

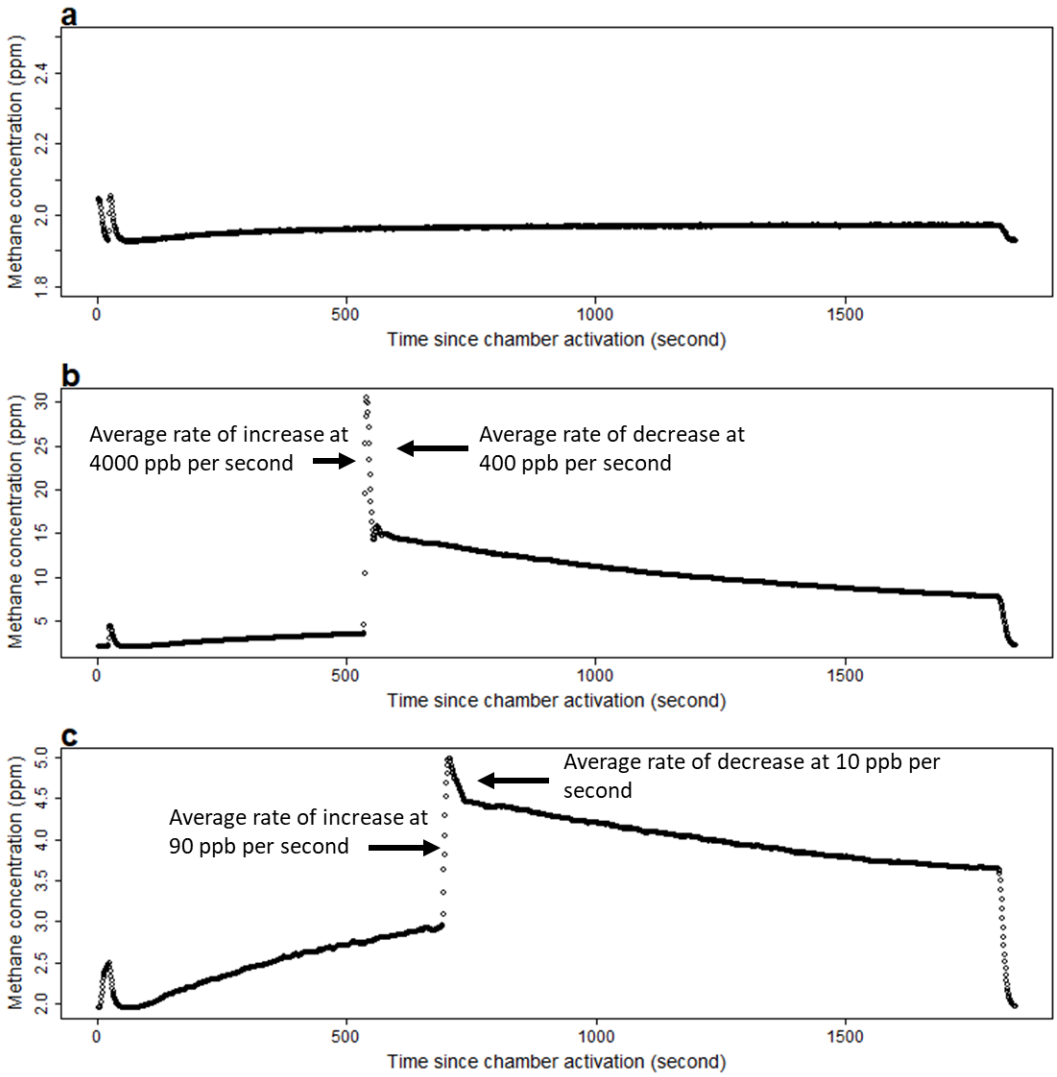

Figure 2.3 Example of chamber measurements for **a**, steady-state flux **b**, strong ebullition and **c**, gentle ebullition.

2.3.6 Calculation of methane and carbon dioxide fluxes

In the open-chamber measurements, the mass flow through the chambers measured by LGR ($Q_{measured}$, μmol) is a mix of mass flow emitted from the ponds ($Q_{emission}$, μmol) and mass flow of injected air ($Q_{injected}$, μmol) (Figure 2.2 a) (Yver Kwok *et al.*, 2015). When a steady-state concentration in the chamber is reached (Figure 2.2 b), the mass flow through the chamber can be determined from the mass balance using the equation:

$$Q_{emission} = Q_{measured} - Q_{injected} \quad (2.1)$$

The mass flow per hour is the gas flux (i.e., CH_4 or CO_2) through the floating chamber. The flux of gases was calculated using the equation:

$$F = \frac{Q_{emission}/dt}{S_{area}} \quad (2.2)$$

Where F is the gas flux (μmol $m^{-2}h^{-1}$). $Q_{emission}/dt$ is the mass flow per hour (μmol h^{-1}) and S_{area} is the surface area of the floating chamber (m^2).

As the mass flow per hour was the production of the gas concentrations measured by LGR at steady-state and the volume of air injected, the mass flow

were calculated using:

$$Q_{measured}/dt = C_{measured} \times V_{areation} \quad (2.3)$$

$$Q_{injected}/dt = C_{injected} \times V_{areation} \quad (2.4)$$

Where $Q_{measured}/dt$ and $Q_{injected}/dt$ are the mass flow through chamber and mass flow of injected air, respectively, over partial time (μmol h^{-1}). $C_{measured}$ and $C_{injected}$ are the gas concentrations measured by LGR and the gas concentrations in the injected air, respectively (μmol L^{-1}). $V_{areation}$ is volume of air injected into chamber per hour (L h^{-1}).

The flux of gases was therefore calculated by:

$$F = \frac{(C_{measured} - C_{injected})}{S_{area}} \times \frac{V_{aeration}}{dt} \quad (2.5)$$

Where F is the flux of gas (CH_4 or CO_2) (μmol m^{-2} h^{-1}), $C_{measured}$ is the concentration of the gas measured in the chamber (μmol L^{-1}) estimated by averaging the concentrations over the steady-state period, $C_{injected}$ is the gas concentration of injected air (μmol L^{-1}), $V_{aeration}/dt$ is the volume of air flowing through a chamber per hour (3.0 L min^{-1}, corrected by gas temperature and pressure) and S_{area} is the surface area of the chamber (0.031 m^2).

2.3.7 Ratio of methane emission to net carbon dioxide exchange

The CO_2 flux measured in the chambers is the net exchange of CO_2, which provides a direct estimate of the ecosystem CO_2 balance (Valentini *et al.*, 2000). Carbon dioxide fluxes followed a regular diel pattern of emission during night and uptake during day (Figure 2.4). Daily net exchange of CO_2 and daily CH_4 emission were calculated by integrating the gas fluxes measured during a single day, using the function "auc" from the package "flux" (version 0.3-0) (Jurasinski, Koebsch and Hagemann, 2012) in R (version 3.2.5). The ratio of CH_4 emission to net exchange of CO_2 was calculated using:

$$R_{emission} = \frac{ME}{NE} \quad (2.6)$$

Where ME and NE are the CH_4 emission rate (μmol $m^{-2}d^{-1}$) and net exchange of CO_2 rate (μmol $m^{-2}d^{-1}$), respectively.

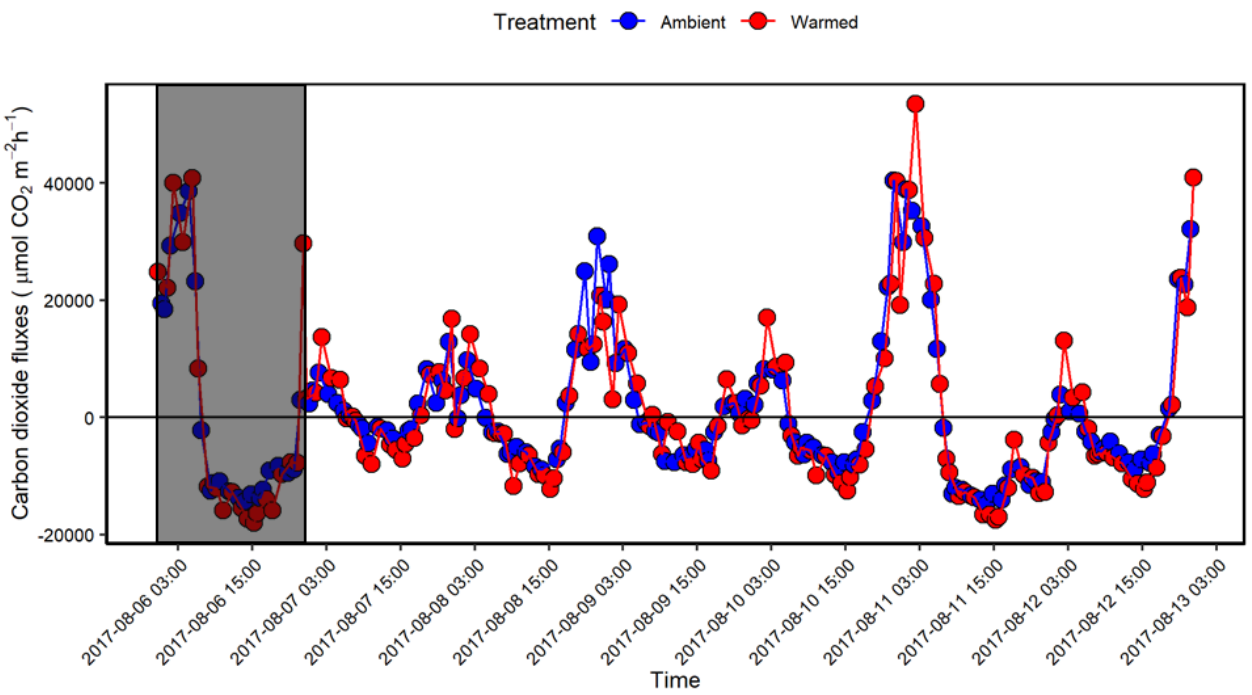

Figure 2.4 Diel patterns of carbon dioxide exchange. Example data set comprising a 1-week segment of carbon dioxide exchange rates. The daily net ecosystem exchange was calculated by trapezium integration of carbon dioxide fluxes over a day (i.e., a 24-hour segment, shaded in grey).

2.3.8 Net global warming potential of carbon gases emitted

Net ecosystem global warming potential (NGWP) of the carbon gases emitted was calculated by summing the positive radiative forcing of CH_4 emission as CO_2 equivalents and the negative radiative forcing of CO_2 uptake using:

$$NGWP_0 = ME \times GWP_0 + Exchange \quad (2.7)$$

$$NGWP_{20} = ME \times GWP_{20} + Exchange \quad (2.8)$$

$$NGWP_{100} = ME \times GWP_{100} + Exchange \quad (2.9)$$

Where $NGWP_0$, $NGWP_{20}$ and $NGWP_{100}$ were the net global warming potential for immediate emission, 20- and 100-year time-horizons', respectively, in the unit of CO_2 equivalents (CO_{2eq}), to fully account for the short-term forcing of CH_4 and long-term impacts of CO_2 (Balcombe *et al.*, 2018). *ME* was the CH_4 emission rate (g CH_4 $m^{-2}yr^{-1}$) and *Exchange*

was the net CO_2 exchange (g CO_2 $m^{-2}yr^{-1}$). GWP_0 was the radiative forcing immediately after emission (120 gCO_{2eq}/gCH_4). GWP_{20} and GWP_{100} were the global warming potential of CH_4 for 20- and 100-year horizon, respectively (84 gCO_{2eq}/gCH_4 and 28 gCO_{2eq}/gCH_4) (IPCC, 2014). If the NGWP>0, the mesocosm ponds contribute to greenhouse effect via CH_4 emission while, in contrast, if NGWP<0, attenuate the greenhouse effect via CO_2 uptake.

2.3.9 Statistical analysis

Estimation of annual budget of CH_4 fluxes using generalized additive mixed effect models (GAMMs)

Plotting natural-log-transformed daily CH_4 emission rates against day of the year since 1st January 2017 showed different shapes and CH_4 emissions among the ponds (Figure 2.5). To account for the variance between mesocosm ponds in their seasonal distribution of net CH_4 emissions and characterize the average annual fluxes and treatment effects, the generalized additive mixed-effect model (GAMM) was used (Zuur, 2009; Yvon-Durocher *et al.*, 2017). The fluxes were firstly fitted as a function of day of the year into a full model using the "gamm4" function from the "gamm4" package (version 0.2-5) which included a treatment on the intercept to characterize the median value of the response variable and a smooth term which defined the shape of seasonal patterns (cubic regression splines). Next, the "dredge" function from "MuMin" package (version 1.15.6) was used to generate a set of models with combinations of terms in the full model and then compared among the models using the AIC (Akaike Information Criterion) and AIC weights (*see* Table 2.2). The annual rate of CH_4 flux from both the warmed and ambient ponds was calculated using the estimates from the best models with lowest AIC scores and multiplying by 365.

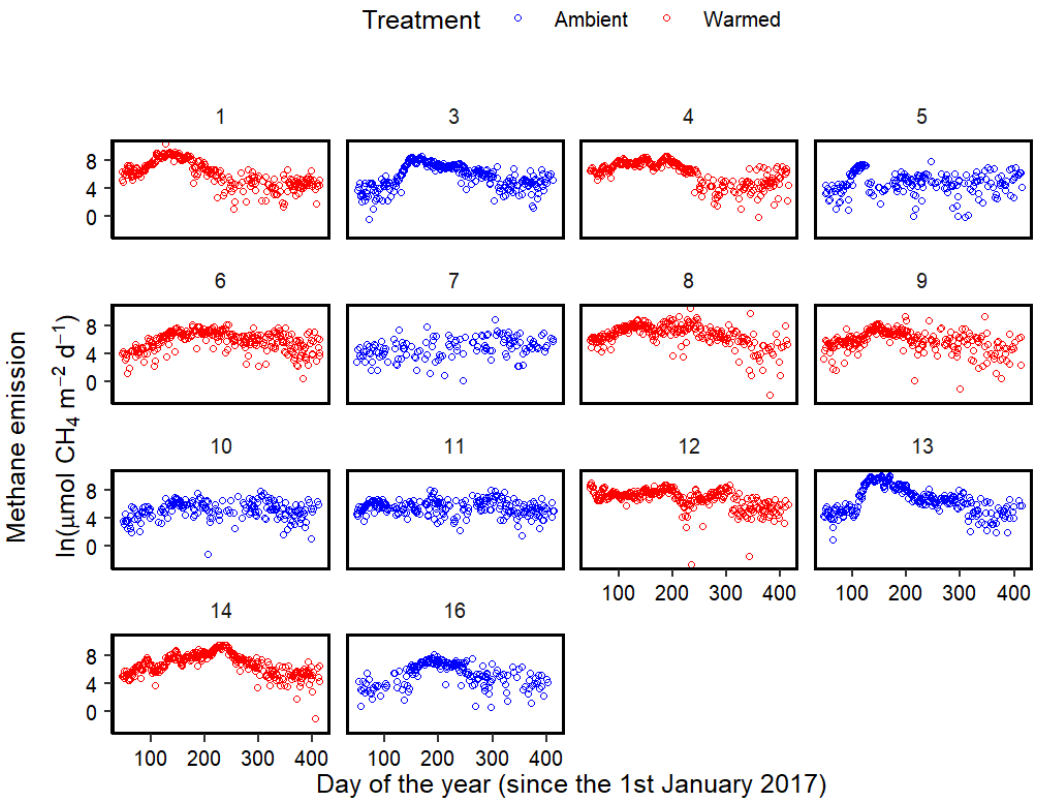

Figure 2.5 Different seasonal variations in CH_4 emissions between mesocosm ponds from February, 2017, to February, 2018.

Estimation of net CO_2 exchange using generalized additive mixed effect models (GAMMs)

The seasonality of net CO_2 exchange was estimated using GAMMs. The model fitting and selection procedures were the same as for CH_4 emissions in the previous section except that the net CO_2 exchange rate was not natural-logarithm-transformed.

Estimation of the temperature sensitivity and rates of methane and carbon dioxide emission using linear mixed effect models

According to the Boltzmann-Arrhenius equation, the temperature sensitivity and rates of CH_4 and CO_2 emission were estimated using:

$$lnME_{ij}(T) = (\overline{\mathrm{E}_{ME}} + a_i + a_{ij})\left(\frac{1}{kT_C} - \frac{1}{kT_{ij}}\right) + \left(\overline{lnME(T_C)} + b_i + b_{ij}\right) \quad (2.10)$$

$$lnER_{ij}(T) = (\overline{\mathrm{E}_{ER}} + a_i + a_{ij})\left(\frac{1}{kT_C} - \frac{1}{kT_{ij}}\right) + \left(\overline{lnER(T_C)} + b_i + b_{ij}\right) \quad (2.11)$$

Where $lnME_{ij}(T)$ and $lnER_{ij}(T)$ are the natural logarithm of rates of CH_4 and CO_2 emission by mesocosm pond i (i =1, 2, …) in month j (j=1, 2, …) at absolute temperature T (K). As the experimental design yielded a hierarchical structure - replicate responses in ponds of both treatment over months (Figure 2.6), the sampling replicate pond and month were treated as nested random effects on the slope ($a_i + a_{ij}$) and the intercept ($b_i + b_{ij}$) of the models to account for the random variation among ponds and among month within ponds from the fixed effects. The slopes of the equation represent the estimated population activation energy (temperature sensitivity) in units of eV (1eV=96.49 kJ mol^{-1}), for CH_4 emission ($\overline{E_{ME}}$) and CO_2 emission ($\overline{E_{ER}}$). k is the Boltzmann constant (8.62×10^{-6} eV K^{-1}). The plot was standardized using the term $\frac{1}{kT_C}$, in which T_C (288.15 K) is the average temperature in the ambient ponds *i.e.*, 15°C in 2017, so that the terms $\overline{lnME(T_C)}$ and $\overline{lnER(T_C)}$ correspond to the average rates of CH_4 and CO_2 emission standardized to 15℃ , respectively. The effects of treatment (i.e., whether ambient or warmed ponds) on both the slope (temperature sensitivity) and intercept (average rates of CH_4 emission) was modelled as fixed effects and their significance was tested using likelihood ratio test by comparing a full model with a reduced one where the "treatment" term was removed (*see* Table 2.4).

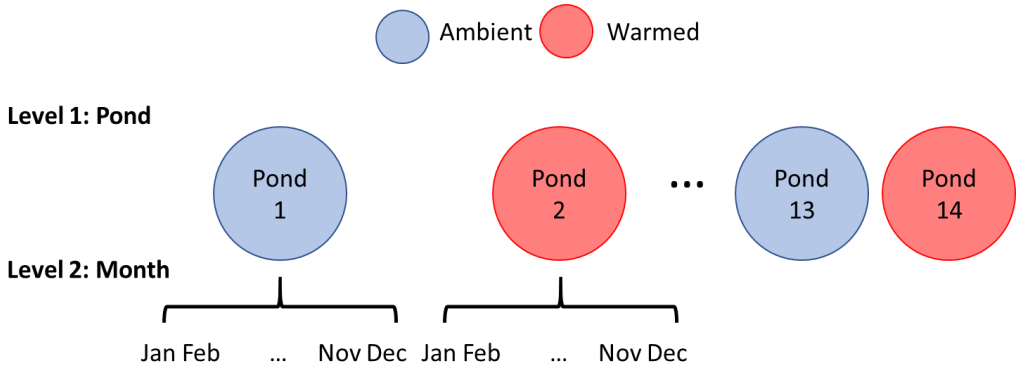

Figure 2.6 The hierarchical structure of CH_4 and CO_2 emission data. The random variance among mesocosm ponds and sampling month were accounted by treating the sampling month within the mesocosm ponds as random effect on the intercept and the slope of the model.

Meta-analysis of global data on CH_4 and CO_2 emission at 15 °C

To test if warming leads to a greater CH_4 emission capacity along a natural temperature gradient from subarctic to subtropical while CO_2 emission capacity is conserved, I performed a meta-analysis of available ecosystem-level CH_4 and CO_2 emissions data from 19 globally distributed sites, of which 68% are wetlands, 11% crop lands and 21% forests, grasslands and open shrubs (see Figure 2.7 for site distribution and Table 2.1 for site names and references). The half-hour aggregated eddy-covariance data were downloaded for 17 sites within the AmeriFlux (https://ameriflux.lbl.gov/) and 2 sites within European Fluxes Database Cluster (http://www.europe-fluxdata.eu/home).

To compare the emission capacity along a natural temperature gradient between CH_4 and CO_2, I only used fluxes where CH_4 fluxes, CO_2 fluxes and air temperature were measured simultaneously. Sites with measurements spanning a time period of <6 months were excluded, to avoid potential bias of average annual temperature of the sites. Data demonstrated a good relationship between CH_4 or CO_2 emission and air-temperature (P<0.05).

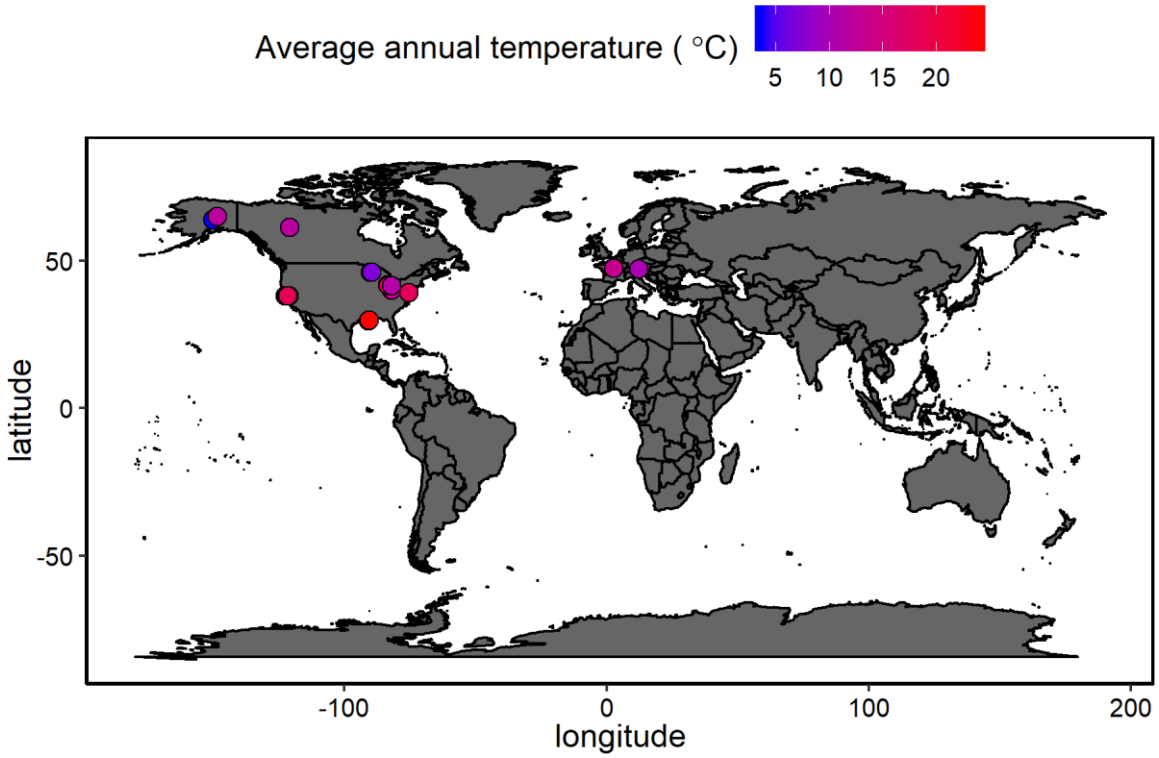

Figure 2.7 Global distribution of the sites included in our meta-analysis (*n*=19). The colour of each point relates to the annual average site temperature.

Because I was interested in the CH_4 and CO_2 emission capacity at a fixed temperature, i.e., here at 15°C, from each site included, rather than the overall capacity across the global sites, a simple linear model was used to quantify the CH_4 and CO_2 emissions at 15 °C at each site separately, by fitting Boltzmann-Arrhenius equation of the form:

$$lnME(T) = \overline{E_{ME}}\left(\frac{1}{kT_C} - \frac{1}{kT}\right) + \overline{lnME(Tc)} \quad (2.12)$$

$$lnER(T) = \overline{E_{ER}}\left(\frac{1}{kT_C} - \frac{1}{kT}\right) + \overline{lnER(Tc)} \quad (2.13)$$

Where *lnME(T)* and *lnER(T)* are the natural-logarithm-transformed CH_4 and CO_2 emissions at absolute temperature T (K). k is the Boltzmann constant (8.62×10^{-6} eV K^{-1}). As the plot was standardized using the term $\frac{1}{kT_C}$, in which T_C (288.15 K) is the fixed temperature, *i.e.*, 15 °C, so that the intercept terms $\overline{lnME(T_C)}$ and $\overline{lnER(T_C)}$ correspond to the average

rates of CH_4 and CO_2 emission at 15 °C, respectively. The relationship between CH_4 and CO_2 emission capacity and natural warming were determined by plotting the average rates of CH_4 and CO_2 emissions at 15 °C against the average annual temperature of each site.

2.3.10 Prediction of methane emission from the apparent activation energy

Activation energy is a measure of temperature sensitivity (Allen, Gillooly and Brown, 2005). The prediction of increase in the CH_4 emissions under the 4 °C warming scenario can be calculated using the apparent activation energy for temperature sensitivity of CH_4 emission to temperature (Allen, Gillooly and Brown, 2005; Yvon-Durocher *et al.*, 2014):

$$\frac{F(T_W)}{F(T_A)} = e^{\frac{\overline{E_{ME}}}{kT_W} - \frac{\overline{E_{ME}}}{kT_A}} \quad (2.14)$$

Where $F(T)$ is CH_4 emission rate and T_W and T_A are the mean annual temperatures of the warmed and ambient ponds (288.15 and 292.15 K, respectively). k is the Boltzmann constant (8.62×10^{-5} eV K^{-1}). $\overline{E_{ME}}$ is the apparent activation energy of CH_4 in equation (2.9). The apparent activation energy of CH_4 emission estimated in this thesis was 0.84 eV, close to the common activation energy yielded in a meta-analysis for 0.96 eV. Under the 4 °C warming scenarios, the apparent activation therefore predicts a 1.60-fold increase in the ecosystem-level CH_4 emission, similar to the 1.70-fold increase using the common activation energy for 0.96 eV.

Table 2.1 Original data sources for the analysis of CH_4 and CO_2 emission capacities from globally distributed sites. n_1 and n_2 represent the number of daily rate measurements of CH_4 emissions and hourly rate measurements of CO_2 emissions for each site, respectively.

Site ID	Site Name	Ecosystem type	n_1	n_2	References
AT-Neu	Neustift	Grassland	539	535	(Sonnentag and Quinton, 2016)
CA-SCB	Scotty Creek Bog	Wetland	639	619	
FR-LGt	La Guette	Wetland	215	78	(Chen and Jiquan, 2016a)
US-CRT	Curtice Walter-Berger cropland	Cropland	246	321	(Schuur and Ted, 2018)
US-EML	Eight Mile Lake Permafrost thaw gradient, Healy Alaska.	Open shrubs	1015	458	(Krauss and Ken, 2016a)
US-LA1	Pointe-aux-Chenes Brackish Marsh	Wetland	206	185	(Krauss and Ken, 2016b)
US-LA2	Salvador WMA Freshwater Marsh	Wetland	531	518	(Desai and Ankur, 2016a)
US-Los	Lost Creek	Wetland	1499	1491	(Baldocchi and Dennis, 2016a)
US-Myb	Mayberry Wetland	Wetland	2687	2669	(Bohrer and Gil, 2016)
US-ORv	Olentangy River Wetland Research Park	Wetland	1132	1052	(Bohrer and Gil, 2018)
US-OWC	Old Woman Creek	Wetland	104	97	(Desai and Ankur, 2016b)
US-PFa	Park Falls/WLEF	Forest	975	551	(Baldocchi and Dennis, 2018)
US-Sne	Sherman Island Restored Wetland	Wetland	575	795	(Vargas and Rodrigo, 2016)
US-StJ	St Jones Reserve	Wetland	250	256	(Baldocchi and Dennis, 2016b)
US-Tw1	Twitchell West Pond Wetland	Wetland	2039	2115	(Baldocchi and Dennis, 2016c)
US-Tw4	Twitchell East End Wetland	Wetland	1668	1662	(Baldocchi and Dennis, 2016d)
US-Twt	Twitchell Island	Cropland	351	2205	(Iwata, Ueyama and Harazono, 2016)
US-Uaf	University of Alaska, Fairbanks	Forest	236	0	(Chen and Jiquan, 2016b)
US-WPT	Winous Point North Marsh	Wetland	793	799	

2.4 Results

2.4.1 Sediment characteristics and comparison of CH_4 emission from experimental ponds to natural ecosystems

Warming has increased the organic carbon (C) and nitrogen (N) in the warmed ponds relative to their ambient controls (*t*-statistic, $P<0.05$) (Figure 2.8). The organic carbon has increased from 0.83% in the ambient ponds to 1.23% in the warmed ponds and the nitrogen has increased from 0.084% in the ambient ponds to 0.11% in the warmed ponds (Figure 2.8 a and b). The C to N ratio and $\delta^{13}C$ were, however, unchanged (*t*-statistic, $P=0.05$ and $P=0.08$ for the C to N ratio and $\delta^{13}C$, respectively) (Figure 2.8 c and d).

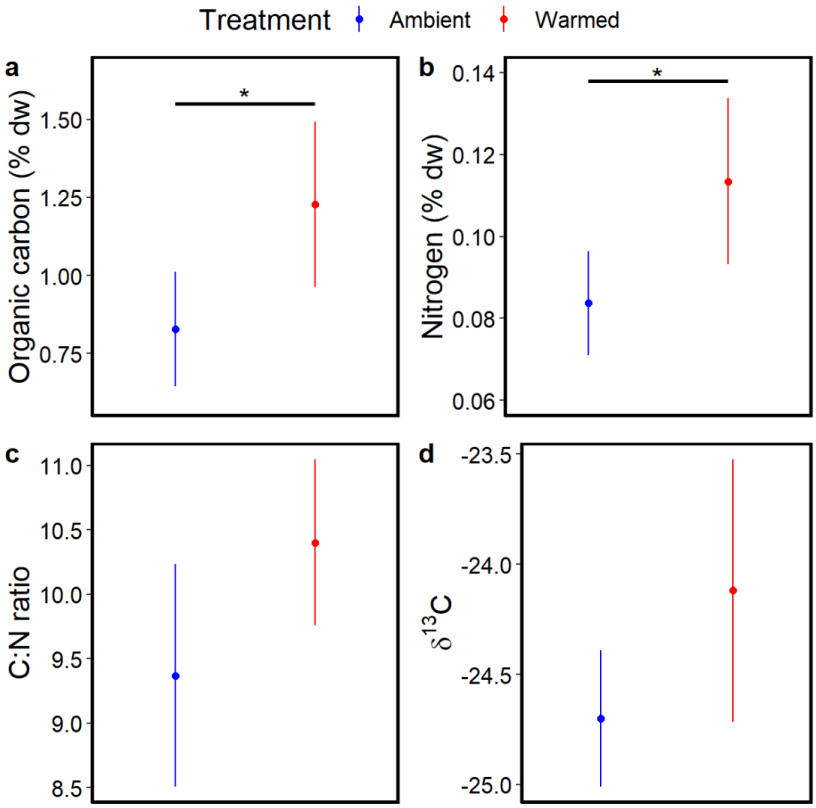

Figure 2.8 Pond sediment characteristics. Organic carbon (**a**), nitrogen (**b**), carbon-to-nitrogen ratio (C:N, **c**) and $\delta^{13}C$ (**d**) of organic matter from pond sediments. Significance for a *t*-statistic comparison between the warmed and ambient ponds is shown by asterisks (*: $P<0.05$).

I further compared the CH_4 concentrations in experimental pond water with natural lakes. The CH_4 concentrations were 1.07 and 0.51 μmol L^{-1} in the warmed and ambient ponds, respectively, undistinguishable from the CH_4 concentrations in the natural ponds of similar surface areas (Figure 2.9).

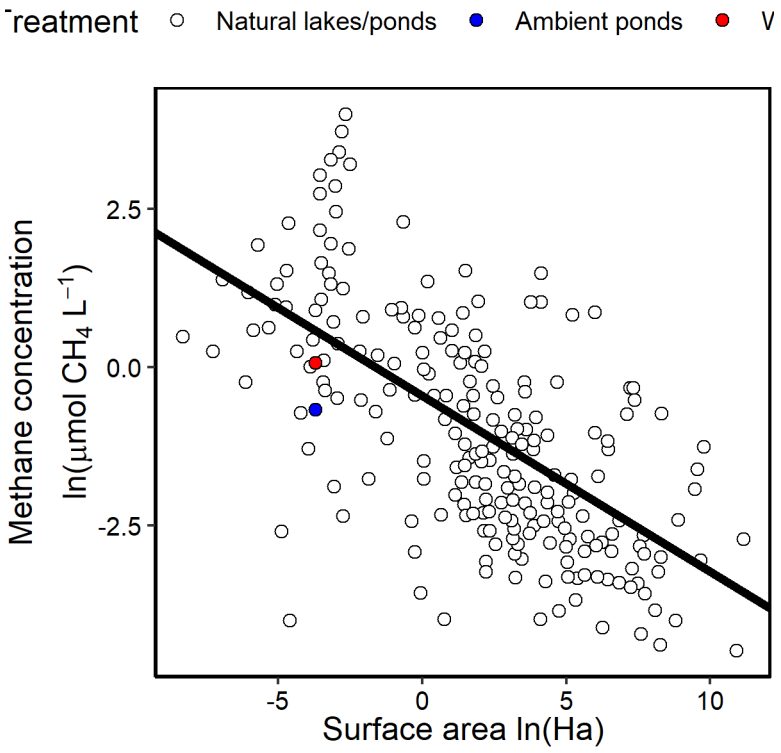

Figure 2.9 Relationship between waterbody surface area and CH_4 concentration for globally distributed lakes, ponds and the experimental mesocosm ponds in this thesis. Data points show the CH_4 concentrations in the mesocosm ponds (red for the warmed and blue for the ambient ponds) and in the global waterbodies from very small ponds to lakes yielded in a recent publication (Holgerson and Raymond, 2016). The analysis demonstrates that the concentrations of CH_4 in the mesocosm ponds are similar to the natural ponds of comparable sizes.

2.4.2 Net carbon dioxide exchange

The carbon cycle in the mesocosm ponds is driven by autochthonous production (Yvon-Durocher, Montoya, Woodward, *et al.*, 2011; Yvon-Durocher *et al.*, 2017). I calculated first the CO_2 exchange to provide a direct estimate of the ecosystem carbon balance in the

mesocosm ponds. During the summer, the mesocosm ponds functioned as CO_2 sinks while during the winter, the mesocosm ponds functioned as CO_2 sources (Figure 2.10 a). While integrating the net CO_2 exchange over the year, the negative values indicated that the mesocosm ponds were sinks for CO_2. The annual net rates of CO_2 exchange were -107 and -118 g C $m^{-2}yr^{-1}$ in the ambient and warmed ponds, respectively (Figure 2.10 b). The annual net CO_2 exchange was marginally lower in the warmed ponds, indicating that warmed ponds fixed more carbon than their ambient controls.

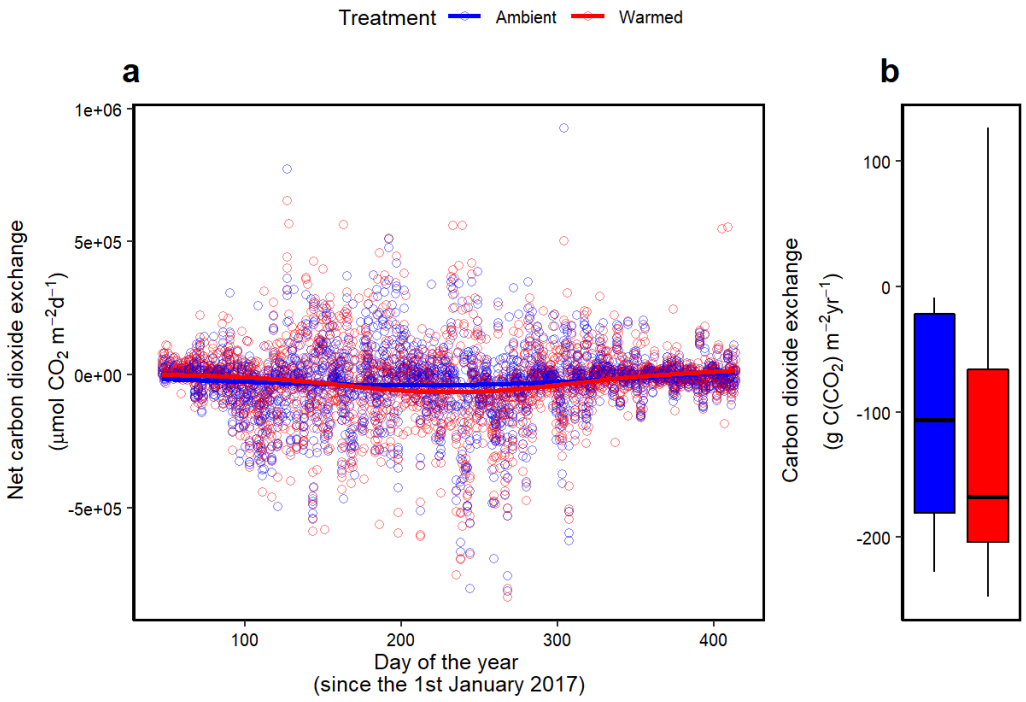

Figure 2.10 Long-term warming has altered the annual budget of net CO_2 exchange. a, Seasonal distribution of net CO_2 exchange. **b**, Annual net CO_2 exchange calculated by integrating the CO_2 flux for each pond over the year. The negative values indicate that the mesocosm ponds were sink for CO_2. The net CO_2 exchange was lower in the warmed ponds relative to their ambient controls (-107 and -118 g C $m^{-2}yr^{-1}$ for warmed and ambient ponds, respectively) suggesting that warmed ponds fixed marginally more carbon than the ambient ponds.

Table 2.2 Multi-model selection procedures for fitting generalized additive mixed effects models to net ecosystem exchange data (*n*=4957). A range of generalized additive mixed effects models (GAMM) were fitted to net CO_2 exchange (NE) as a function of "Treatment" (i.e., warmed or ambient) and DOY (day of the year since 1st January 2017) to assess the effect of long-term warming on net ecosystem exchange. The difference of seasonal flux among the treatment was also tested by comparing the smooth terms s(DOY, by=Treatment) and s(DOY). Models were ranked according to Akaike information criterion (AIC) which measured goodness of fit and model complexity (Zuur, 2009). ΔAIC refers to the AIC differences relative to the smallest AIC value and the AIC weight is the probability that the model is the actual best model (Burnham and Anderson, 2002). The model that best fits the net CO_2 exchange (marked in bold) includes the additive effects of "treatment" and "s(DOY,by=Treatment)", demonstrating that long-term warming has not only lowered the net CO_2 fluxes (indicating more CO_2 fixation) but also changed the seasonality of net daily CO_2 fluxes.

	Model	d.f.	AIC	ΔAIC	AIC Weight
(1)	**NE=Treatment+s(DOY,by=Treatment)**	**8**	**130726.8**	**0.00**	**1**
(2)	NE=s(DOY,by=Treatment)	6	130745.9	19.09	0.000
(3)	NE=Treatment+s(DOY)	7	130753.0	26.23	0.000
(4)	NE=s(DOY)	5	130772.1	45.32	0.000

2.4.3 Annual methane emissions

The net CH_4 emissions exhibited a clear difference in seasonal trends between the warmed and ambient ponds, and, on average, a separation between the treatments (Figure 2.11 a). After 11 years of warming, warmed ponds emit 2.4-fold more CH_4 than their ambient controls (likelihood ratio test, $P<0.01$, 1.02 and 2.46 g C (CH_4) m^{-2} yr^{-1} from the ambient and warmed ponds, respectively). Consequently, a GAMM which included "Treatment" on the intercept and a Treatment-specified smoother term provided the best fit to seasonal CH_4

emission data, demonstrating an increase in median CH_4 emission from warmed ponds as well as a difference in seasonality (Table 2.3).

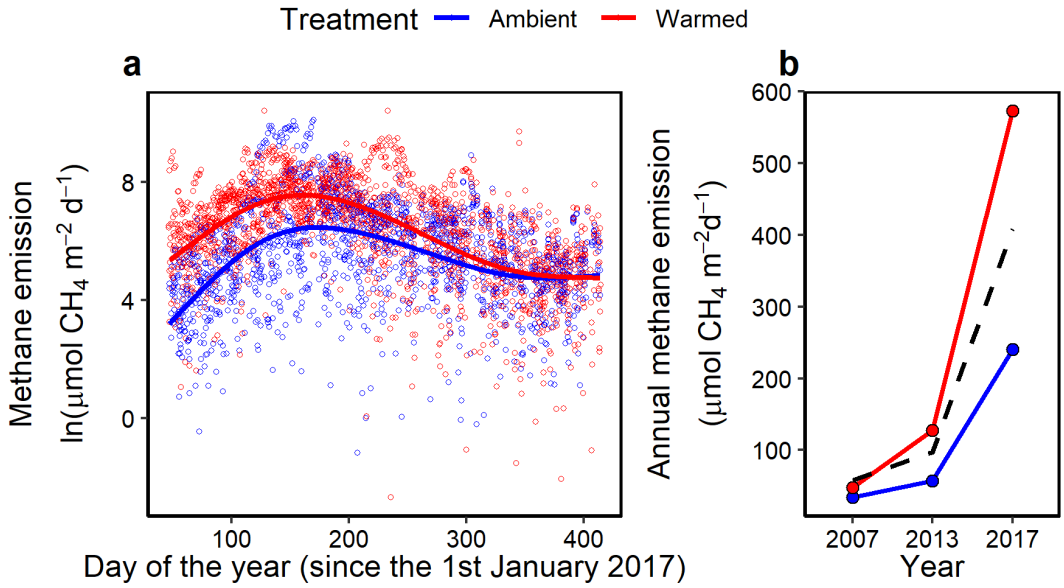

Figure 2.11 Long-term warming has increased annual CH_4 emissions. a, Different seasonal variation in CH_4 emissions from February, 2017, to February, 2018. Median CH_4 emissions were greater in the long-term warmed ponds relative to the ambient controls. **b**, Annual CH_4 emissions from 2007, 2013 and 2017. There is a clear increasing divergence between the warmed (red) and ambient (blue) ponds beyond the 1.60-fold increase predicted for an apparent activation energy of 0.87 eV and the 4°C difference in temperature between the warmed and ambient ponds (black dashed line, *see* equation (2.13)).

More strikingly, there was an increasing divergence of CH_4 emission between the warmed and ambient ponds (Figure 2.11 b). In 2007, after only 1 year of warming, warmed ponds emit only 1.4-fold more CH_4 relative to their ambient controls which, by 2013, had increased to 2.2-fold more CH_4 relative to the ambient ponds. The apparent activation energy based on the 4 °C interval predicts, nevertheless, only a 1.6-fold increase in CH_4 emissions (dashed line in Figure 2.11 b, *see* equation (2.13)). The warmed ponds thus started to emit CH_4 at a rate exceeding the prediction given by consistent apparent activation energy based

on temperature alone. Now in 2017, after 11 years of warming, the difference between the warmed and ambient ponds has increased to 2.4-fold – warming has enhanced the annual CH_4 emission to a greater magnitude far in excess of that predicted by warmer temperatures alone.

Table 2.3 Multi-model selection procedures for fitting generalized additive mixed effects models to the data for seasonal CH_4 emission (*n*=3553). A range of generalized additive mixed effects models (GAMM) were fitted to the daily CH_4 emission (ME) as a function of "Treatment" (i.e., warmed or ambient) and DOY (day of the year since 1st January 2017) to assess the effect of long-term warming on median CH_4 emissions. The differences in seasonal flux between the treatments was test as per in Table 2.2. The model that best fit the CH_4 production was the model (1) marked in bold, which includes the additive effects of "treatment" and "s(DOY,by=Treatment)", demonstrating that long-term warming has not only increased the annual CH_4 emission but also changed the seasonality of CH_4 emission.

Model		d.f.	AIC	ΔAIC	AIC Weight
(1)	**Ln(ME)=Treatment+s(DOY,by=Treatment)**	**8**	**12035.0**	**0.00**	**0.91**
(2)	Ln(ME)=s(DOY,by=Treatment)	7	12039.7	4.71	0.09
(3)	Ln(ME)=Treatment+s(DOY)	6	12194.2	159.24	0.00
(4)	Ln(ME)=s(DOY)	5	12198.9	163.94	0.00

2.4.4 Ratio of methane emission to net carbon dioxide exchange

Mesocosm ponds fix CO_2 via photosynthesis and emit CH_4 and CO_2 via methanogenesis, other respiratory pathways and fermentation. The ratio of CH_4 emission to net CO_2 exchange therefore represents the balance in carbon greenhouse gases between an ecosystem and the atmosphere. Methane emission rates were strongly related to the net CO_2 exchange, and a plot of CH_4 emission rates against net exchange of CO_2 revealed a separation on the intercept, i.e., the proportion of fixed carbon emitted as CH_4 was higher in the warmed

ponds (Figure 2.12 a). Indeed, the ratio of CH_4 emission to net CO_2 exchange was 0.95 % and 2.1 % in the ambient and warmed ponds, respectively (likelihood ratio test, χ^2=10.72, P<0.05).

Radiative forcing of CH_4 is approximately 120 times greater than CO_2 after immediate emission (Balcombe *et al.*, 2018). Global warming potential is the integration of radiative forcing up to a chosen time horizon (e.g., 20 and 100 years) relative to CO_2 (IPCC, 2014). Here, the net ecosystem global warming potential (NGWP) of the warmed and ambient ponds was calculated by summing the negative radiative forcing of CO_2 uptake and the positive radiative forcing of CH_4 emission, in terms of CO_2 equivalents (i.e., CO_{2eq}), to determine the net greenhouse gas balance in mesocosm ponds. The mesocosm ponds contributed to a greenhouse effect via CH_4 emission if NGWP>0, while, in contrast, attenuate the greenhouse effect via CO_2 uptake if NGWP<0.

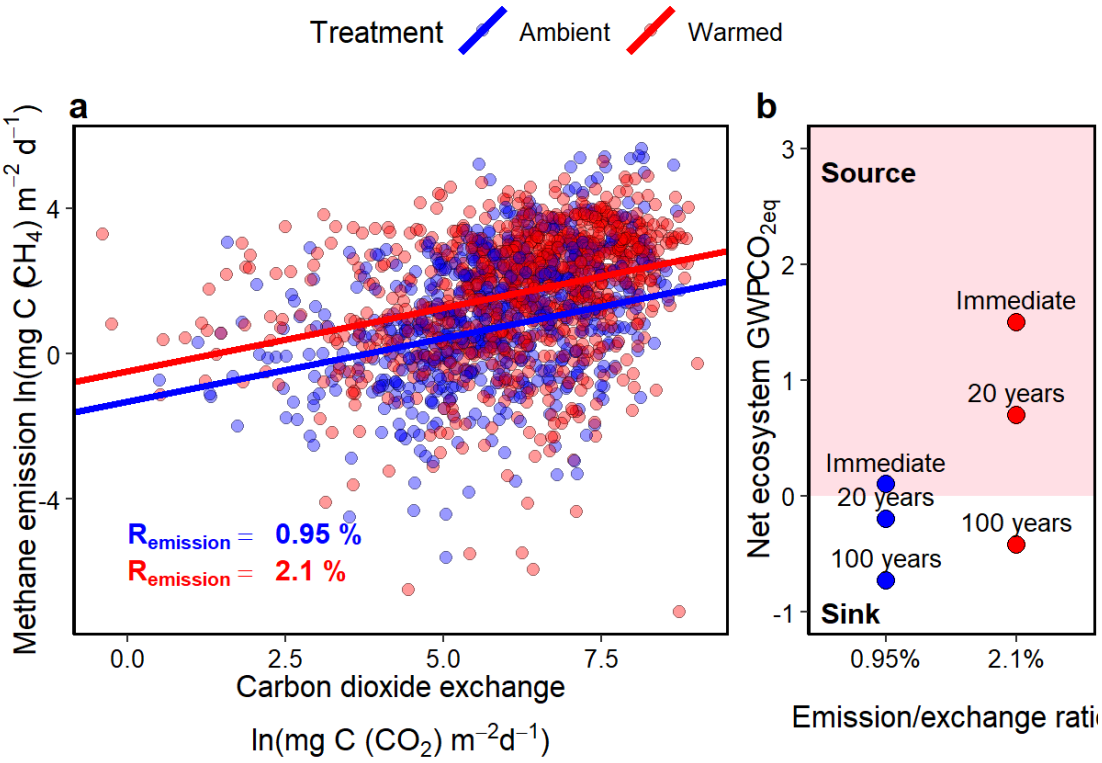

Figure 2.12 Methane emission as a function of net CO_2 exchange. a, Methane emission was strongly correlated with net CO_2 exchange. Long-term warming increased the proportion of the ecosystem fixed carbon emitted as CH_4 by 2.2 fold, from 0.95 % in the ambient ponds to 2.1 % in the warmed ponds. **b**, NGWP declined over time due to relatively short lifespan of CH_4 than CO_2. Ambient ponds turned from carbon greenhouse gas sources to sinks within only 20-year horizon but the long-term warmed ponds would remain as carbon greenhouse gas sources up to an approximate 100-year horizon.

Despite that only 0.95 % and 2.1 % of the fixed carbon was emitted to atmosphere as CH_4 in the warmed and ambient ponds, respectively, the positive forcing of CH_4 would be large enough to offset their CO_2 uptake immediately after emission ($NGWP_0>0$, Figure 2.12 b). Thus, both the warmed and ambient ponds could be considered as carbon greenhouse gas sources after immediate emission. As the proportion of fixed carbon emitted as CH_4 was much lower in the ambient ponds compared to the long-term warmed ponds and the negative net CO_2 exchange would be able to offset the positive forcing of CH_4, the ambient ponds would

turn from carbon greenhouse gas sources to sinks within a 20-year horizon. Consequently, the NGWP of the ambient ponds decreased below 0 ($NGWP_{20}<0$) rapidly for a 20-year horizon. In contrast to the ambient ponds, the warmed ponds would stay as carbon greenhouse gas sources up to an approximate 100-year horizon ($NGWP_{100}>0$, Figure 2.11 b).

Table 2.4 Model selection procedures for fitting linear mixed effect models to CH_4 emission data as function of the net CO_2 exchange rate (NEE) and pond treatment (*n*=1680). The full model included the interactions for 2 fixed effects – NEE and treatment types (i.e., ambient or warmed). The random effects were firstly included on both the intercept and slope to account for the variance across the experimental ponds. The sampling month was not included in the model as CO_2 uptake mainly happened in the summer. The random intercept and slope model had the lowest AIC and was therefore the preferred option. This optimal random effect was then applied, and the significance of *P*-value for the fixed-effect terms were determined via likelihood ratio test on nested models (denoted by subtraction symbols below). The model that best fit the data was marked in bold, i.e., F1 which included the single slope but different intercepts, demonstrating that long-term warming increased the proportion of the ecosystem fixed carbon emitted as CH_4.

Model	**d.f.**	**AIC**	**LogLik**	χ^2	***P*-value**
To determine the optimal random-effect structure:					
Full model + (1+NEE|Pond)	**8**	**6261.0**	**-3112.5**		
Full model + (1|Pond)	6	6273.6	-3130.8	16.65	<0.01
To determine the optimal fixed-effect structure:					
F0) Full model + (1+NEE|Pond)	8	6261.0	-3122.5		
F1) F0 – Treatment×NEE	**7**	**6259.4**	**-3122.7**	**0.41**	**0.52**
F2) F1 - Treatment	6	6268.1	-3128.1	10.72	<0.01
F3) F1 - NEE	5	6285.6	-3137.8	19.53	<0.001

2.4.5 Temperature dependence of methane and carbon dioxide emissions and rates of methane and carbon dioxide emissions at 15 °C

Rates of CH_4 and CO_2 emissions were strongly related to temperature while plotting the natural logarithm of the rates of CH_4 and CO_2 emissions against the standardized temperature $\left(\frac{1}{kT_C} - \frac{1}{kT_{ij}}\right)$ (Figure 2.13 a and b). The apparent activation energy of CH_4 emission, described by the slope of the relationship, was 0.84 eV (95% confidence interval: 0.53~1.16 eV), undistinguishable between the warmed ponds and their ambient controls (likelihood ratio test, χ^2=0.08, P=0.78). And the apparent activation energy of CO_2 emission was 0.86 eV (95% confidence interval: 0.74~1.00 eV), undistinguishable between the warmed and ambient ponds, too (likelihood ratio test, χ^2=0.095, P=0.75).

Despite the consistent temperature dependence of CH_4 emission, after 11 years of warming, there was a clear separation on the intercept while plotting the natural logarithm of rates of CH_4 emissions against standardized temperature $\left(\frac{1}{kT_C} - \frac{1}{kT_{ij}}\right)$, suggesting that the CH_4 emission rates at 15 °C (here 0 for standardized temperature) has been increased by warming (Figure 2.13 a). The CH_4 emission rates at 15 °C have been enhanced by 2-fold from 215 μmol $m^{-2}d^{-1}$ from the ambient ponds to 433 μmol $m^{-2}d^{-1}$ from the warmed ponds (likelihood ratio test, χ^2=5.53, P<0.05). The 2-fold greater CH_4 emission capacity was estimated at the fixed 15 °C (0 for standardized temperature) and was thus lower than the 2.41-fold greater annual CH_4 emissions, calculated by the exponential of the median natural logarithm of CH_4 emissions at *in situ* temperature (Figure 2.11).

In contrast to the increased rates of CH_4 emissions from the long-term warmed ponds, the CO_2 emissions at 15 °C from the warmed ponds was 5486 μmol $m^{-2}h^{-1}$, undistinguishable with that from their ambient controls (likelihood ratio test, χ^2=2.85, P=0.09) (Figure 2.13 b).

Accordingly, the mixed-effect model fitted to the CO_2 emission data with one common intercept provided the best fit (Table 2.5).

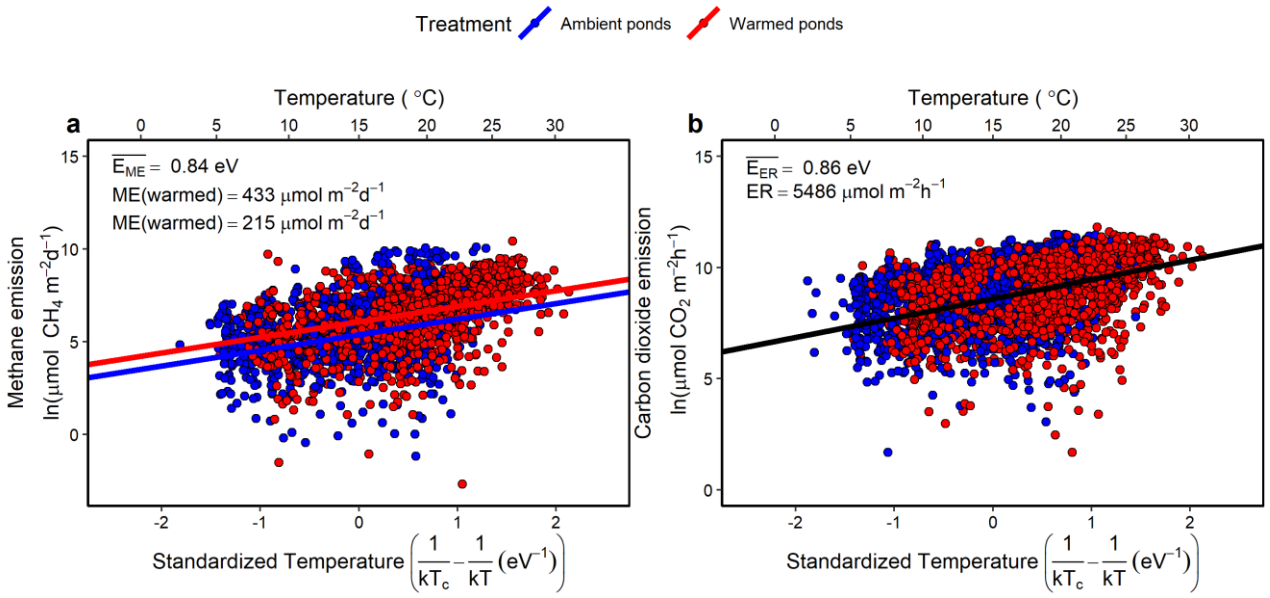

Figure 2.13 Temperature dependence and carbon gases emission capacity. a, The temperature dependence, measured as the apparent activation energy, was the same between the warmed (red) and ambient (blue) ponds at 0.84 eV (likelihood ratio test, χ^2=0.08, P=0.78). But long-term warming has increased the CH_4 emission capacity, average rate of CH_4 emission at 15ºC (here 0 for standardized temperature), by 2-fold, from 215 μmol m^{-2} d^{-1} to 433 μmol m^{-2} d^{-1} (likelihood ratio test, χ^2=5.53, P<0.05). **b**, The temperature dependence of CO_2 emission was the same between the warmed and ambient ponds with an apparent activation energy at 0.86 eV (likelihood ratio test, χ^2=0.08, P=0.78). In contrast to CH_4 emissions, the CO_2 emission capacity, i.e., average rate of CO_2 emission at 15 °C, stayed the same in the warmed and ambient ponds (likelihood ratio test, χ^2=2.85, P=0.09).

Table 2.5 Model selection procedures for fitting linear mixed-effect model to the temperature dependence of CH_4 and CO_2 emission data. The full model included the interactions for 2 fixed effects – standardized temperature (Ts, term $(\frac{1}{kT_C} - \frac{1}{kT_{ij}})$ in equation (2.9) and (2.10)) and treatment types (i.e., ambient or warmed). The random effects were first included on both the intercept and slope to account for the variance across the experimental ponds and sampling months. The nested random intercept and slope model had the lowest AIC and was, therefore, the preferred option. This optimal random-effect structure was then applied to the full model. The significance of *P*-value for the fixed-effect terms were determined via likelihood ratio test on nested models (denoted by subtraction symbols below). The model that best fit to the CH_4 emission is marked in bold, i.e., F1 which included single slope but separate intercepts between the warmed and ambient ponds, demonstrating that long-term warming increased the CH_4 emission at standardized 15 °C but the temperature sensitivity of CH_4 emission stayed conserved. In contrast, the model that best fit to CO_2 emission, also marked in bold, is the model included single slope and single intercept, demonstrating that the apparent activation energy and the rate of CO_2 emission at 15 °C were indistinguishable from the warmed ponds to their ambient controls.

Methane emission (*n*=2771):

Model	**d.f.**	**AIC**	**LogLik**	**χ^2**	***P*-value**
To determine the optimal random-effect structure:					
Full model + (1+Ts|Pond/Month)	**11**	**8206.0**	**-4092.0**		
Full model + (1|Pond/Month)	7	8232.3	-4109.1	34.27	<0.001
To determine the optimal fixed-effect structure:					
F0) Full model + (1+Ts|Pond/Month)	11	8206.0.8	-4092.0		
F1) F0 – Treatment×Ts	**10**	**8204.1**	**-4092.0**	**0.08**	**0.78**
F2) F1 - Treatment	9	8207.6	-4094.8	5.53	<0.05
F3) F1 - Ts	9	8218.5	-4100.8	16.40	<0.001

Carbon dioxide emission (*n*=3200):

Model	d.f.	AIC	LogLik	χ^2	*P*-value
To determine the optimal random-effect structure:					
Full model + (1+Ts|Pond/Month)	**11**	**10799**	**-5388.5**		
Full model + (1|Pond/Month)	7	10820	-5403.2	29.37	<0.001
To determine the optimal fixed-effect structure:					
F0) Full model + (1+Ts|Pond/Month)	11	10799	-5388.5		
F1) F0 – Treatment×Ts	10	10797	-5388.5	0.008	0.78
F2) F1 - Treatment	**9**	**10798**	**-5389.9**	**2.85**	**0.09**
F3) F1 - Ts	9	10832	-5407.3	37.50	<0.001

2.4.6 Meta-analysis of global data on CH_4 and CO_2 emission at 15 °C

Further, I performed a meta-analysis of global CH_4 and CO_2 emission to investigate if the different responses to warming between CH_4 and CO_2 observed in the mesocosm ponds - CH_4 emission capacity increased continuously under warming but CO_2 emission capacity stayed unchanged - would predict ecosystem-level carbon gases emission along a natural temperature gradient. To make the carbon gas emission comparable between mesocosm ponds and natural ecosystems, the global CH_4 and CO_2 emission were also standardized to 15 °C.

The relationships between the natural-logarithm-transformed carbon gas emission capacity against average annual temperature were different between CH_4 and CO_2 (Figure 2.14 a and b). Methane emission capacity correlated positively to average annual temperature for each site (slope=0.13, *t*-test, $P<0.01$), suggesting that naturally warmer ecosystems have a disproportionately higher capacity to emit CH_4. Plotting the CH_4 emission capacity against the average temperature for the warmed (15 °C) and ambient ponds (19 °C), respectively, onto

the global data, demonstrated that the patterns seen in the mesocosm ponds and natural ecosystems agreed well with each other (Figure 2.14 a). In contrast to CH_4 emission capacity, CO_2 emission capacity was indistinguishable between the warmed ponds and their ambient controls. In line with the mesocosm ponds, CO_2 emission capacity was conserved along the natural temperature gradient (*t*-test, P=0.81) (Figure 2.14 b).

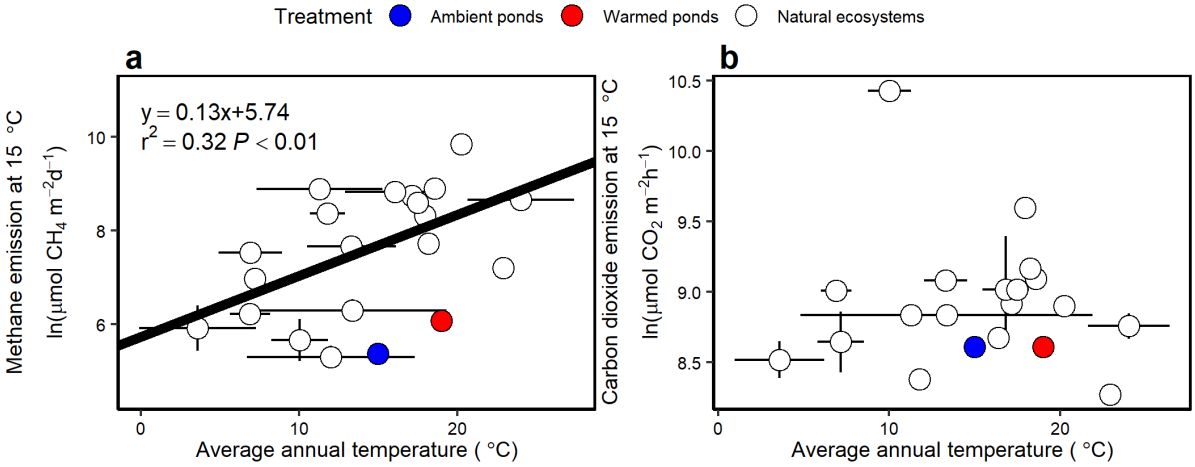

Figure 2.14 Correlations of average annual temperature with carbon gases emissions at 15 °C for globally distributed ecosystems (*n*=19). a, Average annual site temperature is positively correlated with CH_4 emissions at 15 °C (P<0.01). The blue and red symbols mark the average CH_4 emission at 15 °C from the experimental ponds against their average annual temperatures. After 11 years of warming, the CH_4 emission at 15 °C has increased by 2 fold, agreeing with the relationship between global CH_4 emissions and average annual temperatures. **b,** CO_2 emissions at 15 °C is conserved across globally distributed ecosystems (P=0.81), in line with the indistinguishable CO_2 emissions at 15 °C from the long-term warmed ponds (red) and their ambient controls (blue).

2.4.7 Ratio of CH_4 to CO_2 emission

As CO_2 fluxes followed a regular diel pattern of emission during the night and uptake during the day (Figure 2.4), the night-time CH_4 and CO_2 fluxes were used to compare the ratio of CH_4 to CO_2 emission between the warmed and ambient ponds. Long-term warming has increased the CH_4 to CO_2 emission ratio by 1.8-fold as the CH_4 to CO_2 emission ratio was

0.0036 and 0.0021 in the warmed and ambient ponds, respectively (Figure 2.15 a). The higher CH_4 to CO_2 emission ratio leads to a higher net carbon greenhouse gas emission in terms of CO_2 equivalents (CO_{2eq}) by 3 %, 11 % and 15 % for immediate emission, 20-year and 100-year horizon, respectively (Figure 2.15 b). (Balcombe *et al.*, 2018).

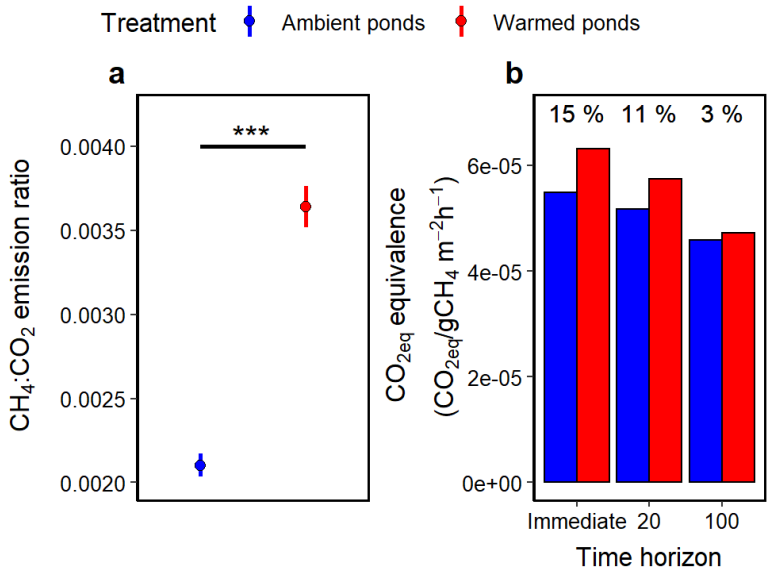

Figure 2.15 Long-term warming increased the ratio of CH_4 to CO_2 emitted. a, The ratio of CH_4 to CO_2 emitted from the warmed ponds was 1.8-fold higher compared to their ambient controls in 2017. **b,** The higher ratio of CH_4 to CO_2 emitted increased the net carbon greenhouse gas emission from the warmed ponds (gCO_{2eq}) by 15 %, 11 % and 3 % for immediate emission, 20-year and 100-year horizon, respectively (Balcombe *et al.*, 2018).

2.5 Discussion

Mesocosm experiments are a useful tool for understanding ecological processes and mechanisms under climate change at ecosystem level (Benton *et al.*, 2007; Stewart *et al.*, 2013). One major difference between mesocosm ponds and natural ecosystems is that the mesocosm ponds were embedded within watershed and therefore received little terrestrially-derived organic carbon (Yvon-Durocher *et al.*, 2017). The carbon cycle in the mesocosm ponds is driven by autochthonous production which may, over the long term, change the

sediment characteristics and the CH_4 emission compared with natural ecosystems. To assess the relevance of mesocosm ponds to natural ecosystems, I first measured the sediment characteristics and CH_4 emissions.

The sediment characteristics, including organic carbon, organic nitrogen, C to N ratio and $\delta^{13}C$ are similar to the sediments in boreal lakes (Santoro *et al.*, 2013). The mesocosm ponds have a surface area of 2.5 m^2, falling within the smallest category of natural ponds in the world. The CH_4 concentrations were 1.07 and 0.51 μmol L^{-1} in the warmed and ambient ponds, respectively, undistinguishable from the CH_4 concentrations in the natural ponds of similar surface areas (Holgerson and Raymond, 2016). In addition, the rates of CH_4 emissions were 1.02 and 2.46 g C $m^{-2}yr^{-1}$ from the warmed and ambient mesocosm ponds, respectively, comparable to the median CH_4 emissions measured in subarctic, boreal and temperate lakes (~3 g C $m^{-2}yr^{-1}$) (Huttunen *et al.*, 2003; Bastviken *et al.*, 2004). These evidences demonstrate that the mesocosm experiment is of direct relevance for understanding carbon cycle in freshwaters under warming at a global scale.

The CO_2 exchange measured in the chambers is the net exchange of CO_2, which provides a direct estimate of the ecosystem balance between photosynthesis and respiration (Whiting *et al.*, 1991; Valentini *et al.*, 2000). The carbon cycle in the mesocosm ponds is driven by autochthonous production (Yvon-Durocher, Montoya, Woodward, *et al.*, 2011; Yvon-Durocher *et al.*, 2017). Indeed, the mesocosm ponds were a sink for CO_2 as the annual net rates of CO_2 exchange were negative for both the warmed and ambient ponds. In the meantime, the net CO_2 exchange in the warmed ponds (-118 g C $m^{-2}yr^{-1}$) was slightly higher than their ambient controls (-107 g C $m^{-2}yr^{-1}$), suggesting that warmed pond fixed more carbon than the ambient ponds. Warming increased slightly the CO_2 absorption, the warmed pond emitted now, after 11 years of warming, disproportionately more CH_4 than their ambient

ponds. The annual CH_4 emission from the warmed pond was 2.46 g C $m^{-2}yr^{-1}$, has been amplified by 2.4-fold relative to the emission from their ambient controls for 1.02 g C $m^{-2}yr^{-1}$. Given the net CO_2 exchange and annual CH_4 emission, 0.95 % of the fixed CO_2 would be emitted as CH_4 in the ambient ponds but in the warmed ponds, 2.1 % of the fixed CO_2 would be emitted.

The reported CH_4 to CO_2 uptake ratios in wetlands, including bogs, fens and swamps, generally ranged from 2% to 7% (Aselmann and Crutzen, 1989; Whiting and Chanton, 1993, 2001; Bellisario *et al.*, 1999; Frolking, Roulet and Fuglestvedt, 2006). In the mesocosm ponds after being warmed by 4 °C for 1 year, the average ratio of CH_4 emission to primary production was elevated by 1.2-fold only (Yvon-Durocher, Montoya, Woodward, *et al.*, 2011). Here, I demonstrate that, after 11 years of warming, the ratio of CH_4 emission to net CO_2 exchange has been increased by 2.2-fold, from 0.95 % in the ambient ponds to 2.1 % in the warmed ponds, suggesting that warming can continuously amplify the fraction of fixed CO_2 emitted as CH_4.

Mesocosm ponds cause negative radiative forcing by absorbing CO_2 and positive radiative forcing by emitting CH_4 (Frolking, Roulet and Fuglestvedt, 2006; Helbig *et al.*, 2017). A larger proportion of fixed CO_2 being emitted as CH_4 would very probably alter the ecosystem service of mesocosm ponds, i.e., the function of mesocosm ponds would transform from a sink to source of carbon greenhouse gases. To test this hypothesis, the balance between CH_4 emission and CO_2 exchange was characterized using the global warming potential. As CH_4 has a higher radiative efficiency but a shorter lifetime in the atmosphere than CO_2, the global warming potential was calculated after immediate emission, over 20- and 100-year horizons, respectively (Balcombe *et al.*, 2018). After immediate emission, both ambient and warmed ponds could be considered as carbon greenhouse sources because the CH_4 equivalents

of CO_2 emitted exceeded the CO_2 uptake. After only a relative short period -20 years-, the lower proportion of fixed carbon emitted as CH_4 (0.95 % compared to 2.1 % in the ambient and warmed ponds, respectively) would allow the ambient ponds to transform from carbon greenhouse gas sources to sinks. In contrast, the warmed ponds, in line with my hypothesis, would stay as carbon greenhouse gas sources as the emitted CH_4 would still exceed the CO_2 uptake. When the long-term climate impacts of carbon greenhouse gas are considered, it is appropriate to extend the integration time to 100 years (28 g CO_{2eq}/gCH_4 for 100-year horizon) (Balcombe *et al.*, 2018). Over 100 years, the warmed ponds turned from greenhouse gas sources to sinks, too, as the radiative forcing of emitted CH_4 would be offset by the CO_2 uptake. Therefore, warming can fundamentally alter the balance between the CH_4 emission and CO_2 exchange, consequently leading to a transform of ecosystem function.

To further characterize the effect of temperature on CH_4 and CO_2 emission, I calculated the temperature dependence as apparent activation energy. The CH_4 emissions from mesocosm ponds were strongly correlated to temperature in both warmed and ambient ponds, yielding an apparent activation energy at 0.84 eV (95% confidence interval: 0.53~1.16). This apparent activation energy is very close to 0.96 eV (95% confidence interval: 0.86~1.07), a well-characterized apparent activation energy yielded in a meta-analysis of 127 studies (Yvon-Durocher *et al.*, 2014). This apparent activation energy was high, indicating a strong positive feedback from CH_4 emission to current warming scenarios. Indeed, 0.84 eV predicts a 1.6-fold increase in the CH_4 emission rate based on the 4 °C of warming (Allen, Gillooly and Brown, 2005). Nevertheless, annual CH_4 emissions are now, after 11 years of warming, 2.4-fold higher from the warmed compared to their ambient controls, exceeding the 1.6-fold predicted based on temperature alone. More strikingly, there has been an ongoing divergence

in CH_4 emissions between the warmed and ambient ponds since the heating started in 2006 (Yvon-Durocher *et al.*, 2010, 2017).

Plotting CH_4 emissions as a function of standardized temperature, there appeared to be a clear separation on the intercept, i.e., CH_4 emission at 15 °C (here 0 for standardized temperature), which refers to an overall capacity of CH_4 emission independent of temperature (Gillooly *et al.*, 2006). The mixed-effect model confirmed a significant 2-fold increase in CH_4 emissions from the warmed ponds at 15 °C relative to their ambient controls at 15 °C. I acknowledge that the 2-fold increase in CH_4 emission capacity is lower than the 2.4-fold increase of annual average CH_4 emission, because the CH_4 emission capacity is represented by CH_4 emission standardized to the same temperature, here at 15 °C, rather than the median daily CH_4 emissions for annual average CH_4 emission. Therefore, the long-term warmed ponds emit more CH_4 than their ambient ponds not simply because of a strong temperature dependence and higher temperatures but also a higher CH_4 emission capacity which cannot be predicted by temperature alone. In contrast to CH_4, the CO_2 emission seemed to be predicted by temperature as increasing physiologically as function of temperature and the emission capacity at 15 °C staying the same.

To test whether the prediction by mesocosm ponds applies to natural ecosystems, I further performed a meta-analysis of CH_4 and CO_2 emissions from 19 globally distributed sites. In line with the mesocosm ponds predict – warming can continuously amplify the CH_4 emission capacity while the CO_2 emission capacity would stay unchanged, the CH_4 emission capacity was positively correlated with average annual temperature but the CO_2 emission capacity was, nevertheless, the same. More importantly, plotting the CH_4 and CO_2 emission capacity against the average annual temperature in ponds onto the global emissions agreed

well with each other, confirming again that, the mesocosm ponds are useful tools to understand and predict the carbon cycle at ecosystem level under warming.

The overall capacity of gas emission standardized to the fixed temperature is expected to vary among taxa, abundance and environmental conditions including substrate availability (Gillooly *et al.*, 2006). The observed 2-fold increase in the overall capacity of CH_4 emission therefore strongly suggest that the fundamental control mechanism of temperature on CH_4 emissions between the warmed and ambient ponds has altered. For CO_2, in contrast, the unchanged CO_2 emission capacity under warming suggests functional redundancy of ecosystem respiration (Louca *et al.*, 2018). Moreover, the production of CH_4 and CO_2 in freshwater ecosystem is not isolated as the two major methanogenic pathways produce CH_4 and CO_2 at different ratios: acetoclastic methanogenesis produces 50% CH_4 and 50% CO_2 while hydrogenotrophic methanogenesis produces 100% CH_4 (Liu and Whitman, 2008). Potential shifts in methanogenic pathways (relative contribution of acetoclastic and hydrogenotrophic methanogenesis) or methanogen community properties (methanogen abundance or composition) can therefore also contribute to the distinct responses between CH_4 and CO_2 emission to warming (Singh *et al.*, 2010).

The distinct responses to warming predicts a substantial increase in the ratio of CH_4 to CO_2 emission if the Earth continues to warm. The ratio of CH_4 to CO_2 emitted from the warmed pond has been increased by 1.8-fold, increasing the global warming potential of the carbon-gases emitted by 11 % for a 20-year horizon. The increase in the very ratio of CH_4 to CO_2 emission is very important because the concentrations of CH_4 and CO_2 in the atmosphere appear to contribute significantly to global temperature changes (Petit *et al.*, 1999). Current atmospheric concentrations of CH_4 and CO_2 are 403 ppm and 1.86 ppm, respectively (Data from https://www.esrl.noaa.gov/gmd/ccgg/trends/ and

https://www.esrl.noaa.gov/gmd/ccgg/trends_ch4/, for CO_2 and CH_4 concentrations, respectively), equivalent to a ratio of 0.0046 to 1. The ratio of CH_4 to CO_2 atmospheric concentration is very similar to the emission ratio from the ambient ponds, but, in contrast, the CH_4:CO_2 emission ratio from the warmed ponds is almost twice as high as the CH_4:CO_2 ratio in the atmosphere. Given that CH_4 is a more potent greenhouse gas than CO_2, warmer freshwater ecosystems would therefore act to increase the global warming potential by emitting disproportionately high CH_4 relative to CO_2 emissions.

2.6 Conclusion

Here the results demonstrate that long-term warming has continuously enhanced the CH_4 emission to a greater magnitude, far in excess of that predicted by 4ºC higher temperatures alone. After 11 years of warming by 4°C, the CH_4 emission rates in the warmed ponds are now 2.4-fold greater than their ambient controls. The substantial increase in CH_4 emission altered the carbon greenhouse gas balance as a greater proportion of fixed CO_2 was emitted as CH_4 in the long-term warmed ponds relative to their ambient controls. More importantly, there was a distinct response of carbon greenhouse gas emission between CH_4 and CO_2 to warming - the CH_4 emission standardized to 15°C representing the CH_4 emission capacity has been enhanced while the CO_2 emission capacity stayed unchanged. Exactly as the mesocosm ponds predicted, a meta-analysis of global CH_4 and CO_2 revealed a positive correlation of the CH_4 emission capacity against average annual temperature at each site but the same CO_2 emission capacity across natural temperature gradient. Ultimately, the distinct responses between CH_4 and CO_2 emission lead to a greater net carbon greenhouse gas emitted to atmosphere. These apparent emergent properties in the freshwater carbon cycle suggest that, as the Earth warms, freshwater will emit increasing more CH_4 in excess of that predicted by

warmer temperatures alone and ultimately breaks the carbon greenhouse carbon balance, serving as a positive feedback that enhances warming in the future.

Chapter 3 Long-term warming enhanced methanogenesis and altered the methanogen community composition

3.1 Abstract

Methanogenesis is very sensitive to temperature and expected to increase exponentially with warming (Duc, Crill and Bastviken, 2010; Gudasz *et al.*, 2010; Marotta *et al.*, 2014). Methanogens drive methanogenesis and their community compositions can change over time due to environmental perturbations (Fey and Conrad, 2000; Høj, Olsen and Torsvik, 2008). Understanding how methanogenesis will respond to the expected increase in mean global temperature and how changes in methanogen community compositions regulate CH_4 production, especially in the long-term (> 10 years), is therefore fundamental to predicting CH_4 cycle feedbacks. Here I show, using a freshwater pond experiment, that long-term warming (+4 °C) significantly enhanced the CH_4 production capacity, which was driven by an amplification of the methanogen abundance and their CH_4 production efficiency. Hydrogenotrophic methanogenesis was more sensitive to warming than acetoclastic methanogenesis, probably due to its higher apparent activation energy (1.40 eV versus 1.08 eV), making it more energetically favorable under warming. Therefore, hydrogenotrophic methanogen community was altered, while, in contrast, the acetoclastic methanogen community remained unchanged. Parallel to the selective alteration of methanogen community, there was a permanent 3-fold increase in the ratio of CH_4 to CO_2 produced in the long-term warmed sediments – an emergent property that suggests warmer freshwaters are more efficient at making CH_4. These findings show that warming can alter methanogen

community structures and drive a shift towards a more hydrogenotrophic-based methanogenesis, ultimately making the CH_4 cycle more efficient at making CH_4.

3.2 Introduction

Most natural CH_4 emissions originate with methanogenic archaea - methanogens, that actively transform simple organic carbon substrates into CH_4 (Thauer *et al.*, 2008; Gudasz *et al.*, 2010; Crawford and Stanley, 2016). Warming increases methanogenesis exponentially (Schulz, Matsuyama and Conrad, 1997; Gudasz *et al.*, 2010; Marotta *et al.*, 2014; Shelley *et al.*, 2015) as methanogenesis is very sensitive to temperature - its temperature sensitivity (activation energy of 0.96 eV) being considerably higher than respiration (0.65 eV) and photosynthesis (0.3 eV) (Allen, Gillooly and Brown, 2005; Yvon-Durocher *et al.*, 2012, 2014) and methanogenesis is, therefore, has a strong potential to cause a positive feedback to climate warming.

In a recent meta-analysis, the average temperature sensitivity of CH_4 emissions, despite of variation among global sites, has been shown to be indistinguishable with that of CH_4 production by pure cultures and anaerobic microbial communities (Yvon-Durocher *et al.*, 2014). Yet average CH_4 emissions from different wetland, paddy soils or aquatic ecosystems cannot be predicted based on differences in their average temperatures alone (Dinsmore, Billett and Dyson, 2013; Wallin *et al.*, 2014; Yvon-Durocher *et al.*, 2014). This inability to predict ecosystem-level CH_4 emission by temperature alone, implies that changes in methanogenesis in response to climate warming in the long term are more complex than a simple exponential response to temperature.

Methanogens are restricted to a limited number of substrates, converting CO_2 with H_2 (hydrogenotrophic), acetate (acetoclastic) and other methylated substances (methylotrophic,

e.g. methanol, methylamine) into CH_4 (Liu and Whitman, 2008). In freshwaters, acetoclastic and hydrogenotrophic methanogenesis are the most important methanogenic pathways, theoretically accounting for 70 % and 30 % of the total CH_4 production, respectively (Conrad, 1999). Indeed, this percentage is consistent with data from lakes (Kuivila *et al.*, 1989; Winfree *et al.*, 2015) and paddy soils (Rothfuss and Conrad, 1992). As CH_4 is a more potent greenhouse gas than CO_2 (IPCC, 2014), the pathway of CH_4 production is critical to the ratio of carbon gas produced (CH_4:CO_2) as acetoclastic producing 50 % CH_4 and 50% CO_2 ($CH_3COOH \rightarrow CH_4+CO_2$) and hydrogenotrophic producing CH_4 only ($4H_2+CO_2 \rightarrow CH_4+2H_2O$) (Liu and Whitman, 2008; Thauer *et al.*, 2008). Warming has been shown to increase the relative contribution of hydrogenotrophic methanogenesis in lake sediment (Schulz, Matsuyama and Conrad, 1997; Glissmann *et al.*, 2004; Nozhevnikova *et al.*, 2007), paddy soils (Fey and Conrad, 2000; Conrad, Klose and Noll, 2009) and permafrost (Metje and Frenzel, 2007). Yet whether the methanogenic activity will shift towards more hydrogenotrophic in the course of global warming remains unknown.

Understanding how methanogenesis might respond to climate warming is further complicated by the difficulty in linking methanogenic community structure to CH_4 producing processes. Environmental perturbations select specific metabolic functions and generally cause changes in community structures (Louca *et al.*, 2018). The response of methanogen community compositions to temperatures is, however, often contradictory to changes observed in methanogenic pathways. For example, the relative abundance of acetoclastic methanogens (*Methanosaetaceae*) has been shown either to increase or to remain the same with temperature increases (Chin, Lukow and Conrad, 1999; Høj, Olsen and Torsvik, 2008). These experiments, restricted to a relatively short-term response (less than 90 days), might not be able to capture changes in community composition (Bier *et al.*, 2015). Therefore, the

key unanswered questions are: 1, does warming enhance methanogenesis over a long-term scale (for example, > 10 years); 2, does warming alter the relative contribution of methanogenic pathways to total CH_4 production and 3, how does warming shape the methanogen community over time?

To answer these questions, I used the long-term warmed, artificial-pond experiment to investigate the effect of moderate warming, of + 4 °C above ambient temperature since 2006, on the sediment's CH_4 production capacity and methanogen community characteristics. The sediment CH_4 production capacity was quantified using controlled microcosm incubations every month from January, 2016, to December, 2016. Then, experiments with a range of methanogenic substrates were performed to investigate whether increased CH_4 production was associated with specific methanogenic pathways. The methanogen community characteristics, including methanogen abundance, diversity and composition, were analyzed using molecular techniques targeting the critical functional gene (*mcrA*).

3.3 Materials and Methods

3.3.1 Sediment collection and incubation with additional substrates

Sediment cores (typically 6 cm to 10 cm depth) were collected by hand using a small corer (Ø 34 mm, polycarbonate) every month from January, 2016, to December, 2016, (except for July) from three warmed and ambient ponds, selected randomly. The sediments were stored in zip-lock bags and kept cool with freezer blocks for transport back to laboratory (< 4 h) and then kept intact at 4 °C in a dark cold room before further treatment.

Sub-samples (~3 g) of the bottom sediment layers (> 3 cm in depth) from each corer were transferred into 12.5 ml gas-tight vials (Labco Exetainer®) in an anoxic glove box (CV204; Belle Technologies). Sodium acetate (Sigma-Aldrich®, for molecular biology),

hydrogen (H_2, research grade, BOC, Industrial Gases, Guilford, UK), sodium formate (Sigma-Aldrich®, ACS reagent), betaine (perchloric acid titration, Sigma-Aldrich®, ⩾98 % purity) and methanol (Sigma-Aldrich®, anhydrous) were used as additional methanogenic substrates (Liu and Whitman, 2008). Pond water (3.6 ml), after being flushed with oxygen-free nitrogen (N_2, BOC) for 10 minutes, as well as the substrate stock solution (0.4 ml, 100 mM) were added to each vial to create final concentrations of 10 mM for each substrate. The vials were then sealed. For the addition of H_2, 1 ml of the pure H_2 was injected through the septum into each vial using a gas-tight syringe (1 ml, Hamilton) to create an initial concentration in the headspace of about 17 %. A further set of vials were left unamended as controls. All the prepared vials were then placed in temperature-controlled incubators covering from 10 °C to 26 °C in approximately 5 °C increments and incubated for up to 4 days in total (*see* Figure 3.1 for flow chart showing the experimental design).

3.3.2 Quantification of CH_4 production

Methane production was measured every 24 h for 4 days by taking 100 µL of headspace gas from each vial and analysing it in a gas chromatograph fitted with a flame-ionization detector (GC/FID; Agilent Technology UK Ltd., South Queensferry, UK). A stainless-steel column (1.83 m×3.18 mm Ø) packed with Porapak (Q 80/100) was used with an oven temperature of 30 °C. Zero grade N_2 was used as the carrier gas (14 mL min^{-1}) and the FID run with hydrogen and air (7/93 %) (zero grade, BOC, Industrial Gases, Guilford, UK) at a flow rate of 40 and 430 mL min^{-1}, respectively, at 300 °C. Concentrations of CH_4 were calculated from peak areas calibrated against known standards by diluting pure CH_4 (BOC, Industrial Gases, Guilford, UK). The total amount of CH_4 in each vial (headspace and dissolved in the liquid phase) was calculated using Bunsen coefficients (Wiesenburg and Guinasso, 1979).

3.3.3 Quantification of CO_2 production

The total CO_2 production was the sum of the change of CO_2 in the headspace and the dissolved inorganic carbon ($\Sigma DIC = CO_2 + HCO_3^- + CO_3^{2-}$) in the water phase. The production of carbon dioxide in the headspace was quantified together with the production of CH_4 using the same technique (*see* previous section 3.3.2). The dissolved inorganic carbon was quantified at the end of incubation by transferring 3 ml of the supernant in each vial carefully with a syringe into a separate 3 ml gas-tight vial (Labco Exetainer®, Lampeter, UK). One milliliter of water was then forced out by injecting oxygen-free nitrogen. After acidifying with 100 µl hydrochloride acid (HCl, 1M) and shaking vigorously for 30 s, the concentration of CO_2 in the headspace was measured as above. The initial concentration of ΣDIC was measured using original pond water using the same techniques.

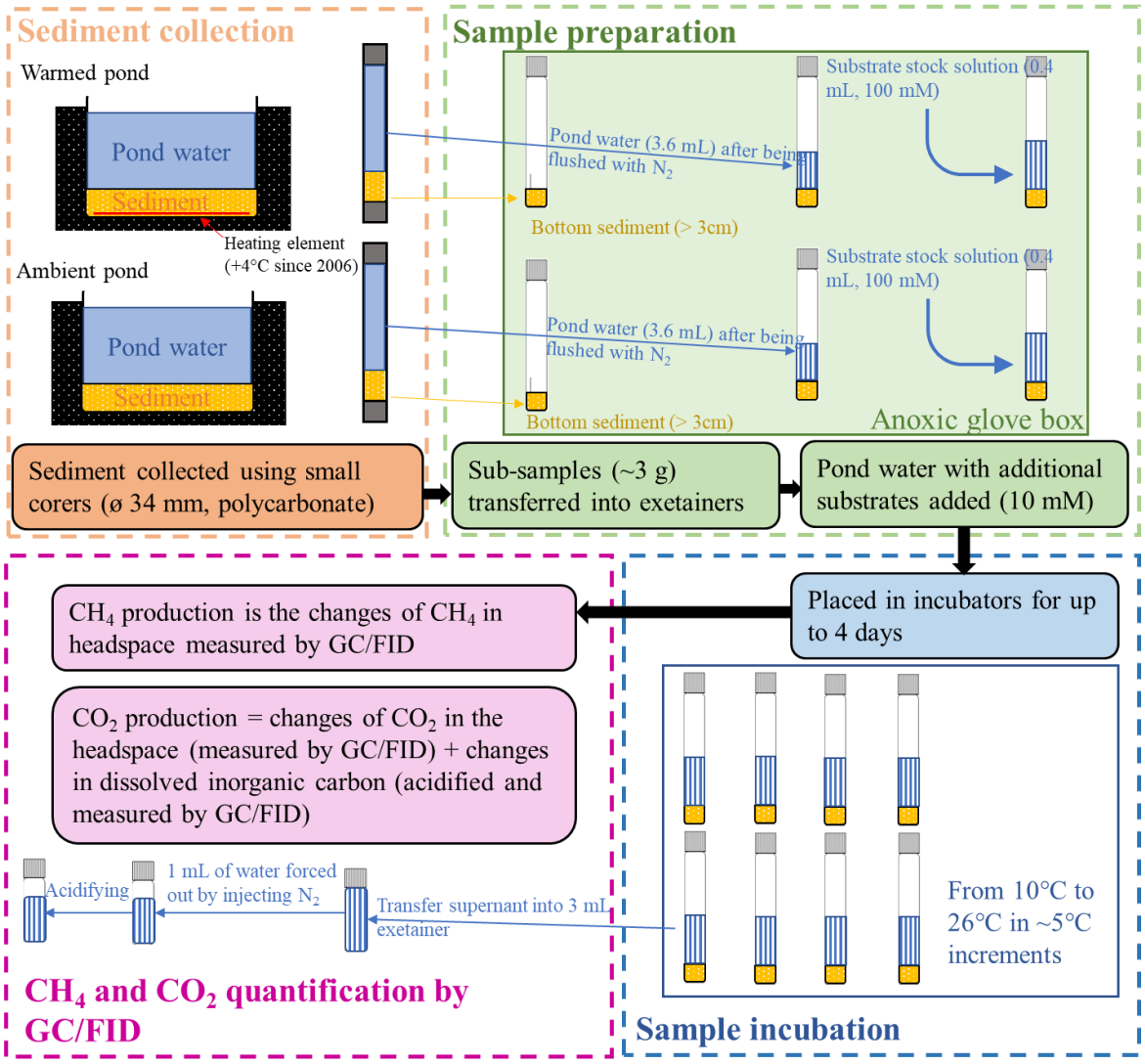

Figure 3.1 Flow chart of the sediment methane production experiment.

3.3.4 Statistical analyses

According to the Boltzmann-Arrhenius equation, the temperature sensitivity and capacity of CH_4 production was estimated using (Yvon-Durocher *et al.*, 2014):

$$lnF_{ij}(T) = \left(\overline{E_{MP}} + a_i + a_j\right)\left(\frac{1}{kT_C} - \frac{1}{kT_{ij}}\right) + \left(\overline{lnF(T_C)} + b_i + b_j\right) + \varepsilon_{ij} \quad (3.1)$$

$$lnG_{ij}(T) = \left(\overline{E_{CP}} + a_i + a_j\right)\left(\frac{1}{kT_C} - \frac{1}{kT_{ij}}\right) + \left(\overline{lnG(T_C)} + b_i + b_j\right) + \varepsilon_{ij} \quad (3.2)$$

Where $lnF_{ij}(T)$ and $lnG_{ij}(T)$ are the natural logarithm of the rate of CH_4 and CO_2 production, respectively, by any sediment sample of mesocosm pond *i* (*i* =1, 2, …), collected in month *j* (*j*=1, 2, …) at absolute temperature *T* (K). The slopes, $\overline{E_{MP}}$epresents the estimated population activation energy, *i.e.*, the temperature sensitivity in units of eV (1eV=96.49 kJ mol^{-1}), for CH_4 production. *k* is the Boltzmann constant (8.62×10^{-6} eV K^{-1}). The plot was standardized using the term $\frac{1}{kT_C}$, in which T_C (288.15 K, i.e., 15 °C) is the average temperature in the ambient ponds in 2017, so that the terms, $\overline{lnF(T_C)}$, corresponds to the average capacity of CH_4 production at T_C. As the experimental design yielded replicate responses in ponds of both treatment over months, sampling month and replicate pond were treated as crossed random effects on the slope ($a_i + a_j$) and on the intercept ($b_i + b_j$) of the models to account for the random variations among months and ponds from the fixed effects. ε_i is the unexplained error with normal distribution N (0, σ^2). The effects of treatment (i.e., ambient or warmed ponds), as well as the effect of additional substrates for CH_4 production, on both the slope (temperature sensitivity) and intercept (average capacity of CH_4 production at T_C) were modelled as fixed effects.

The data were fitted into linear mixed-effect models using the "lmer" function from the lme4 package (version 1.1-12) of R statistical software (version 3.2.5) (R Core Team, 2014; Bates *et al.*, 2015). Model selection was performed by a top-down strategy starting with fitting a full model with all explanatory terms (e.g. treatment and additional substrates) and their possible interactions (Zuur, 2009). First, the significance of random effects on both the slope and intercept were determined by comparing their AICs (Akaike information criterion) to assess whether including the random effects improved the model (Pinheiro and Bates, 2000). Then the optimal random effects revealed in the previous step was applied. The significance

of fixed effects was tested using likelihood ratio test: the terms in the model were dropped sequentially and the significance of the dropped term was determined by comparing the fits of alternative model fitted with and without the term of interest (Zuur, 2009).

The CH_4 production capacity and temperature sensitivity was obtained via the *post-hoc* pairwise comparisons of the estimated marginal means for the pond treatment with different substrates using the "emmeans" function from the "emmeans" package (version 1.1.3).

3.3.5 DNA extraction from pond sediments

Sampling for methanogen community composition analysis and functional gene abundance analysis was conducted every month from March to August in 2016. Cores were collected from 8 warmed and 8 ambient experimental ponds using cut-off 25 mL syringes. The sediments from the depth beneath 2 cm were transferred to a falcon tube. The samples were stored at -80 °C before further extraction.

Extraction of DNA from 0.5 g of the sediment was performed using the DNeasy® PowerSoil® Kit (Qiagen group) according to the manufacturer's instructions. The quantification of DNA was performed with NanoDrop (Thermo ScientificTM) according to the manufacturer's directions. The DNA yield was approximately 1 to 4 $\mu g\ g^{-1}$ of wet sediment.

3.3.6 Polymerase chain reaction (PCR) amplification and sequencing

The *mcrA* gene, which encodes α-subunit of methyl coenzyme M reductase, was used as a molecular marker of methanogenic diversity (Lever and Teske, 2015). The *mcrA* gene was amplified with the primer set mcrIRD (forward: 5'-TWYGACCARATMTGGYT-3'; reverse: 5'-ACRTTCATBGCRTARTT-3') (Lever and Teske, 2015). Amplification was performed in a total volume of 50 μL in 0.2-mL reaction tubes (flat cap, STAR LAB). Each

reaction mixture contained 25 µL of MyTaq™ Red Mix (2×, Bioline), 1.0 µL of forward primer (10 µM), 1.0 of reverse primer (10 µM), 3.0 µL of DNA template and 20.0 µL of water.

The amplifications were performed in a Thermal Cycler (T100™, Bio-Rad) following the thermal program: (1) denaturation at 95 °C for 5 min, (2) 40 cycles of denaturation at 95 °C for 45 s, annealing at 51°C for 45 s and extension at 72 °C for 60 s, (3) extension at 72 °C for 5 min. PCR products (3 µL) were checked by electrophoresis on a fluorescent dye (GelRed® Nucleic Acid Gel Stain) stained 1 % agarose gel.

PCR products were sequenced on the Illumina MiSeq platform (300 bp paired-end, Illumina, Inc, San Diego, CA, USA) at the Genomics Service, University of Warwick (UK). Before sequencing, the PCR products were cleaned using Agencourt® AMPure® XP beads (Beckman Coulter). Barcodes and linkers were added by a 10-cycle PCR (initial denaturation at 95°C for 3 min, 10 cycles of 98°C for 20 sec, 55°C for 15 sec, 72°C for 15 sec, a final elongation step at 72°C for 5 min). Final PCR products were quantified by Qubit dsDNA BR Assay Kit with Qubit 2.0 Fluorometer (Invitrogen, CA, USA), 250 ng of PCR product from each sample was normalised to 4 nmoles (SequalPrep Normalization Plate Kit, Invitrogen, CA, USA) and combined for sequencing.

3.3.7 Processing of sequence data

The downstream sequence analysis was conducted using QIIME2 (version 2018.2.0) (Caporaso *et al.*, 2010) on the Apocrita HPC facility at Queen Mary University of London, supported by QMUL Research-IT (King, Butcher and Zalewski, 2017) (*see* Figure. 3.1 for flow chart of the bioinformatic and analytical components of the project).

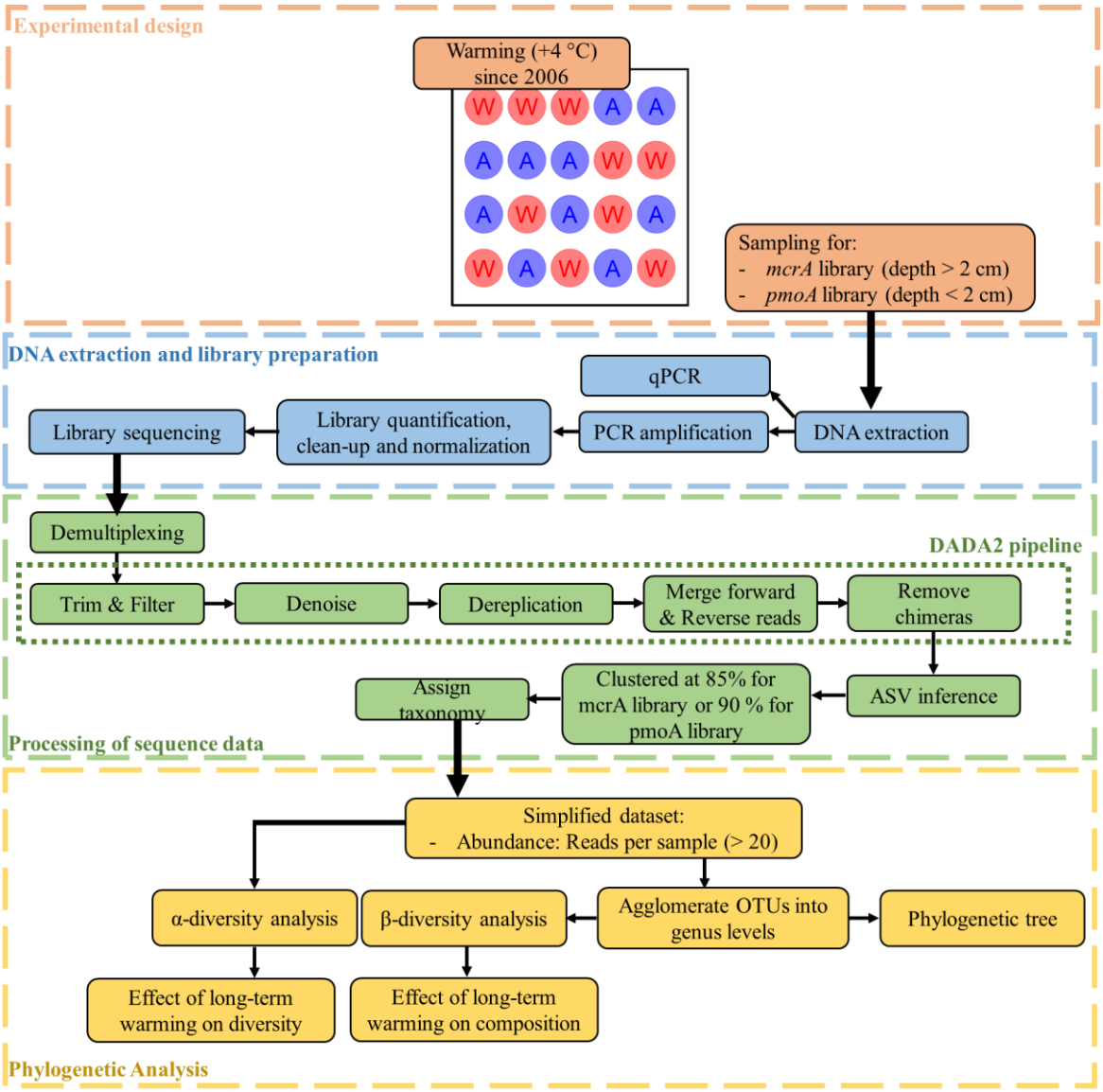

Figure 3.2 Flow chart of the experimental design (orange), DNA extraction and library preparation (blue), processing of sequence data (green) and phylogenetic analysis (yellow) of the microbial community composition analysis and functional gene abundance analysis.

Paired-end demultiplexed files were imported into a QIIME2 artifact and then processed using DADA2 pipeline implemented in q2-dada plugin in QIIME2 for modelling and correcting amplicon errors (Callahan *et al.*, 2016). Primer sequences were trimmed from the paired-end sequences and removed low-quality data with a quality score less than 35 and removed chimeras. Amplicon Sequence Variants (ASVs), which represent exact sequence

variants down to the single-nucleotide level, were then inferred by DADA2 (Callahan, McMurdie and Holmes, 2017). To analyse the sequence data at the genus-level, ASVs were clustered into Operational Taxonomic Units (OTUs) using a 85 % similarity threshold taking into account the nucleotide substitution rate of functional genes (Pester *et al.*, 2004; Oakley *et al.*, 2012).

Table 3.1 Taxonomy assignment to the *mcrA* OTUs at 85 % identity.

	Family	Species	Sequence reads	
			Ambient	Warmed
1	unclustered *Methanomicrobiales*	unclustered *Methanomicrobiales*	227766	225753
2	*Methanocellaceae*	*Methanocella*	149	83
3	*Methanocaldococcaceae*	*Methanocaldococcus*	69	13
4	*Methanomicrobiaceae*	*Methanoplanus*	316	320
5	*Methanothermaceae*	*Methanothermus*	141	161
6	unclustered *Thermoplasmata*	unclustered *Thermoplasmata*	648	271
7	*Methanosarcinaceae*	*Methanohalophilus*	394	1012
8	*Methanospirillaceae*	*Methanospirillum*	256777	184696
9	*Methanosaetaceae*	*Methanosaeta*	257132	287992
10	*Methanomicrobiaceae*	*Methanomicrobium*	174	223
11	*Methanobacteriaceae*	*Methanothermobacter*	0	31
12	*Methanobacteriaceae*	*Methanobacterium*	69265	107752
13	*Methanosarcinaceae*	*Methanosalsum*	0	25
14	*Methanomicrobiaceae*	*Methanoculleus*	0	73
15	*Methanosarcinaceae*	*Methanomethylovorans*	0	320
16	*Methanoplasmatales*	unclustered *Methanoplasmatales*	46	28
17	*Methanosarcinaceae*	unclustered *Methanosarcinaceae*	7285	5071

Taxonomy was assigned to individual OTUs using pre-trained Naïve Bayes classifier implemented feature-classifier plugin in QIIME2 (Table 3.1). The classifier was trained on 85 % *mcrA* OTUs where the sequences have been extracted at the appropriate *mcrA* (mcrIRD) primer sites. To further process sequence data, the package "phyloseq" in R was used (McMurdie and Holmes, 2013). Sample containing sequence reads below the 5000 individual sequences was removed (only one sample from *mcrA* library was removed). The final dataset contained 68 unique OTUs with a total of 1,633,993 high-quality sequences for the *mcrA* library.

3.3.8 Phylogenetic analysis

Variation in richness (α-diversity)

For each sample, the observed OTUs richness, Shannon's diversity index, Chao1 index and evenness were measured. The differences between treatments were determined using mixed effect models treating each experimental pond as a random effect. Likelihood ratio test (LRT) was used to compare full and reduced models to test the significance of long-term warming on α-diversity.

Variation in community composition (β-diversity)

Principal Coordinate Analysis (PCoA) was performed using Bray-Curtis dissimilarity index to visualize the dissimilarity in community composition between treatments. The dissimilarity index was generated using Hellinger standardized datasets agglomerated at the genus level (Oksanen *et al.*, 2018). To quantify the effect of long-term warming on community composition, the scores of samples along the PCoA axis with the two largest eigenvalues (together capturing above 50 % of the variation) were fitted into mixed-effect models using "lmer" function from lmerTest package (version 2.0-36) (Kuznetsova, Brockhoff and Christensen, 2017), fitting experimental pond and sample-collection month as nested random

effects. The significance of treatment on scores were determined based on *F*-tests and *P*-values generated using "anova" function from lmerTest package which applied Satterthwaite's method for denominators degrees-of-freedom and F-statistic.

Permutational Multivariate Analysis of Variance (PERMANOVA) is a geometric partitioning of multivariate variance in response to factors (Anderson, 2017). Here the "adonis" function from the vegan package (version 2.4-6) (Oksanen *et al.*, 2018) which partitions variation in the distance matrix between the warmed and ambient ponds was performed using a permutation test with pseudo-*F* ratios. The results from PCoA and PERMANOVA were similar to each other.

Differences in taxonomic abundance

The R package DESeq2 (version 1.18.1) which uses negative binomial generalized linear models was used to obtain maximum likelihood estimates to investigate the changes in taxonomic abundance between treatments (i.e., warmed or ambient ponds) (Love, Huber and Anders, 2014). The DESeq2 package was designed specifically for RNA-seq data but has been proposed for analysing microbiome data (McMurdie and Holmes, 2014). I appreciate that DESeq2 tends toward a higher false discovery rate with uneven library sizes; our *mcrA* library, however, exhibited even sizes between the warmed and ambient ponds at the genus level (Table 3.1). Changes in taxonomic abundance between treatments was determined at genus level by controlling the false discovery rate at 0.01.

3.3.9 PCR cloning

The *mcrA* PCR products were ligated into a linear plasmid vector of pCR™2.1 vector, provided in the TA Cloning kit (TA Cloning™ Kit, with pCR™2.1 Vector and One Shot™ TOP10 Chemically Competent *E. coli*, Invitrogen), and then cloned into One Shot® cells

using chemical transformation. The white colonies were randomly picked using X-Gal (solution, ready-to-use, Thermo Scientific) medium containing ampicillin (100 µg ml^{-1}). The DNA plasmid was extracted using a GeneJET Plasmid Miniprep Kit following the manufacturer's instructions (Thermo Scientific) and sent for sequencing by TubeSeq Service provided by Eurofins Genomics Ltd. The identities of the *mcrA* gene sequences were confirmed by searching the international sequence databases using the BLAST programs (https://blast.ncbi.nlm.nih.gov/Blast.cgi). Plasmid DNA containing the *mcrA* gene inserts were used for standard curves in qPCR analysis (*see* the following section 3.3.9).

3.3.10 Quantitative polymerase chain reaction (qPCR)

Total methanogen abundance of each individual sample (each pond for every month) was estimated by measuring the copy numbers of *mcrA* gene, which often present as a single-copy gene on chromosome (Narihiro and Sekiguchi, 2015). The *mcrA* primer set mcrIRD (forward: 5'-TWYGACCARATMTGGYT-3'; reverse: 5'-ACRTTCATBGCRTARTT-3') was used (Lever and Teske, 2015). Amplifications were done in 384-well plate using CFX384 Touch™ Real-Time PCR Detection System (Bio-Rad). The reactions were carried out in a total volume of 10 µL containing: 5 µL of SsoAdvanced™ Universal SYBR® Green Supermix (2×, Bio-Rad), 0.2 µL of forward primer (10 µM), 0.2 µL of reverse primer (10 µM), 1 µL of DNA template and 3.6 µL of molecular biology quality water. The plasmid DNA of an *mcrA* clone (*see* previous section 3.3.8) were used as standards. The copy numbers of *mcrA* gene per µL for standards were calculated using (McGenity, Timmis and Nogales, 2017):

$$Copies\ numbers\ per\ \mu L = \frac{N_A \times DNA\ plasmid\ concentration}{Bases\ pair\ number\ \times Average\ weight\ of\ a\ single\ base\ pair} \quad (3.2)$$

Where N_A is Avogadro's number (6.02×10^{23} copies mol^{-1}) and average weight of a single base pair is 660 Daltons. The DNA plasmid concentration (g μL^{-1}) was quantified using Qubit™ Fluorometer and Qubit™ dsDNA BR Assay kit by following the manufacturer's guidelines. The bases pair numbers (bp) were provided by TubeSeq Service provided by Eurofins Genomics Ltd (*see* previous section 3.3.8).

Standard curves with 10^1 to 10^7 copies of *mcrA* gene insert per µL were constructed by serial diluting a clone using molecular biology quality water. The qPCR thermal program was as follows: (1) initial denaturation at 98 °C for 3 min; (2) 40 cycles of denaturation at 98 °C for 15 s, annealing at 55°C for 15 s and extension at 72 °C for 60 s; (3) final extension at 72 °C for 10 s. Fluorescent signal was acquired after each cycle at 72 °C. Product specificity and size was confirmed by melt curve analysis after the final extension by increasing the temperature from 62 to 95 °C in 0.5 °C increments every 5 s. Each sample was performed in three replicates.

3.3.11 Cell-specific activities of methanogens

Cell-specific activities were calculated for methanogens by dividing CH_4 production capacity at 15 °C by *mcrA* gene copy abundances in each sample.

3.4 Results

3.4.1 Sediment methane production capacity

Microcosm sediment slurry incubations showed that warmed ponds sediments now produce 2.53-fold more CH_4 than the ambient ponds (*post-hoc* pairwise comparison: $P<0.05$, CH_4 production by unamended control in Figure 3.2), indicating that warming had indeed increased the CH_4 producing capacity of the sediments. I further studied any response of CH_4 production in the sediments with additional substrates (Figure 3.2). The addition of acetate,

hydrogen, methanol and formate stimulated the CH_4 production capacity in the sediments from both ambient and warmed ponds; however, the addition of two hydrogenotrophic substrates, hydrogen and formate, had a significantly greater effect on the CH_4 production in the warmed ponds compared to their ambient controls. The addition of betaine had no effect on the CH_4 production capacity while the addition of propionate even reduced the CH_4 production capacity in the sediments. Consequently, a linear mixed-effect model that included a 'treatment' by 'substrate' interaction on the intercept provided the best fit to the data (Table 3.2), demonstrating that the effects of additional substrates on CH_4 production capacity in the sediment were significant.

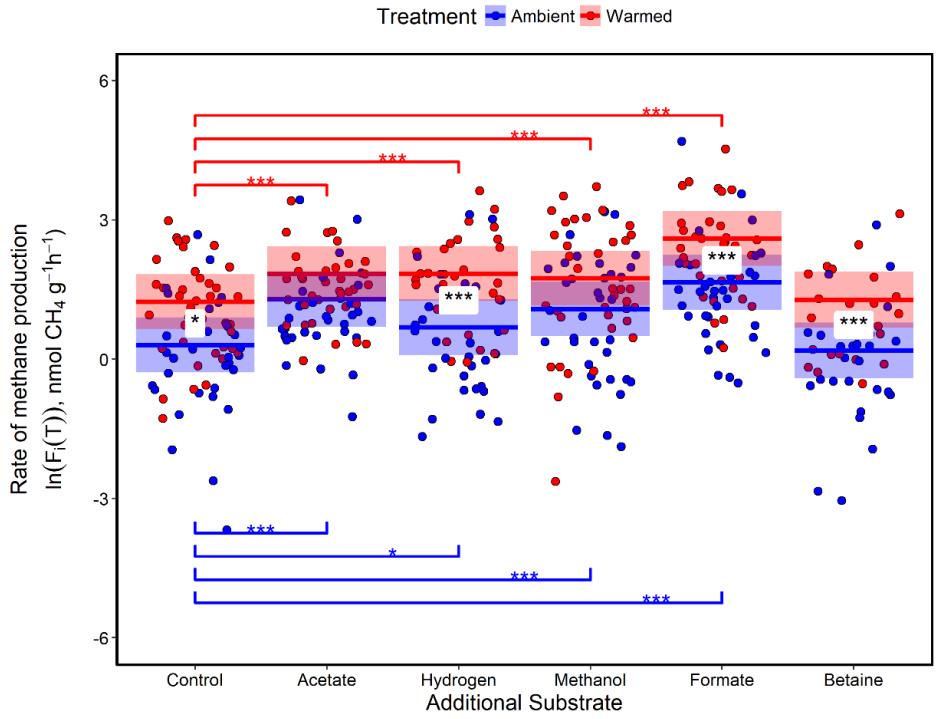

Figure 3.2 Effect of long-term warming on the CH_4 production in sediment. Long-term warming (red) increased the average rates of CH_4 production at 15 °C (centred temperature), with a preferential stimulation by hydrogen and formate, relative to the ambient controls (blue). Shaded areas indicate the 95 % confidence interval. The level of statistical significance compared to the controls (asterisks above or below the data points) and pairwise comparisons between treatments (asterisks between estimation lines) in a *post hoc* pairwise comparison were presented (*: $P<0.05$, ***: $P<0.001$).

3.4.2 The temperature dependence of CH_4 production

I used short-term temperature manipulations to show the temperature dependence of CH_4 production in the sediments. The sediment CH_4 production was slightly less sensitive to temperature in the warmed ponds (Figure 3.3 a). The average apparent activation energy of CH_4 production in the warmed pond sediment was 0.57 eV, slightly lower than that in the ambient pond sediment at 0.78 eV (likelihood ratio test, d.f.=24, χ^2=5.63, P<0.05). The CH_4 production amended with hydrogen had a significantly higher temperature sensitivity (apparent activation energy) than the other methanogenic substrates (*post-hoc* pairwise comparisons: P<0.01, Figure 3.3 b). The apparent activation energy of CH_4 production in the sediment with additional hydrogen was 1.40 eV while the other substrates all had a similar apparent activation energy at ~ 1.0 eV.

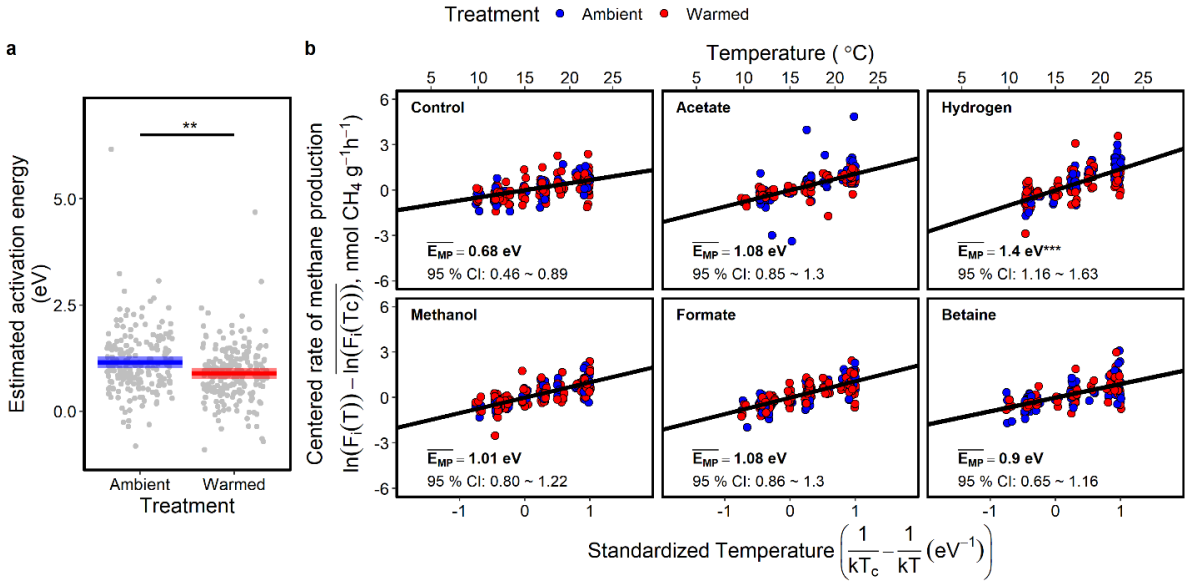

Figure 3.3 Temperature dependence of CH_4 production with additional substrates. a, Estimated population activation energy of CH_4 production for every sample from warmed (red) or ambient (blue) pond sediment. **b,** Estimates of temperature dependence of CH_4 production with additional substrates. Asterisks indicate the level of statistical significance compared to the controls in a post hoc pairwise comparison (*: P<0.05, **: P<0.01, ***: P<0.001). Note the estimated marginal means (i.e., the means for the substrates averaged between the ambient and warmed treatment effects) of the apparent activation energy were presented here for comparison between additional substrates.

Table 3.2 Model selection procedures for fitting the LMEM to the data for methane production with temperature and additional substrates (n=1508). The full model included additive terms and their interactions for 3 fixed effects – standardized temperature (*Ts*, term $(\frac{1}{kT_C} - \frac{1}{kT_{ij}})$, *see* equation 3.1), treatment types (i.e., ambient or warmed) and additional substrates. The random effects were first included on both the intercept and slope to account for the variance across the experimental ponds and sampling months. The crossed random intercept model had the lowest AIC and was, therefore, the preferred option. The optimal random effect was then applied to the full model. The significant P-value of fixed-effect terms were determined via likelihood ratio test on nested models (denoted by subtraction symbols below). The model F1 included treatment effect on slope and interactive effect between additional substrates and treatment types on intercept provided the best and was marked in bold.

Model	d.f.	AIC	LogLik	χ^2	*P*-value
To determine the optimal random-effect structure:					
Full model + (1+Ts|Pond) + (1+Ts|Month)	35	4343.7	-2136.8		
Full model + (1|Pond) + (1+Ts|Month)	33	4341.0	-2137.5	1.35	0.51
Full model + (1|Pond) + (1|Month)	**31**	**4337.0**	**-2137.0**	**0.016**	**0.99**
To determine the optimal fixed-effect structure:					
F0) Full model + (1|Pond) + (1|Month)	31	4337.0	-2137.5		
F1) F0 – Treatment×Substrate×Ts	**25**	**4328.9**	**-2139.5**	**3.90**	**0.69**
F2) F1 – Treatment×Ts	24	4332.6	-2142.3	5.63	<0.05
F3) F1 - Substrate×Ts	19	4336.4	-2149.2	19.49	<0.01
F4) F1 - Treatment×Substrate	19	4342.5	-2152.2	25.55	<0.01

Above 22 °C, the rates plateaued, and the data were excluded from the model.

3.4.3 Methanogen abundance and cell-specific activity

Methanogen abundance (qPCR of the *mcrA* gene) was 1.50-fold higher in the warmed compared to the ambient ponds (*t*-test, $P<0.05$, Figure 3.4). The cell-specific methanogen activity (CH_4 production at 15 °C per *mcrA* gene copy) was even greater: 0.59 fmol CH_4 copy^{-1} h^{-1} and 0.35 CH_4 copy^{-1} h^{-1} for warmed and ambient ponds respectively, demonstrating that the methanogens in the warmed ponds appeared to be ~ 60 % more efficient at making CH_4 than their ambient counterparts.

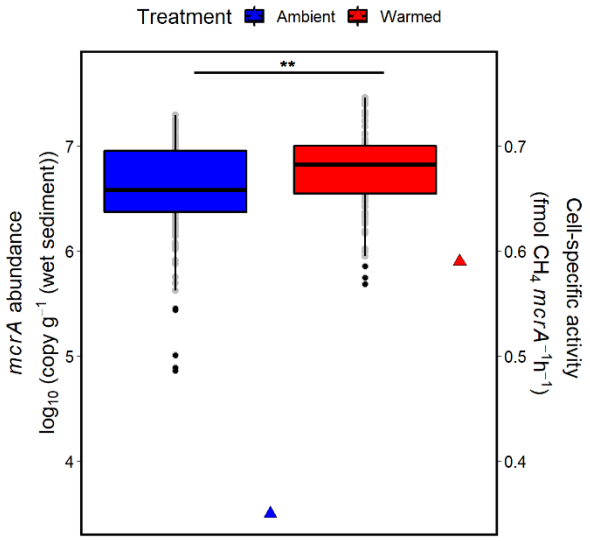

Figure 3.4 Functional gene copy numbers of methanogens (*mcrA*) in the sediments and (bars) their cell-specific activity (triangle). Asterisks indicate the level of statistical significance of a comparison between the warmed (red) and ambient (blue) ponds (**: $P<0.01$).

3.4.4 Methanogen community

α-diversity describes microbial richness and evenness. Here I present the α-diversity of the methanogen community between the warmed and ambient ponds, using the observed OTUs and Chao1, Shannon's diversity, and evenness (calculated as inverse Simpson's diversity/Observed OTUs) (Figure 3.5). The α-diversity of the methanogen community was the same between the warmed and ambient ponds (likelihood ratio test, all *P*-values > 0.05), demonstrating that long-term warming did not change the richness or evenness of the methanogen community in the sediments.

Despite the stable community richness and evenness, β-diversity, i.e., the community composition, had changed after 11 years of warming (PERMANOVA, $P<0.01$, Figure 3.6 a). To further assess the dissimilarity in the methanogen community composition between the warmed and ambient ponds, PCoA analysis was performed, where the distance between any

two points represents the dissimilarity between those two samples (Paliy and Shankar, 2016). I analysed sample scores along a PCoA axis to determine the effect of treatment. The scores of every sample varied significantly between the warmed and ambient pond sediments along PCoA1 axis (F-test, $P<0.05$), which explained 34 % variation of the data. No difference could be detected in the scores between the warmed and ambient ponds along PCoA2 axis, but PCoA2 explained 23% variation of the data only. Therefore, and similar to PERMANOVA result, the methanogen community composition had changed after 11 years of warming.

Further, a community analysis specifically identified a significant shift in two hydrogenotrophic genera between the warmed and ambient ponds (Figure 3.6 b). The relative abundance of the hydrogenotrophic *Methanobacterium* increased significantly from 8.45 % to 13.24 %, whereas, in contrast, the other hydrogenotrophic *Methanospirillum* decreased from 31.31 % to 22.69 % between the warmed and ambient ponds, respectively (adjusted *P*-value < 0.01, Figure 3.6 b). But no changes in any other methanogens, i.e., acetoclastic methanogens, were observed.

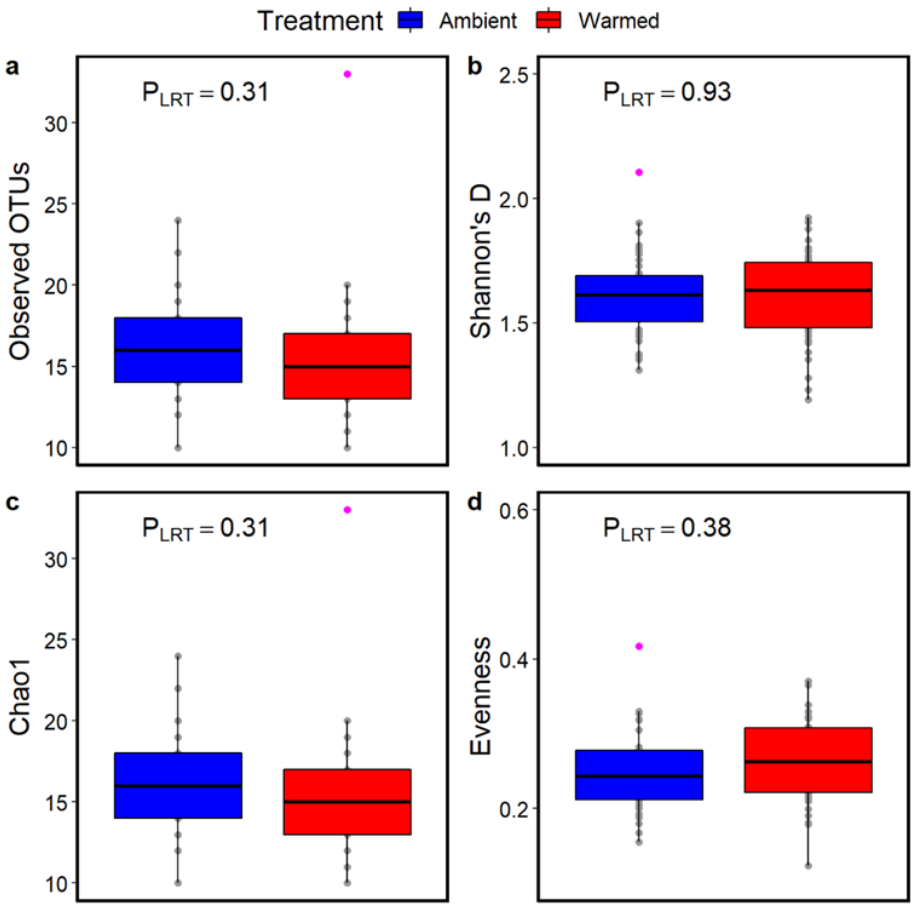

Figure 3.5 Alpha diversity between the warmed and ambient ponds of *mcrA* library sequence reads. Effect of long-term warming on species richness (a), Shannon's diversity (b), Chao1 diversity (c) and evenness (d). Statistical significance (*P*-values) is determined by a likelihood ratio test.

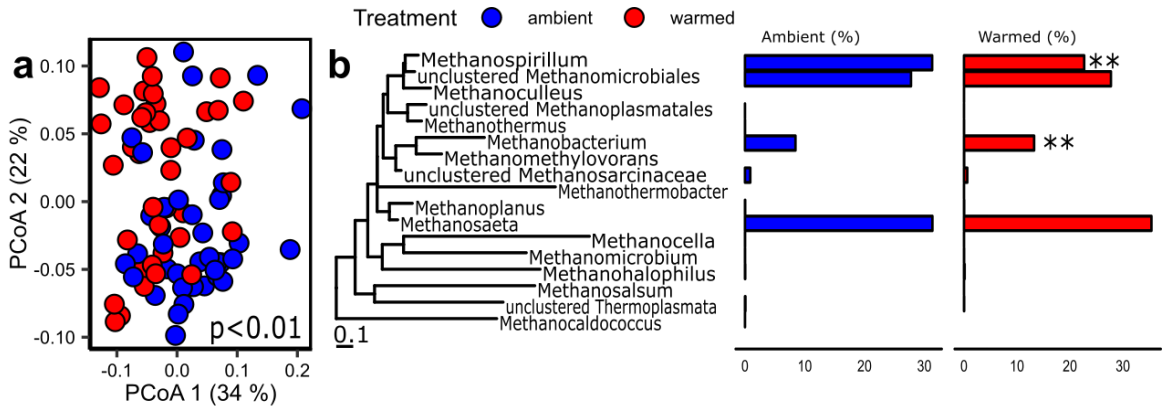

Figure 3.6 Effect of long-term warming on *mcrA* community compositions. Principal coordinate analysis (PCoA), using Bray-Curtis analysis and a Hellinger standardized dataset (agglomerated at genus level), demonstrating a highly significant shift in the methanogen community between ambient (blue) and warmed (red) ponds (**a**). The distance between sample dots represents the dissimilarity in taxonomic compositions. The numbers in brackets represent variation accounted for by the principal coordinate axes. *P*-value from PERMANOVA analysis was reported. Differential abundance analysis at genus level detected significant shifts in the relative abundance of two hydrogenotrophic methanogen genera (*Methanospirillum* and *Methanobacterium*) (**b**). Asterisks indicate the level of statistical significance for a pairwise comparison between ambient and warmed ponds (**: adjusted *P*-value<0.01).

3.4.5 The ratio of CH_4 to CO_2 production in pond sediments

Hydrogenotrophic methanogenesis, being more energetically favourable at higher temperatures, appeared to drive a selective alteration towards a more hydrogenotrophic-based methanogenesis which would result in a higher CH_4 to CO_2 production ratio. To test this hypothesis, the ratio of CH_4 to CO_2 production in the sediments was measured. The ratio of CH_4 to CO_2 production at 15 °C had increased by 3.2-fold, from 0.19 in the ambient ponds to 0.60 in the long-term warmed ponds (Figure 3.7).

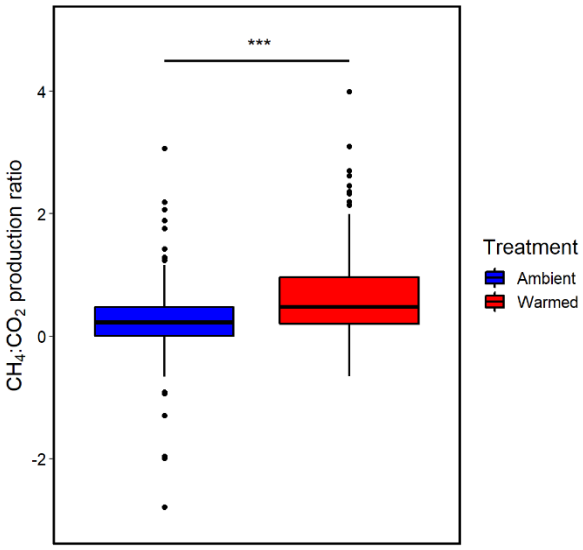

Figure 3.7 The ratio of CH_4 to CO_2 produced by warmed pond sediments (red) is now 3.2-fold higher than for their ambient controls (blue) at 15 °C. Asterisks indicate the level of t-statistic statistical significance of a comparison between the warmed and ambient ponds (***: P<0.001).

3.4.6 The CO_2 production capacity in pond sediments

The increase in CH_4 to CO_2 production ratio depends on changes not only in CH_4 production pathways but also CO_2 productions, such as fermentation. Here I further explored the CO_2 production capacity in the pond sediments. Plotting the natural-logarithm-transformed rates of CO_2 production against the standardized temperature demonstrated that the CO_2 production rates in the pond sediments were positively correlated with standardized temperature but were the same for the warmed ponds and their ambient controls (Figure 3.8). Fitting the CO_2 production rate into mixed-effect models confirmed that the intercept, i.e., the CO_2 production capacity standardized to 15 °C, was statistically undistinguishable between the warmed ponds and their ambient controls (likelihood ratio test, d.f.=1, χ^2=1.10, P=0.29) and produced a CO_2 production capacity at 3.7 nmol CO_2 $g^{-1}h^{-1}$. Consequently, a mixed-effect

model that included common intercept and slope for the warmed and ambient ponds provided the best fit to the CO_2 production data (Table 3.3).

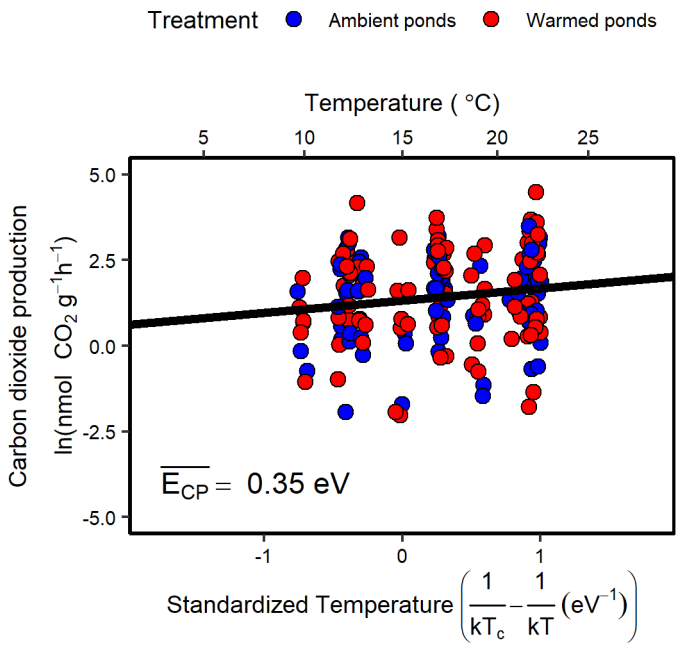

Figure 3.8 Temperature dependence and capacity of CO_2 production in pond sediments. The activation energy of CO_2 production in pond sediments, which is represented by the slope, was 0.35 eV (95% CI:0.10 ~ 0.59), undistinguishable between the warmed and ambient ponds (likelihood ratio test, d.f.=1, χ^2=0.69, P=0.41). The CO_2 production capacity was represented by the CO_2 production rate standardized to 15 °C, i.e., the intercept, was also the same for the warmed and ambient ponds (likelihood ratio test, d.f.=1, χ^2=1.10, P=0.29).

Table 3.3 Model selection procedures for fitting the LMEM to the data for CO_2 production with temperature and additional substrates (n=182). The full model included additive terms and their interactions for 2 fixed effects – standardized temperature (*Ts*, term $(\frac{1}{kT_C} - \frac{1}{kT_{ij}})$, *see* equation 3.2) and treatment types (i.e., ambient or warmed). The random effects were first included on both the intercept and slope to account for the variance across the experimental ponds and sampling months. The crossed random intercept model had the lowest AIC and was, therefore, the preferred option. The optimal random effect was then applied to the full model. The significant *P*-value of fixed-effect terms were determined via likelihood ratio test on nested models (denoted by subtraction symbols below). The model F2 included one common slope and intercept for the warmed and ambient ponds provided the best and was marked in bold.

Model	**d.f.**	**AIC**	**LogLik**	χ^2	***P*-value**
To determine the optimal random-effect structure:					
Full model + (1+Ts|Pond) + (1+Ts|Month)	11	540.0	-258.98		
Full model + (1|Pond) + (1+Ts|Month)	9	538.6	-260.31	2.65	0.27
Full model + (1|Pond) + (1|Month)	**7**	**535.2**	**-260.61**	**0.61**	**0.74**
To determine the optimal fixed-effect structure:					
F0) Full model + (1|Pond) + (1|Month)	7	535.2	-260.61		
F1) F0 – Treatment ×Ts	6	533.9	-260.96	0.69	0.41
F2) F1 – Treatment	**5**	**533.0**	**-261.51**	**1.10**	**0.29**
F3) F2 – Ts	4	538.7	-265.4	7.69	<0.01

Above 22 °C, the rates plateaued, and the data were excluded from the model.

3.5 Discussion

In *Chapter 2*, I demonstrated, using the high-frequency chamber measurements, that 11 years of warming has enhanced the CH_4 emission capacity standardized to 15°C. A meta-analysis of global CH_4 emission revealed a positively correlation of the CH_4 emission capacity against average annual temperature at each site, vindicating the mesocosm pond prediction -

freshwater would emit disproportionately more CH_4 under warming. Indeed, there had been an ongoing divergence in CH_4 emissions between the warmed ponds and their ambient controls - warming now, after 11 years, has increased CH_4 emission by 2.47-fold, far exceeding the predicted 1.70-fold increase due to temperature alone (based on 4 °C offset and an activation energy of 0.96 eV). These findings suggested that the CH_4 cycle has not responded to warming through a simple physiological change, but rather to shifts in the activities and the structures of the methanogen community.

In this Chapter, I show that warming had indeed increased the CH_4 production capacity of the sediments. Warmed sediments now produced 2.53-fold more CH_4 than the ambient controls. Organic carbon fuels methanogenesis in freshwaters (Whiting and Chanton, 1993; Yvon-Durocher *et al.*, 2015). Organic carbon contents have increased by 1.50-fold in the warmed ponds compared to their ambient controls (*see* Figure 2.7, due to enhanced ecosystem development and primary production (Yvon-Durocher *et al.*, 2015). Accordingly, the methanogen abundance increased by 1.50-fold in the warmed sediments compared to their ambient controls. But the 1.50-fold increase in methanogen abundance were not enough to account for the 2.53-fold more CH_4 production in the warmed ponds relative to their ambient controls. Hence, cell specific methanogen activity (CH_4 production per *mcrA* gene measured at 15 °C) was almost 2-fold greater (0.59 fmol CH_4 h^{-1} $copy^{-1}$ compared to 0.35 fmol CH_4 h^{-1} $copy^{-1}$, for warmed and ambient ponds, respectively). Therefore, the warmed methanogens appear to be ~60 % more efficient at making CH_4 than their ambient counterparts and can explain the disproportionate increase in CH_4 emission seen in *Chapter 2*.

The other apparent emergent property seen in *Chapter 2* is that warming has enhanced the ratio of CH_4 to CO_2 emission. Here I further demonstrated that the CH_4 to CO_2 production has been enhanced in the warmed pond sediments relative to their ambient controls. Increases

in CH_4 to CO_2 production depend on changes not only in CH_4 production pathways but also the CO_2 production capacities, for example, fermentation. As the CO_2 production capacity was undistinguishable between the warmed ponds and their ambient controls, these increases in apparent methanogen efficiency and CH_4 to CO_2 ratio would therefore be hard to rationalize without a fundamental change the structure of the methanogen structure. For example, the two most important substrates for methanogenesis are acetate and hydrogen (Conrad, 1999; Liu and Whitman, 2008). Acetoclastic methanogenesis produces 50 % CH_4 and 50 % CO_2 while hydrogenotrophic methanogenesis produces CH_4 only (acetoclastic: $CH_3COOH \rightarrow CH_4+CO_2$; hydrogenotrophic: $4H_2+CO_2 \rightarrow CH_4+2H_2O$) (Liu and Whitman, 2008). The increase in both the methanogen efficiency and CH_4 to CO_2 ratio therefore suggested a shift towards a more hydrogenotrophic based methanogen community. To corroborate this hypothesis, the methanogen community in both warmed and ambient sediments were analysed using molecular techniques (*mcrA* gene which encodes α-subunit of methyl coenzyme M reductase) (Lever and Teske, 2015). Indeed, the community analysis confirmed changes in the relative abundances of two hydrogenotrophic genera (*Methanobacterium* and *Methanospirillum*) but no change was detected in acetoclastic genera. The relative abundance of hydrogenotrophic genus *Methanobacterium* increased, while the other hydrogenotrophic genus *Methanospirillum* decreased. After 11 years of warming, the diversity of methanogen was conserved as its richness and evenness remained unchanged, but the marginal changes in the relative abundance of two hydrogenotrophic genera appeared to have increased the contribution from hydrogenotrophic methanogenesis to CH_4 production, leading to an increasing ratio of CH_4 to CO_2 emitted.

Sediment incubation experiments with methanogenic substrates were performed to investigate a mechanism for changes in the methanogen community. There was a preferential

stimulation of the CH_4 production by hydrogen in the warmed compared to the ambient controls and the hydrogenotrophic methanogenesis showed a significantly higher temperature sensitivity (1.40 eV compared to 1.08 eV for acetoclastic methanogenesis). Therefore, warming makes hydrogenotrophic methanogenesis more energetically favourable, providing a mechanism to drive the shift towards a more hydrogenotrophic methanogenesis.

Short-term (< 3 months) experiments in lake sediment (Schulz, Matsuyama and Conrad, 1997; Glissmann *et al.*, 2004; Nozhevnikova *et al.*, 2007), paddy soils (Fey and Conrad, 2000; Conrad, Klose and Noll, 2009) and permafrost (Metje and Frenzel, 2007) have shown that the relative contribution of hydrogenotrophic methanogenesis decreased at lower temperatures primarily due to competition with homoacetoclastic bacteria for hydrogen and/or relatively low *in situ* hydrogen concentrations (Conrad *et al.*, 1989; Schulz, 1996; Nozhevnikova *et al.*, 1997; Fey and Conrad, 2000; Kotsyurbenko, 2005). Here I demonstrate for the first time that long-term warming of 4°C favours hydrogenotrophic over acetoclastic methanogenesis, permanently altering the methanogen community composition and increasing the ratio of produced and emitted CH_4 to CO_2.

Microorganisms can grow rapidly under favourable conditions, compared to plants and animals, leading to varying community compositions (Prosser *et al.*, 2007). In contrast to changes towards hydrogenotrophic methanogenic pathway at higher temperatures, changes in methanogen community composition reported in previous studies are ambiguous and contradictory. For example, the relative abundance of the acetoclastic methanogen *Methanosaetaceae* has been shown to decrease with higher temperature in the paddy soils, in line with the higher contribution from hydrogenotrophic methanogenesis to the total CH_4 production (Chin, Lukow and Conrad, 1999). But in contrast, *Methanosaetaceae* was also reported to be increasing at higher temperatures, replacing the high-acetate-requiring

Methanosarcinaceae (Fey and Conrad, 2000; Høj, Olsen and Torsvik, 2008). These contradictory findings for linking methanogen community changes to warming make it difficult to predict the response of methanogenesis under current warming scenarios.

One main factor to take into account while linking microbial community composition to physiological processes - under any environmental perturbation - is the time scale (Bier *et al.*, 2015). Previous studies have been limited to relatively short-term responses to changes in temperature (< 3 months); however, our long-term mesocosm experiment shows, for the first time, that 11 years of warming of 4 °C appears to serve as a selective pressure for hydrogenotrophic methanogens. At higher temperatures, hydrogenotrophic methanogenesis is more energetically favourable (apparent activation energy of 1.4 eV compared to 1.08 eV and 1.01 eV for acetoclastic and methylated methanogenesis, respectively), driving changes in two hydrogenotrophic methanogen genera (*Methanospirillum* and *Methanobacterium*) and having ultimately changed the methanogen community compositions after 11 years of warming.

3.6 Conclusion

Methane emissions in freshwaters originate from methanogenesis, therefore, understanding how methanogenesis responds to current warming scenarios is fundamental to predicting their future impacts on the global climate. In *Chapter 2*, an ongoing divergence in the CH_4 emissions between the long-term warmed ponds (+ 4 °C for 11 years) and their ambient controls was observed. The emissions from warmed ponds were greater than would be predicted by warming alone. Here, I demonstrate that, increased CH_4 emissions were driven by a substantial amplification of CH_4 production, which cannot be fully accounted by the increase in methanogen abundance only. Indeed, warming has increased the cell-specific methanogen efficiency for CH_4 production. The increasing methanogen efficiency and CH_4 to CO_2 production ratio was in line with a shift in hydrogenotrophic methanogen genera,

which can be rationalized by short-term temperature manipulations - CH_4 production from hydrogen showed a greater positive sensitivity to warming than from acetate (1.40 eV compared to 1.08 eV for hydrogenotrophic and acetoclastic methanogenesis, respectively), making hydrogenotrophic CH_4 production more energetically favourable at higher temperatures. These findings provide experimental evidence that long-term warming can alter methanogen community structure and shift towards a more hydrogenotrophic-based methanogenesis, leading to a greater capacity of CH_4 production and an increased CH_4 to CO_2 production ratio, which fuels the CH_4 emission beyond the prediction by warming alone and ultimately make warmer freshwaters more efficient at making CH_4.

Chapter 4 Methanotrophy responds physiologically to warming with a conserved methanotroph community

4.1 Abstract

Methanotrophy is the sole biological CH_4 sink. Aerobic bacterial methanotrophs can decrease CH_4 emissions by oxidizing the majority of the CH_4 produced in anoxic freshwaters. Methanotrophy is often strongly substrate limited and therefore changes in temperature may have little effect on the rate of CH_4 oxidation. Warming has been shown to enhance methanogenesis and so alleviating some of the substrate limitation experienced by methanotrophs; yet how methanotrophic activity and methanotroph communities would respond to long-term warming is unknown. To better predict CH_4 emissions in a warmer world, it will be essential to understand the response of methanotrophs to climate warming. Here I show that, after 11 years of warming (+ 4 °C since 2006), methanotrophy was able to respond physiologically to higher temperature and CH_4 while the methanotroph community structure stayed the same. Despite that the *ex situ* CH_4 oxidation capacity was undistinguishable between the warmed ponds and ambient ponds in the laboratory slurry incubation, there was a marked kinetic and temperature effect of CH_4 oxidation. The apparent activation energy was 0.57 eV, which enables the CH_4 oxidation to be 1.37-fold greater *in situ* based on the 4 °C offset between the warmed and ambient ponds. Similarly, as warming has increased the CH_4 concentrations, this can be tracked by a 1.9-fold increase in CH_4 oxidation capacity *in situ*. As the oxic zone at the sediment surface was ~40% shallower in the warmed ponds, the *ex situ* CH_4 oxidation activity in slurry incubation can be underestimated by having counted inactive methanotrophs. Combined, the kinetic effect, temperature effect and the effect of sampling the same depths of methanotrophy accounted for a 3.59-fold increase in CH_4 oxidation in the

warmed ponds, oxidizing 95% of the extra CH_4 production under warming and not the required 98% that would prevent CH_4 emission from increasing. The methanotroph abundance did increase by 2.45-fold in the warmed ponds but would need to increase by 2.64-fold to offset the greater warming-induced CH_4 production. In the laboratory, the growth efficiency of methanotrophs appeared to be impaired by both higher temperature and higher CH_4 concentrations, and thus lack the potential to reach the required abundance to balance CH_4 production and the methanotroph community would stay the same. Our findings proved experimental evidence that methanotrophy can increase with temperature and higher CH_4 availability, i.e., the exact conditions induced by warming, yet the overall capacity of CH_4 oxidation would be limited through impaired growth efficiency to prevent CH_4 emission from increasing.

4.2 Introduction

Methanotrophy is the sole biological CH_4 sink. Methanotrophic bacteria, or methanotrophs, are able to oxidize up to 90 % of the CH_4 produced in freshwaters (Schutz, Seiler and Conrad, 1989; Frenzel, Thebrath and Conrad, 1990; King, 1990). Natural CH_4 emissions are regulated by the balance between methanogenesis and any subsequent methanotrophy because CH_4 escapes from anaerobic environments to the atmosphere when it is not oxidized by methanotrophs (Hanson and Hanson, 1996). Thus, as a key process in the global CH_4 cycle, understanding how methanotrophs respond to warming is crucial to predicting the effects of a changing climate on the net CH_4 emissions.

The temperature sensitivity of CH_4 oxidation is often suppressed under substrate limitation (Lofton, Whalen and Hershey, 2014; Shelley *et al.*, 2015). At low CH_4 concentrations, methanotrophy does not respond to increases in temperature but demonstrates a marked kinetic effect; while at higher CH_4 concentrations – although CH_4 is still limiting

but to a lesser extent – methanotrophy interacts with both CH_4 concentration and temperature (Bender and Conrad, 1992; Shelley *et al.*, 2015). As warming has been shown to increase methanogenesis exponentially in freshwaters (Gudasz *et al.*, 2010; Marotta *et al.*, 2014) and so potentially alleviating substrate limitation experienced by the methanotrophs (Shelley *et al.*, 2015), methanotrophy therefore has the potential to offset the warming-induced increase in CH_4 production. Nevertheless, previous experiments were restricted to relatively short-term responses (< 3 months) of methanotrophy to warming alone (Knoblauch *et al.*, 2008; van Winden *et al.*, 2012), and how methanotrophy responds to warming and warming-induced higher CH_4 concentrations over the long-term (> 10 years) remains unknown.

In *Chapter 2* and *3*, increases in CH_4 emission and production were demonstrated after 11 years of warming beyond the increase predicted by temperature alone, raising an unanswered question: how do methanotrophic activity and the affiliated bacterial communities respond to long-term warming? Predicting changes in methanotrophy under long-term warming will not only require an understanding of the CH_4 oxidation capacity that interacts with temperature and substrate availability, but also the methanotroph community characteristics, as changes in CH_4 fluxes have been shown to be related to shifts in methanotroph composition (Nazaries *et al.*, 2011) and abundance (Freitag *et al.*, 2010).

Traditionally, methanotrophs can be divided into type I (*Methylococcaceae* family) and type II (*Methylocystaceae* and *Beijerinckiaceae* families), based on their physiology, biochemistry and morphology (Hanson and Hanson, 1996; McDonald *et al.*, 2008). Short-term experiments incubating tundra- and paddy -soils under a range of temperatures have shown that rising temperatures appear to increase the relative abundances of the type II methanotrophs (Mohanty, Bodelier and Conrad, 2007; Knoblauch *et al.*, 2008; Ho and Frenzel, 2012). These experiments were limited to the short-term impact of temperature only, whether

the shifts towards a more type II abundant methanotroph community would be seen over the long-term under a condition of higher temperature and more abundant CH_4, i.e., the exact conditions induced by warming, is, nevertheless, not clear.

Here, in this Chapter, I used the long-term warmed, mesocosm pond experiment to investigate the effect of moderate warming (+ 4 °C above ambient temperature since 2006) on the CH_4 oxidation capacity and methanotroph community characteristics. Now after 11 years of warming, the kinetic effect and temperature response of CH_4 oxidation in the pond sediments was quantified. Furthermore, oxygen penetration profiles into the pond sediment were measured to rationalize methanotroph abundance and their cell-specific activity. The methanotroph community characteristics, including methanotroph abundance, diversity and composition, were analysed using molecular techniques targeting the critical functional gene *pmoA*.

4.3 Materials and Methods

4.3.1 Dissolved oxygen and penetration-profile measurements of oxygen in sediments

Dissolved oxygen concentrations in the overlying water were measured every 10 minutes from October, 2015, to October, 2016, in 8 warmed and 8 ambient ponds, using oxygen sensors (miniDOT oxygen logger, PME, California USA).

Penetration profiles of dissolved oxygen into the sediments were measured in April, 2016. Sediments were collected by hand using a small corer (Ø 8.8 cm, polycarbonate). The concentration of dissolved oxygen in the sediment was then measured at a resolution of 100 µm, using a 50-µm oxygen sensor (OX50; Unisense AS, Denmark) attached to an automated micromanipulator controlled by micro-profiling software (SensorTrace PRO; Unisense AS) (Neubacher, Parker and Trimmer, 2011).

4.3.2 Sediment collection and methane oxidation experiments

Sediment cores were collected from 8 warmed and 8 ambient ponds using truncated syringes (25 ml) in May, June and July, 2017, for temperature dependence experiments. In December, 2018, sediment corers were collected from 8 warmed and 8 ambient ponds using the same techniques for the kinetic effect experiment. The sediment cores were stored in zip-lock bags and kept cool with freezer blocks for transport back the laboratory (< 4 h) and then kept intact in the dark at 4 °C before further treatment.

The top 2 cm of sediment from each corer, along with the overlying pond water (4 mL), were transferred into 12 ml gas-tight vials (Labco Exetainer®). The vials were then sealed leaving an air headspace. The effect of long-term warming on both the temperature and kinetic concentration response of CH_4 oxidation were quantified. For the temperature response experiment, the vials were enriched with 200 µL of ^{13}C-CH_4 (99 % atom) to give an initial headspace concentration at ~1300 µmol L^{-1} and 40 µmol L^{-1} in the water phase. Control vials were set up without ^{13}C-CH_4 enrichment. All vials were incubated on a shaker (RPM=130) in temperature-controlled rooms (5 °C, 10°C, 15°C and 22°C). I appreciate that the concentration of CH_4 in the vials was higher than that in the experimental ponds (~1.07 and 0.51 µmol L^{-1} in the warmed and ambient pond water, respectively, *see* Figure 4.2 a and b) but higher concentrations of CH_4 enabled short, overnight incubations (for ~22 h) under different temperatures and without any conflating substrate limitation and I, in turn, characterised any concentration, kinetic effect. For the kinetic response experiments, the vials were enriched with ^{13}C-CH_4 to generate a range of initial concentrations from 1 to 60 µmol L^{-1} in water phase. All vials were incubated on a shaker (RPM=130) at room temperature (22°C). The vials with ^{13}C-CH_4 concentrations less than 15 µmol L^{-1} were incubated for less than 12 h and those with

higher initial concentrations were incubated overnight for ~ 20h. The incubations were stopped by injecting 200 µL of Zinc Chloride ($ZnCl_2$, 3.7M) to inhibit any microbial activity.

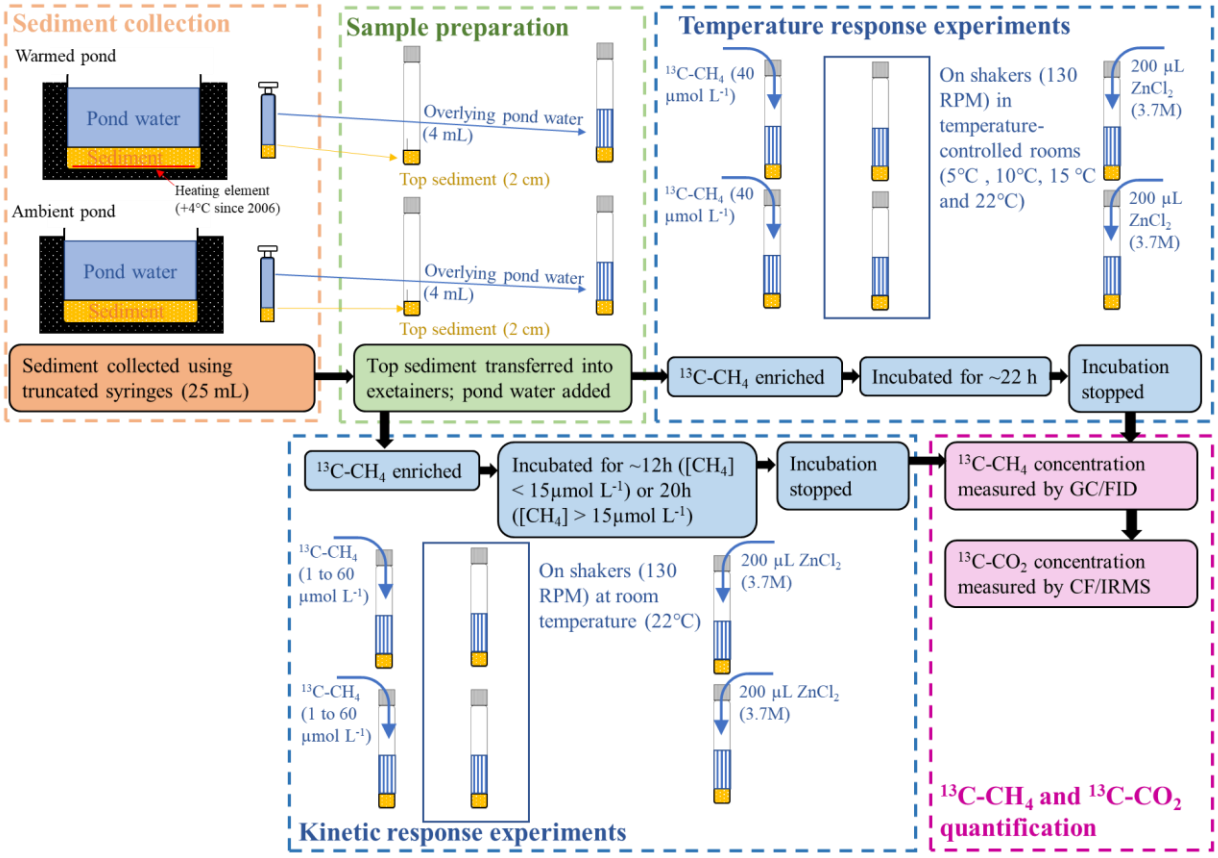

Figure 4.1 Flow chart of the experiments quantifying the effect of long-term warming on both the temperature and kinetic concentration response of CH_4 oxidation.

4.3.3 Quantification of methane oxidation and carbon conversion efficiency

The ^{13}C-CH_4 in the headspace of vials was quantified using a gas chromatograph fitted with a flame-ionization detector (*see Chapter 3* for details). The ^{13}C-CO_2 in the headspace was quantified by continuous flow isotope ratio mass spectrometry (CF/IRMS). Total ^{13}C as dissolved inorganic carbon ($\sum DIC = CO_2 + HCO_3^- + CO_3^{2-}$) was quantified at the end of each incubation, as per Trimmer et al. (2015). Summation of ^{13}C-CO_2 in headspace and ^{13}C-DIC equalled the total ^{13}C-CH_4 metabolised into inorganic carbon. As proxy for their growth-

efficiency, the fraction of CH_4 assimilated into methanotroph biomass (carbon conversion efficiency) was then measured using the fraction of ^{13}C-CH_4 recovered as ^{13}C-inorganic carbon as per Trimmer et al. (2015): $1 - \frac{\Delta^{13}C-inorganic}{\Delta^{13}C-CH4}$ where Δ represented the production or consumption of ^{13}C-DIC or ^{13}C-CH_4.

4.3.4 Statistical analyses

All statistical analyses were performed in R (version 3.2.5) (R Core Team, 2014).

Seasonality of the *in situ* dissolved oxygen concentrations and dissolved methane concentrations in the overlying pond water

Generalized additive mixed effect models (GAMMs) were used to characterize the seasonality of the *in situ* dissolved oxygen concentrations and the *in situ* dissolved CH_4 concentrations. The replicate ponds were treated as random effects on the intercept. The response variable (i.e., dissolved oxygen concentrations or dissolved CH_4 concentrations) were fitted as a function of day of the year into a full model using "gamm4" function from "gamm4" package (version 0.2-5), which included a treatment on the intercept which characterized the median value of the response variable and a smooth term which defined the shape of seasonal patterns (cubic regression spline). A set of models with combinations of terms in the full model was generated using the "dredge" function from MuMin package (version 1.15.6) (Barton, 2018). The models were compared using the AIC and AIC weights (Table 4.2 and 4.5).

Kinetics of methane oxidation

The kinetics of CH_4 oxidation was characterised by Michaelis-Menten model, taking the form:

$$MO_i(C_{CH4}) = \frac{(V_{max} + a_i) \times C_{CH4}}{(K_M + b_i) + C_{CH4}} \quad (4.1)$$

Where MO_i represents the rate of $^{13}C\text{-}CH_4$ oxidation by any sediment sample of mesocosm pond i (i =1, 2, …). C_{CH4} is the initial $^{13}C\text{-}CH_4$ concentrations (μmol L^{-1}). The parameters V_{max} and K_M were determined by fitting self-starting nonlinear mixed-effect models using the "nlme" function from nlme package (version 3.1-137) (Pinheiro *et al.*, 2018). The mesocosm ponds were fitted into the models as random effects to account for their variations on the parameter V_{max} (a_i) and on the parameter K_m (b_i). The significance of the treatment (*i.e.*, warmed or ambient ponds) as a fixed effect was tested using the Likelihood ratio test (Pinheiro and Bates, 2000) (*see* Table 4.3).

Temperature sensitivity and capacity of methane oxidation

According to the Boltzmann-Arrhenius equation, the temperature sensitivity and capacity of CH_4 production and oxidation were tested using (Gillooly *et al.*, 2001; Yvon-Durocher *et al.*, 2014):

$$lnG_i(T) = (\overline{E_{MO}} + a_i)\left(\frac{1}{kT_C} - \frac{1}{kT_i}\right) + \left(\overline{lnG(T_C)} + b_i\right) \quad (4.2)$$

Where $\ln G_i(T)$ is the natural logarithm of the rate of CH_4 oxidation by any sediment sample of mesocosm pond i (i =1, 2, …). The slopes, $\overline{E_{MO}}$, represent the estimated population activation energy, *i.e.*, the temperature sensitivity in units of eV (1eV=96.49 kJ mol^{-1}), for CH_4 oxidation and k is the Boltzmann constant (8.62×10^{-6} eV K^{-1}). The plot was standardized using the term $\frac{1}{kT_C}$, in which T_C (288.15 K, i.e., 15 °C) is the average temperature in the ambient ponds in 2017, so that the terms, $\overline{lnG(T_C)}$, corresponds to the average capacity of CH_4 oxidation at T_C. As the experimental design yielded replicate responses in ponds of both treatments, the replicate ponds was treated as random effects on the slope (a_i) and on the

intercept (b_i) of the models to account for the random variation among ponds from the fixed effects. ε_i is the unexplained error with normal distribution N (0, σ^2). The effects of treatment (i.e., whether ambient or warmed pond sediment) on both the slope (temperature sensitivity) and intercept (average capacity of CH_4 oxidation at T_C) were modelled as fixed effects (Table 4.4).

Prediction of methane oxidation from apparent activation energy

The prediction of increase in the CH_4 oxidation under the 4 °C warming scenario can be calculated using the apparent activation energy for temperature sensitivity of CH_4 oxidation to temperature (Allen, Gillooly and Brown, 2005; Yvon-Durocher *et al.*, 2014):

$$\frac{MO(T_W)}{MO(T_A)} = e^{\frac{\overline{E_{MO}}}{kT_W} - \frac{\overline{E_{MO}}}{kT_A}} \quad (4.3)$$

Where $MO(T_W)$ and $MO(T_A)$ are the CH_4 oxidation activity and T_W and T_A are the mean annual temperatures of the warmed and ambient ponds (288.15 and 292.15 K, respectively). $\overline{E_{MO}}$ is the apparent activation energy yielded at 0.57 eV in equation (4.2). k is the Boltzmann constant (8.62×10^{-5} eV·K^{-1}).

Carbon conversion efficiency

The fraction of CH_4 assimilated into methanotroph biomass (carbon conversion efficiency i.e., CCE) was used as a proxy for the methanotroph growth efficiency. To characterise the temperature sensitivity of the CCE, CCE values was fitted as a response variable into a mixed effect model of the form:

$$CCE_i(T) = (slope + a_i) \times (T - T_C) + \left(\overline{CCE(T_C)} + b_i\right) \quad (4.4)$$

Where $CCE_i(T)$ is the CCE of methanotrophy (%) by any sediment sample of mesocosm pond i (i =1, 2, …) at temperature T and, again, the plot was centered to the average

annual temperature in the ambient ponds (15 °C), so that the term $\overline{CCE(T_C)}$ represents the average CCE at 15 °C.

To characterize the kinetic concentration effect of carbon conversion efficiency (CCE), the CCE values were fitted into mixed-effect model using:

$$\mathrm{CCE}_i(C_{CH4}) = (slope + a_i) \times C_{CH4} + \left(\overline{\mathrm{CCE}(C_{CH4,0})} + b_i\right) \quad (4.5)$$

Where $\mathrm{CCE}_i(C_{CH4})$ represents the carbon conversion efficiency by any sediment of mesocosm pond *i* (*i* =1, 2, …). C_{CH4} is the initial concentration of $^{13}C\text{-}CH_4$. The intercept term $\overline{CCE_i(\mathrm{C}_{CH4,0})}$ is the average carbon conversion efficiency at an initial concentration of $^{13}C\text{-}CH_4$ at 0 μmol L^{-1}. The random effect terms a_i and b_i represent the variation among mesocosm ponds on the slopes and the intercepts, respectively. The effect of treatment (*i.e.*, warmed or ambient ponds) was fitted into the model as fixed effect. The significance of the treatment as fixed effect was tested using Likelihood Ratio Test (LRT) as described in following section.

4.3.5 DNA extraction

Sampling for methanotroph community composition analysis and functional gene abundance analysis was conducted every month from March to July in 2017. Cores were collected from 8 warmed and 8 ambient experimental ponds using cut-off 25 mL syringes. The sediments of the top 2 cm were transferred to an Eppendorf tube. The samples were stored at -80 °C before further extraction. Extraction of DNA from 0.5 g of the sediment was performed using the DNeasy® PowerSoil® Kit (Qiagen group) according to the manufacturer's instructions. The quantification of DNA was performed with NanoDrop (Thermo ScientificTM) according to the manufacturer's instructions. The DNA yield was approximately 1 to 4 μg g^{-1} of wet sediment.

4.3.6 Polymerase chain reaction (PCR) amplification, cloning and sequencing

The *pmoA* gene, which encodes particulate methane monooxygenase, was used as a molecular marker of methanotroph diversity. The *pmoA* gene was amplified by a seminested PCR using the primer pair 189F (5'-3': GGNGACTGGGACTTCTGG)-A682R(5'-3': GAASGCNGAGAAGAASGC) in the first round and A189F (5'-3': GGNGACTGGGACTTCTGG)-A650R (5'-3': ACGTCCTTACCGAAGGT) in the second round (Horz *et al.*, 2005). PCRs were performed in 25 µL reaction mixtures in a 96-well PCR plate (STAR LAB) containing 12.5 µL of MyTaq^{TM} Red Mix (2×, Bioline), 1.0 µL of each primer (10 µM), 1.0 µL of DNA template and 9.5 µL of molecular biology quality water.

For the first round, a touch-down PCR was used from 62 °C to 52 °C: after each cycle, the annealing temperature was decreased by 0.5 °C until it reached 52 °C (Horz *et al.*, 2005). The amplifications were performed in a Thermal Cycler (T100^{TM}, Bio-Rad) following the thermal program: (1) denaturation at 94 °C for 3 min, (2) 30 cycles of denaturation at 94 °C for 45 s, annealing from 62 to 52 °C for 60 s and extension at 72 °C for 180 s, (3) extension at 72 °C for 10 min. For the second round, the amplifications were performed following the thermal program: (1) denaturation at 94 °C for 3 min, (2) 22 cycles of denaturation at 94 °C for 45 s, annealing at 56 °C for 60 s and extension at 72 °C for 60 s, (3) extension at 72 °C for 10 min. PCR products (3 uL) were checked by electrophoresis on a fluorescent dye (GelRed® Nucleic Acid Gel Stain) stained 1 % agarose gel.

PCR products were sequenced on the Illumina MiSeq platform using the same methods as described in *Chapter 3*.

4.3.7 Processing of sequence data

The downstream sequence analysis was conducted using QIIME2 as in *Chapter 3*. To analyse the sequence data at the genus-level ASVs were clustered into Operational Taxonomic Units (OTUs) using a similarity threshold (90 % for *pmoA* sequences) taking into account the nucleotide substitution rate of functional genes (Pester *et al.*, 2004; Oakley *et al.*, 2012).

Table 4.1 Taxonomy assignment to the pmoA OTUs at 90 % identity.

	Family	**Species**	**Sequence reads**	
			Ambient	**Warmed**
1	*Methylococcaceae*	typeIb	713570	597859
2	*Methylocystaceae*	*Methylosinus*	535	1848
3	*Methylococcaceae*	*Methylomonas*	13	0
4	*Methylococcaceae*	*Methylobacter*	1372	158
5	pmoA-2	unclustered pmoA-2	235	410
6	*Methylococcaceae*	TUSC-like	1062	14
7	unclustered *Proteobacteria*	unclustered *Proteobacteria*	362	0
8	*Methylocystaceae*	typeIIa	4784	100
9	*Methylocystaceae*	unclustered *Methylocystaceae*	166	88
10	environmental_samples	typeIIb	2012	79
11	MO3	unclustered MO3	2532	1681
12	unclustered *Methylococcales*	unclustered *Methylococcales*	0	181
13	*Beijerinckiaceae*	Methylocapsa_related	2399	5
14	unclustered *Rhizobiales*	unclustered *Rhizobiales*	149	12
15	*Methylococcaceae*	unclustered *Methylococcaceae*	0	28
16	*Methylocystaceae*	*Methylocystis*	357045	324967

Taxonomy was assigned to individual OTUs using pre-trained Naïve Bayes classifier implemented feature-classifier plugin in QIIME2 (Table 4.1). The classifier was first trained on 90 % *pmoA* OTUs where the sequences have been extracted at the appropriate *pmoA* (A189F-A650R) primer sites. To further process sequence data, the package "phyloseq" in R was used (McMurdie and Holmes, 2013). The final dataset contained 65 unique OTUs with 2,013,666 sequence reads for *pmoA* library.

4.3.8 Phylogenetic analysis

The variation in riches (α-diversity), in community composition (β-diversity) and in differences in taxonomic abundance was analysed using the same method as in *Chapter 3*.

4.3.9 PCR cloning

The PCR cloning was performed using the same methods as in *Chapter 3*.

4.3.10 Quantitative polymerase chain reaction (qPCR)

The total methanotroph population of each individual sample was estimated by measuring *pmoA* gene copy numbers using the primer set A189F-A650R (Bourne, McDonald and Murrell, 2001). Amplifications were done in 384-well plate using CFX384 Touch™ Real-Time PCR Detection System (Bio-Rad). The reactions were carried out in a total volume of 10 µL containing: 5 µL of SsoAdvanced™ Universal SYBR® Green Supermix (2×, Bio-Rad), 0.2 µL of forward primer, 0.2 µL of reverse primer, 1 µL of DNA template (10 µM) and 3.6 µL of water. Standard curves with 10^1- to 10^7-fold serial dilutions of plasmid DNA containing the target gene were constructed by serial diluting the plasmid DNA containing *pmoA* gene inserts (*see Chapter 3* for calculation of copy numbers of *pmoA* gene per µL for standards). The qPCR thermal program was as follows: (1) initial denaturation at 98 °C for 3 min; (2) 40 cycles of denaturation at 98 °C for 15 s, annealing at 55°C for 15 s and extension at 72 °C for

60 s; (3) final extension at 72 °C for 10 s. Fluorescent signal was acquired after each cycle at 72 °C. Product specificity and size was confirmed by melt curve analysis after the final extension by increasing the temperature from 62 to 95 °C in 0.5 °C increments every 5 s. Each sample was performed in three replicates.

4.3.11 Cell-specific activies of methanotrophs

Cell-specific activities were calculated for methanotrophs by dividing CH_4 oxidation capacity at 15 °C by *pmoA* copy abundances in each sample.

4.4 Results

4.4.1 Dissolved methane concentrations and kinetics of methanotrophy in the sediments

There was a marked kinetic effect demonstrating a strong physiological potential to oxidize CH_4 (Figure 4.2 c) over the range initial starting concentration of CH_4 from 1 to 60 μmol L^{-1}. The capacity to oxidize CH_4 in both the warmed and ambient pond sediments was the same (P=0.93 and P=0.44 for treatment on V_{max} and K_m, respectively, Table 4.3). The calculated maximum CH_4 oxidation (*Vmax*) in the pond sediments were 514 nmol CH_4 $g^{-1}h^{-1}$.

Warming increased *in situ* CH_4 concentrations in the warmed ponds by 2.1-fold (Figure 4.2 a and b). The average CH_4 concentrations were 1.07 and 0.51 μmol L^{-1} in the warmed and ambient pond water, respectively (P<0.05, Figure 4.2 b). Though the CH_4 oxidation activity was the same in the *ex situ* slurry incubation, given the strong kinetic potential to oxidize CH_4, the 2.1-fold higher CH_4 concentrations were tracked by a 1.9-fold increase in *in situ* CH_4 oxidation activity in the warmed pond sediment relative to their ambient controls (by Michaelis-Menten model, *see* equation 4.1).

Table 4.2 Model selection procedures for fitting the GAMM to the data of CH_4 concentration (*n*=485). A range of generalized additive mixed effects models (GAMM) were fitted to the dissolved CH_4 concentration data (dCH_4) as a function of "Treatment" (i.e., warmed or ambient) and DOY (day of the year since 1st January, 2017) to assess the effect of long-term warming on the *in situ* CH_4 concentrations in the overlying water. The seasonality of CH_4 concentrations was tested by comparing the smooth terms s(DOY, by=Treatment) and s(DOY). Models were ranked according to Akaike information criterion (AIC) which measured goodness of fit and model complexity (Zuur, 2009). ΔAIC refers to the AIC differences relative to the smallest AIC value and the AIC weight is the probability that the model is the actual best model (Burnham and Anderson, 2002). The model with the best fit to the CH_4 concentrations is marked in bold i.e., F0): CH_4 concentrations was higher in the warmed ponds but warmed and ambient ponds had the same seasonality of CH_4 concentrations.

Model	d.f.	AIC	ΔAIC	AIC Weight
F0) dCH_4 = s(DOY)+Treatment	**6**	**1204.9**	**0.00**	**0.73**
F1) dCH_4 = s(DOY)	5	1207/8	2.98	0.16
F2) dCH_4 = s(DOY, by=Treatment)+Treatment	8	1209.2	4.31	0.085
F3) dCH_4 = s(DOY, by=Treatment)	7	1212.1	7.26	0.019

Table 4.3 Model selection procedures for fitting the nonlinear mixed-effect models to the data of methanotrophy kinetics (*n*=158). Michaelis-Menten model ($MO_i(C_{CH4}) = \frac{(V_{max}+a_i)\times C_{CH4}}{(K_M+b_i)+C_{CH4}}$) was fitted to the CH_4 oxidation capacity data (MO) with a range of initial starting concentrations of CH_4. The mesocosm ponds (a_i and b_i) were fitted into the models as random effects (Vm+k~1) to account for their variation on the parameters (V_{max} and K_m) from the fixed effects. The optimal model appears to be the model with the mesocosm ponds as the random effects on the parameter V_{max} only as it had the lowest AIC (marked on bold). The significance of treatment (i.e., warmed or ambient) on fixed effect (V_{max} and K_m) was determined via Likelihood Ratio Test on nested models (denoted by subtraction symbols below). The model that best fits the kinetic effect response of CH_4 oxidation was the one with indistinguishable V_{max} and K_m between the warmed and ambient ponds (model F2, marked on bold).

Model	**d.f.**	**AIC**	**LogLik**	***P*-value**
To determine the optimal random-effect structure:				
Full model + (Vm+k~1)	7	2108.21	-1047.11	
Full model + (Vm~1)	**6**	**2106.21**	**-1047.10**	**0.93**
Full model + (K~1)	6	2168.51	-1078.26	<0.001
To determine the optimal fixed-effect structure:				
F0) MO~(Vmax+Treatment) + (Km~+Treatment)	6	2106.21	-1047.10	
F1) MO~(Vmax+Treatment) + (Km~1)	5	2104.21	-1047.10	0.98
F2) MO~(Vmax~1) + (Km~1)	**4**	**2102.78**	**-1047.39**	**0.45**

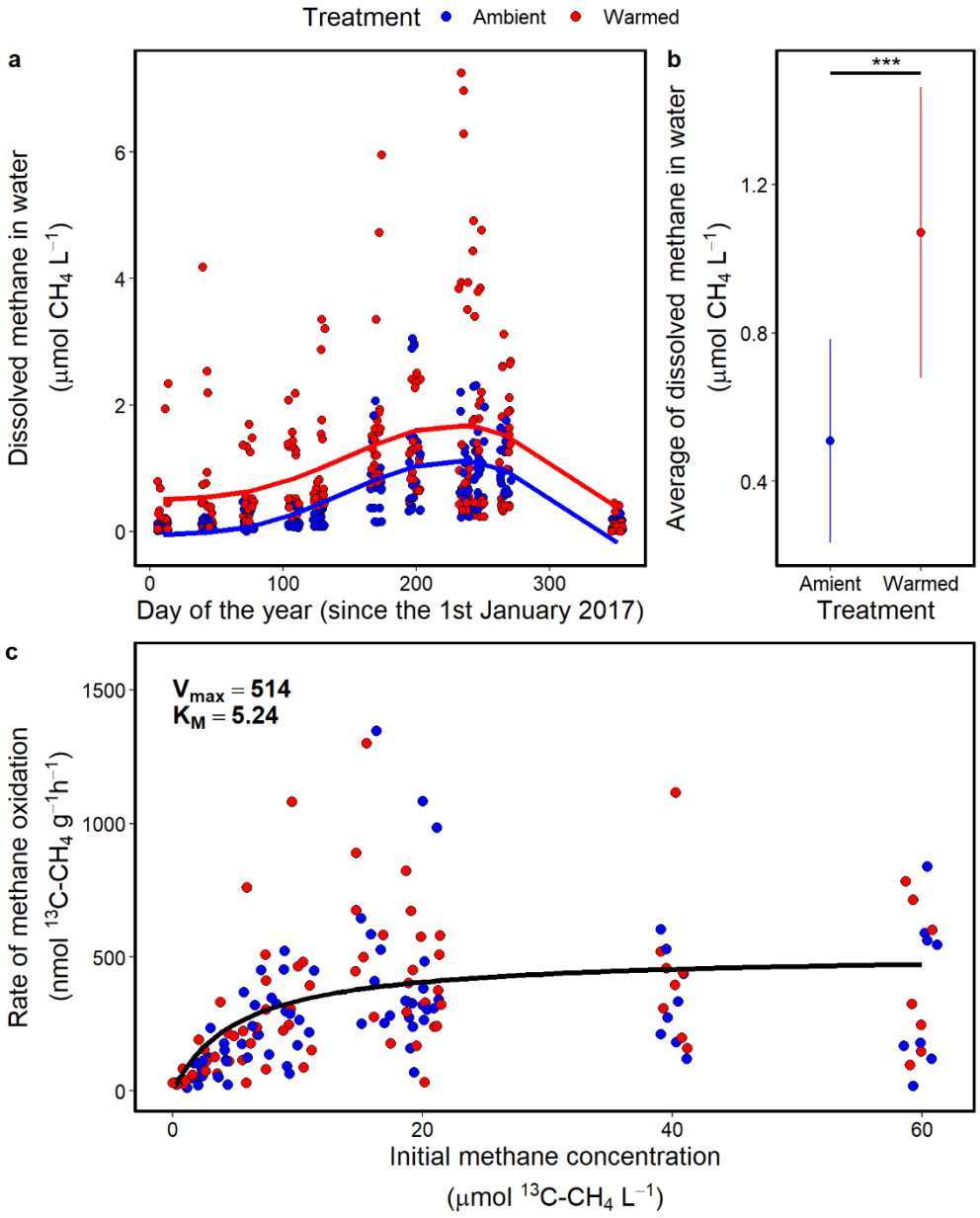

Figure 4.2 CH_4 concentrations and kinetic concentration response of CH_4 oxidation. Seasonal *in situ* CH_4 concentrations in the overlying water from January to December, 2017 (**a**). The solid lines denote the estimates from the best filling GAMM model where each experimental pond is treated as a random effect. The averages of dissolved CH_4 concentrations in the overlying water were 1.07 and 0.51 µmol L^{-1} in the warmed and ambient pond, respectively (**b**). Statistical significance between the warmed and ambient ponds is shown by asterisks (*t*-test, ***: $P<0.001$). The CH_4 oxidation capacity of the methanotrophs increasing as a function of initial starting concentrations of CH_4, fitted into a Michaelis-Menten kinetics (solid line) (**c**).

4.4.2 The temperature dependence of CH_4 oxidation

Plotting the natural-logarithm-transformed CH_4 oxidation rates against the standardized temperature demonstrated that the capacity to oxidize CH_4 was the same between the warmed and ambient ponds (Likelihood Ratio Test, P=0.068) (Figure 4.3). The CH_4 oxidation capacity standardized to 15 ° (here intercept at 0), was calculated for 244.69 nmol CH_4 $g^{-1}h^{-1}$. The slope of the natural-logarithm-transformed CH_4 oxidation rates against the standardized temperature plotting represents the temperature sensitivity of CH_4 oxidation. The temperature sensitivity of CH_4 oxidation, expressed as apparent activation energy, was 0.57 eV, indistinguishable between the warmed and ambient ponds, too (Likelihood Ratio Test, P=0.24).

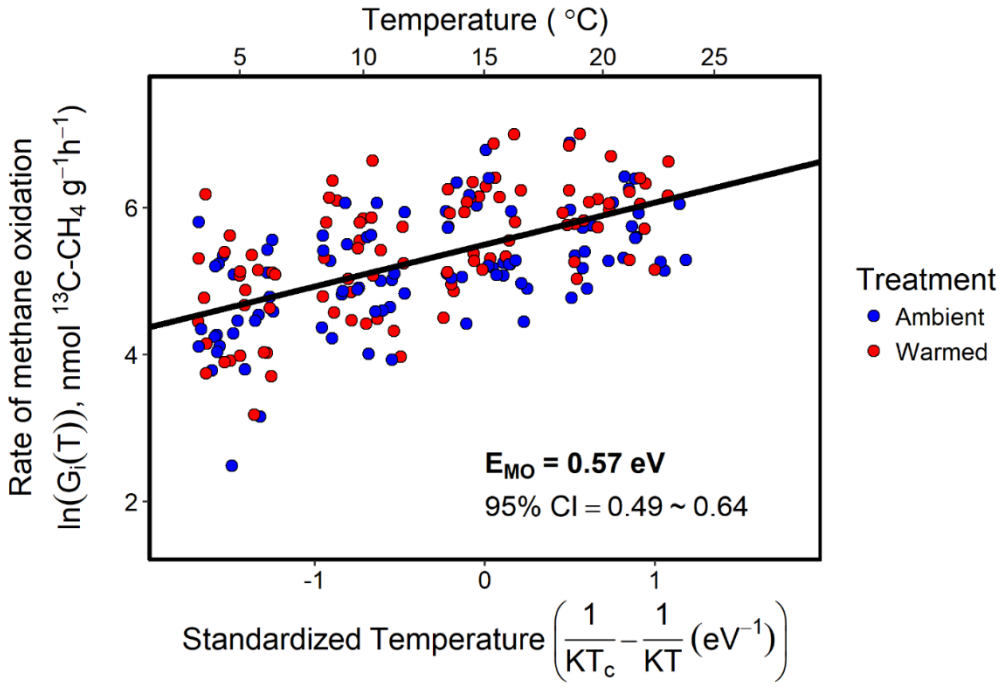

Figure 4.3. The temperature sensitivity of CH_4 oxidation. The temperature sensitivity and capacity were indistinguishable between the warmed (red) and ambient (blue) ponds.

Despite that the *ex situ* CH_4 oxidation capacity was the same in the slurry incubation experiments, the capacity to oxidize CH_4 would be 1.37-fold greater in the warmed pond

sediments *in situ* (*see* equation (4.3)), based on the 4°C offset between the warmed and ambient ponds (Allen, Gillooly and Brown, 2005). Altogether, 4°C of warming and warming-induced increases in CH_4 concentrations could account for a 2.62-fold increase in CH_4 oxidation capacity in the warmed ponds relative to their ambient controls.

Table 4.4 Model selection procedures for fitting the LMEM to the data of temperature sensitivity of methane oxidation (*n*=192). The full model included additive terms and their interactions for two fixed effects – centered temperature at 15 °C (Tc, term $\left(\frac{1}{kT_C} - \frac{1}{kT_{ij}}\right)$ in equation 4.2) and treatment types (i.e., ambient or warmed). The random effects were firstly included on both the intercept and slope to account for the variance across the experimental ponds. The random intercept and slope model had the lowest AIC and therefore the preferred option. The optimal random effect was then applied, and the significant *P*-value of fixed-effect terms were determined via likelihood ratio test on nested models (denoted by subtraction symbols below). The model that best fit the CH_4 oxidation was marked in bold, i.e., F1 which included a single intercept and slope provided the best fit, demonstrating that the CH_4 oxidation and temperature sensitivity was the same between the warmed and ambient ponds.

Model	**d.f.**	**AIC**	**LogLik**	χ^2	***P*-value**
To determine the optimal random-effect structure:					
Full model + (1+Tc|Pond)	**8**	**287.12**	**-135.56**		
Full model + (1|Pond)	5	383.68	-186.84	102.56	<0.001
To determine the optimal fixed-effect structure:					
F0) Full model + (1+Tc|Pond)	8	287.12	-135.56		
F1) F0 – Treatment×Tc	**7**	**286.48**	**-135.56**	**1.36**	**0.24**
F2) F1 - Treatment	6	287.81	-137.91	3.33	0.068
F3) F2 - Tc	5	329.75	-159.88	43.94	<0.001

4.4.3 Methanotroph abundance and cell-specific activity

The abundance of methanotrophs (qPCR of *pmoA* gene) was 2.45-fold higher in the warmed ponds (*t*-test, $P<0.001$). The cell-specific activity in the warmed pond sediments, defined as the CH_4 oxidation capacity at 15 °C per *pmoA* gene, was less than half that in the ambient controls (10.20 pmol copy^{-1} h^{-1} compared to 25.04 pmol copy^{-1} h^{-1} for the ambient ponds). Therefore, a large fraction (~60 %) of the methanotrophs were inactive in the warmed pond sediments (Figure 4.4).

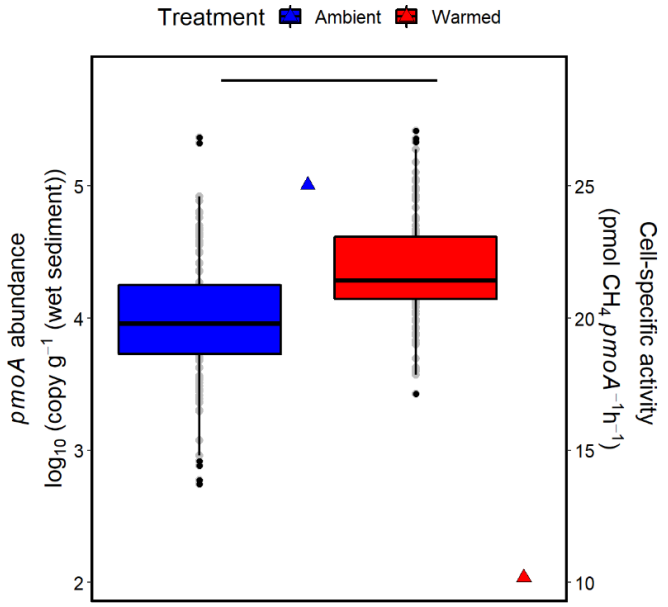

Figure 4.4 Long-term warming increased the methanotroph abundance (bars) in the warmed pond sediments but decreased the cell-specific methanotroph activity (triangle). Significance for a comparison between the warmed and ambient ponds is shown by asterisk (***: $P<0.001$).

4.4.4 Oxygen profiles in the sediment

Methanotrophs are inactive while methane- or oxygen-starved (Roslev and King, 1995; Singh *et al.*, 2010) and therefore, their activity is confined to a thin, oxic zone at the sediment surface (Reim *et al.*, 2012). To further rationalize the large fraction of inactive methanotrophs

in the warmed sediments, the oxygen profiles were measured. There are differences in the oxygen seasonality between the warmed and ambient ponds (Figure 4.5 a). The averages of *in situ* dissolved oxygen in the warmed ponds were lower than the ambient ponds (Figure 4.5 b, *t*-test, $P<0.001$). Consequently, a generalized additive mixed-effect model which included a smoother term differentiating the shapes between the warmed and ambient ponds and a treatment (i.e., warmed and ambient) on the intercept provided the best fit to the data.

The vertical profiles of oxygen were measured too. Oxygen declined more rapidly in the warmed ponds than their ambient controls (Figure 4.5 c), leading to a 40 % narrower depth of oxygen penetration in the warmed pond sediment (4.86 compared to 6.67 mm in the ambient pond sediment). Therefore, the cell-specific activity, reported above, would have been under-estimated by counting inactive methanotrophs in the anoxic sediment layers. Using oxic depth as a proxy for the active methanotrophy layer, the effect of sampling the same depths in the warmed and ambient ponds for CH_4 oxidation capacity measurements accounts for another 1.37-fold increase in the warmed sediments ($\frac{D_{samling}}{4.86\ mm} / \frac{D_{sampling}}{6.67\ mm} = 1.37$, $D_{sampling}$ is the sampling depth (20 mm)).

Table 4.5 Model selection procedures for fitting the GAMM to the data of oxygen concentration (*n*=5120). A range of generalized additive mixed effects models (GAMM) were fitted to the dissolved oxygen concentration data (dO2) as a function of "Treatment" (i.e., warmed or ambient) and DOY (day of the year since 20th October, 2015) to assess the effect of long-term warming on median oxygen concentrations in the overlying water. I aslo test whether the seasonal oxygen concentrations differed among the treatments by comparing the smooth terms s(DOY, by=Treatment) and s(DOY). Models were ranked according to Akaike information criterion (AIC) which measured goodness of fit and model complexity (Zuur, 2009). ΔAIC refers to the AIC differences relative to the smallest AIC value and the AIC weight is the probability that the model is the actual best model (Burnham and Anderson, 2002).

Model	d.f.	AIC	ΔAIC	AIC Weight
F0) dO2 = s(DOY, by=Treatment)+Treatment	**8**	**48910.5**	**0.00**	**0.95**
F1) dO2 = s(DOY, by=Treatment)	7	48916.4	5.91	0.05
F2) dO2 = s(DOY)+Treatment	6	49906.5	966.00	0
F3) dO2 = s(DOY)	5	49912.4	1001.90	0

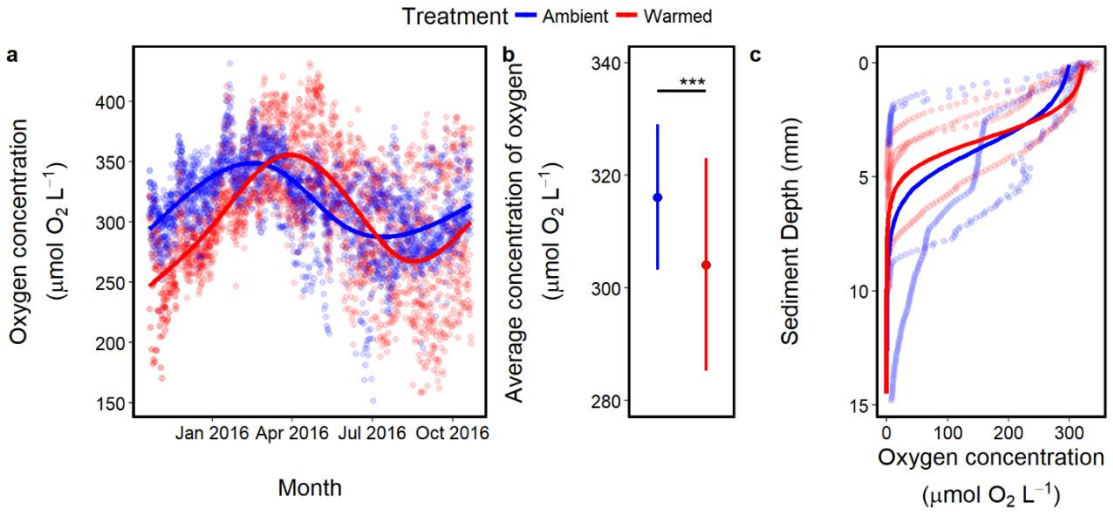

Figure 4.5. Effect of long-term warming on oxygen concentrations. a, Seasonality of the *in situ* dissolved oxygen concentrations in the overlying water of the warmed (red) and ambient (blue) ponds from October, 2015 to October, 2016. **b**, Averages of the *in situ* dissolved oxygen concentrations was lower in the warmed pond water than their ambient counterparts (t-test, ***:P<0.001). **c**, oxygen profiles measured for intact corers at 15 °C. The oxygen concentrations declined faster with depths in the warmed ponds, resulting a narrower oxic layer (4.86 mm compared to 6.67 mm for the ambient ponds).

4.4.5 Carbon conversion efficiency as a proxy for methanotroph growth

The carbon conversion efficiency, i.e., what fraction of CH_4 oxidized is assimilated into biomass, is used as a proxy for methanotroph-growth-efficiency. The carbon conversion efficiency was the same between the warmed and ambient pond sediments as a function of

temperatures (Figure 4.6 a, Likelihood Ratio Test, P=0.63 and P=0.63 for the significance of comparison between the warmed and ambient ponds on the intercept and slope, respectively). Plotting the CCE against the temperature demonstrated a negative correlation, suggesting that the growth of methanotrophy was attenuated at higher temperatures. The slope calculated in the best fit model to CCE data was 0.58 per °C, equivalenting to a decrease of CCE by 2.32 % based on the 4° offset between the warmed and ambient ponds.

There was a relationship between CCE of methanotrophy with the CH_4 concentrations, too. The CCE was negatively correlated to initial starting CH_4 concentrations, suggesting that the growth efficiency of methanotrophy was impaired at higher CH_4 concentrations, though the CCE was indistinguishable between the warmed and ambient ponds (Figure 4.6 b, Likelihood Ratio Test, P=0.77 and P=0.38 for the significance of comparison between the warmed and ambient ponds on the intercept and slope, respectively). As the CH_4 concentrations in the warmed ponds was 2.1-fold greater than their ambient controls, the CCE of methanotrophs in the warmed ponds would be 0.1% lower than their ambient controls.

Table 4.6 Model selection procedures for the LMEM fitted to carbon conversion efficiency data. The full model included additive terms and their interactions for two fixed effects – centered temperature at 15 °C (Tc, term $T - T_C$ in equation (4.3)) and treatment types (i.e., ambient or warmed). The random effects were first included on both the intercept and slope to account for the variance across the experimental ponds. The random intercept and slope model had the lowest AIC and therefore the preferred option. The optimal random effect was then applied, and the significant *P*-value of fixed-effect terms were determined via likelihood ratio test on nested models (denoted by subtraction symbols below). The model that best fit the CH_4 production was marked in bold.

Carbon conversion efficiency as function of temperature (*n*=191):

Model	**d.f.**	**AIC**	**LogLik**	**χ^2**	***P*-value**
To determine the optimal random-effect structure:					
Full model + (1+Tc|Pond)	**8**	**1041.2**	**-512.61**		
Full model + (1|Pond)	6	1051.7	-519.85	14.48	<0.01
To determine the optimal fixed-effect structure:					
F0) Full model + (1+Tc|Pond)	8	1041.2	-512.61		
F1) F0 – Treatment×Tc	7	1039.5	-512.72	0.23	0.63
F2) F1 - Treatment	**6**	**1037.7**	**-512.84**	**0.23**	**0.63**
F3) F2 - Tc	5	1069.0	-529.51	33.34	<0.01

Carbon conversion efficiency as function of methane concentration (*n*=69):

Model	**d.f.**	**AIC**	**LogLik**	**χ^2**	***P*-value**
To determine the optimal random-effect structure:					
Full model + (1+Tc|Pond)	8	460.51	-223.25		
Full model + (1|Pond)	**6**	**458.78**	**-223.39**	**2.27**	**0.32**
To determine the optimal fixed-effect structure:					
F0) Full model + (1+Tc|Pond)	6	458.78	-223.39		
F1) F0 – Treatment×Tc	5	456.86	-223.43	0.083	0.77
F2) F1 - Treatment	**4**	**455.63**	**-223.82**	**0.77**	**0.38**
F3) F2 - Tc	3	463.93	-228.97	10.30	<0.01

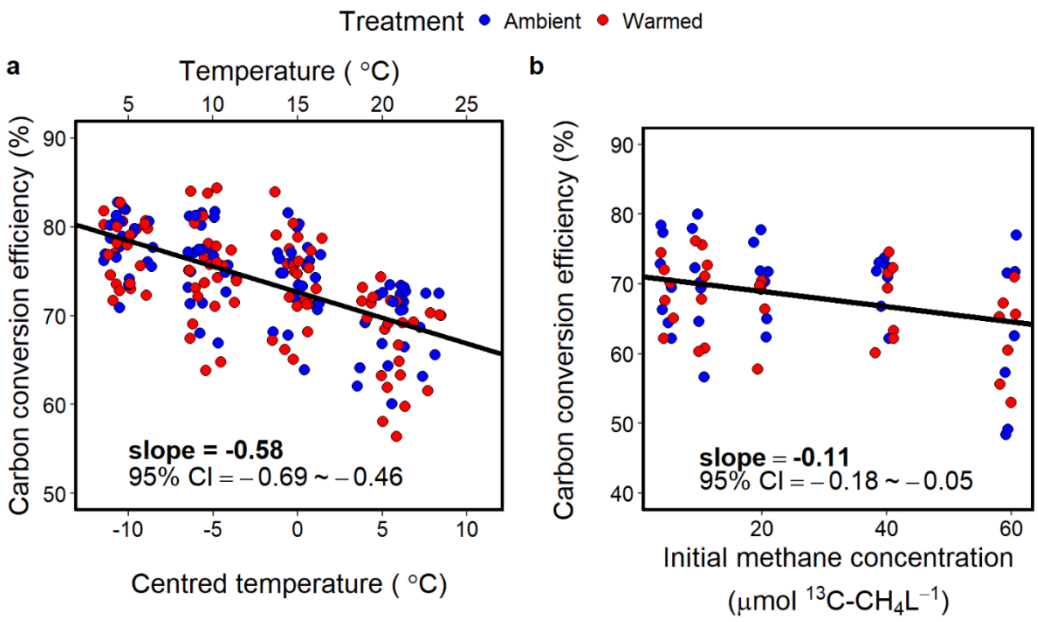

Figure 4.6. The carbon conversion efficiency of methanotrophy. a, the carbon conversion efficiency of methanotrophy was attenuated at higher temperatures. **b,** the carbon conversion efficiency was impaired at higher CH_4 concentrations.

4.4.6 Alpha diversity of the methanotroph community

The methanotroph community diversity, calculated using the observed OTUs, Shannon's Diversity, Chao 1 diversity and evenness index revealed that long-term warming did not alter the methanotroph community diversity (Figure 4.7, Likelihood Ratio Test, P>0.05).

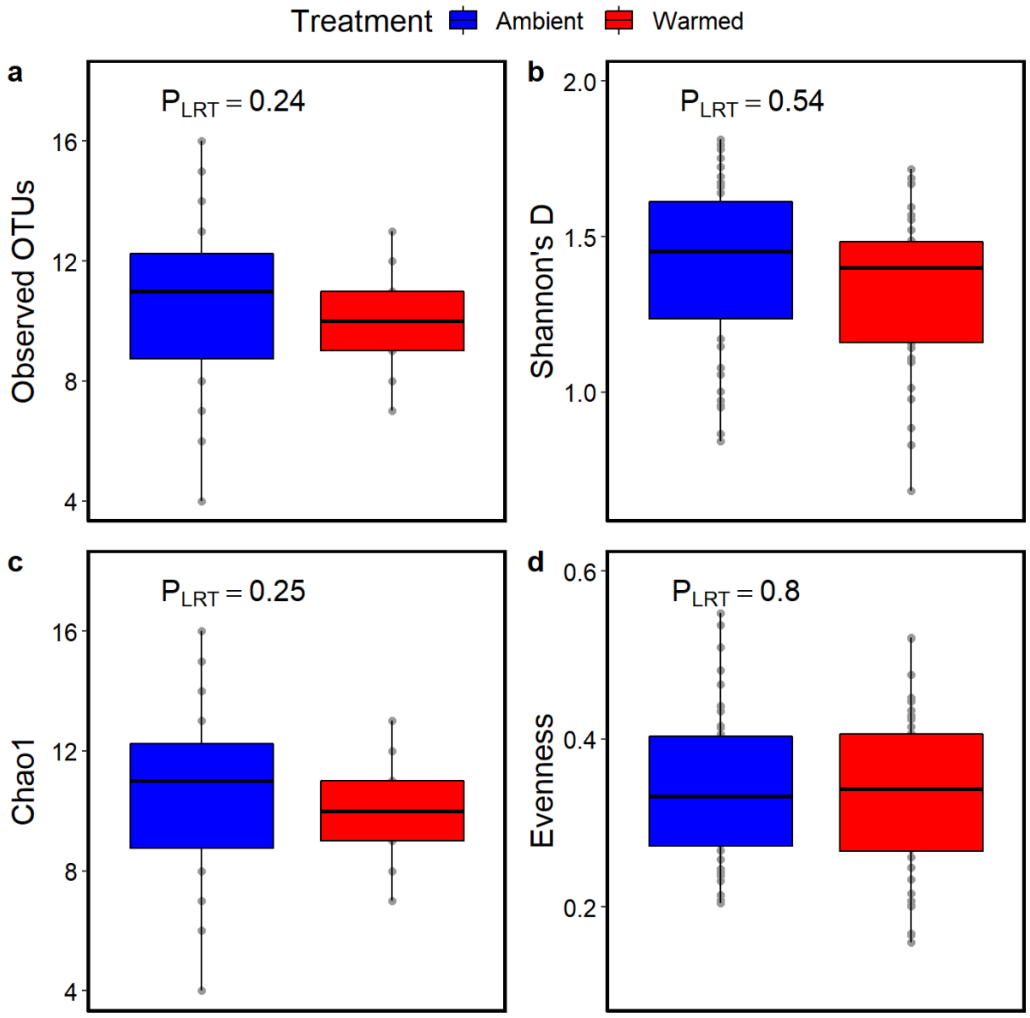

Figure 4.7 Alpha diversity calculated for methanotroph community. Observed OTUs, Shannon's Diversity, Chao 1 diversity and evenness of the methanotroph community were identical between the warmed and ambient ponds.

4.4.7 Methanotroph community

The effect of long-term warming on the methanotroph community composition was analysed by comparing the sample scores along the first two PCoA axes. The sample scores were indistinguishable on either of the PCoA axis between the warmed and ambient pond (Likelihood Ratio Test, *P*=0.85 and *P*=0.51 for the significance between the warmed and ambient ponds along the PCoA1 and PCoA2, respectively), demonstrating a conserved methanotroph community composition under warming (Figure 4.8 a). Similarly,

PERMANAOVA analysis did not detect any difference either (P<0.10). To further investigate any shift in the relative abundances of the existing methanotroph genera, negative binomial generalized linear modelling was applied. There was no change in the relative abundance of methanotroph genera between the warmed and ambient ponds (Figure 4.8 b, adjusted P-value > 0.01).

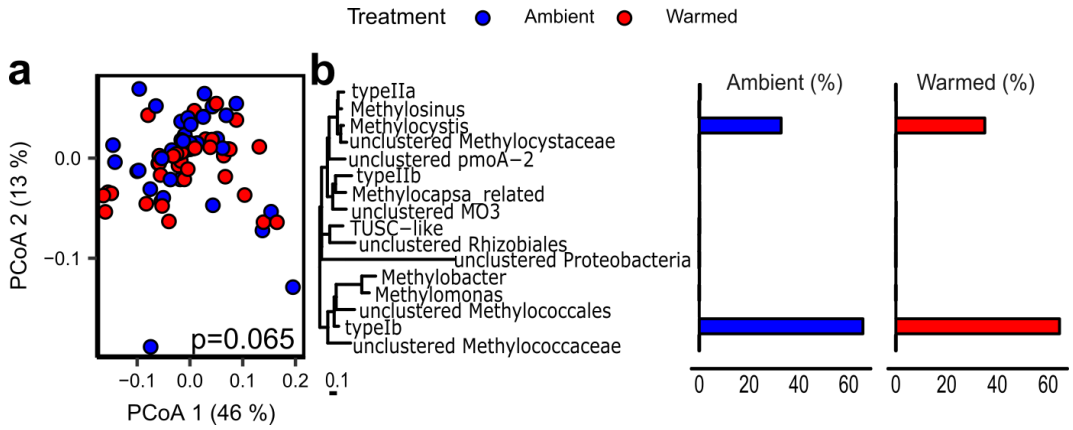

Figure 4.8 Effect of long-term warming on the methanotroph community composition. **a**, Principal Coordinate Analysis (PCoA), using Bray-Curtis analysis and a Hellinger standardized dataset (at genus level), demonstrating a conserved community composition between the warmed (red) and ambient (blue) ponds (PERMANOVA analysis, P<0.10). **b**, no significant shifts were observed in the relative abundance of any of the methanotroph genera between the warmed and ambient ponds.

4.5 Discussion

In *Chapter 2*, an increase in CH_4 emissions beyond that predicted by an increase in temperature alone was observed and, further in *Chapter 3*, the increased CH_4 emissions were shown to be driven by a substantial amplification of CH_4 production, methanogen abundance and efficiency. Here in this chapter, I demonstrated that methanotrophy increased with temperature and substrate availability without any shifts in community compositions.

Methane oxidation is often substrate limited in ecosystems and follows a kinetic response (Whalen, Reeburgh and Sandbeck, 1990; Shelley *et al.*, 2015). Warming has been

shown to increase the CH_4 production in the sediments, accordingly, the CH_4 concentrations in the warmed ponds were higher than that in their ambient controls (1.07 versus 0.51 μmol L^{-1} in the ambient ponds). To investigate how methanotrophy responded to this warming-induced increase in substrate availability, the kinetic response of CH_4 was investigated using a Michaelis-Menten model. The CH_4 oxidation capacity followed the same kinetic response as the Michaelis-Menten constants V_{max} and K_m were the same for the warmed and ambient ponds (*see* equation 4.1). The calculated V_{max}, i.e., the maximum CH_4 oxidation capacity, for CH_4 oxidation was 514 nmol g^{-1} h^{-1}, comparable to those reported in lakes (Deutzmann, Wörner and Schink, 2011) and in rivers (Shelley *et al.*, 2015). But the calculated K_m, the half-saturation constant, was 5.25 μmol L^{-1}, lower than those reported in lakes and rivers, indicating that methanotrophs are able to rapidly exploit the greater CH_4 concentrations in the warmed ponds. Indeed, warming increased CH_4 concentrations by 2.1-fold, which was tracked by a 1.91-fold increase in CH_4 oxidation activity.

There was a temperature effect, too. The apparent activation energy (0.57 eV) was the same between the warmed and ambient ponds and comparable to previously reported in pure cultures and landfill cover soil (Whalen, Reeburgh and Sandbeck, 1990; King and Adamsen, 1992). The 4 °C offset between the warmed and ambient ponds would thus enable oxidation activity to be 1.37-fold greater *in situ*. Altogether, 4 °C of warming and induced increases in CH_4 concentrations would increase the CH_4 oxidation capacity of the warmed ponds by 2.6-fold (2.1-fold for kinetic effect ×1.37-fold for the temperature effect) but in order for the CH_4 emissions to remain the same under warming, the methanotrophic response would need to be 3.9-fold greater to consume 98% of the CH_4 produced.

Methanotrophs are inactive while methane- or oxygen-starved (Roslev and King, 1995; Singh *et al.*, 2010). In the pond sediments, oxygen penetrated into the sediment to a depth

about 1 mm only as respiration consumes oxygen quickly (Frenzel, Thebrath and Conrad, 1990). The activity of methanotrophs is therefore confined to a very thin zone at oxic-anoxic interface (Reim *et al.*, 2012). The cell-specific, CH_4 oxidation activity (at 15 °C per *pmoA* gene copy) in the warmed ponds was less than half that in the ambient controls and a large fraction, ~ 60 % of methanotrophs appeared to be inactive. As oxygen penetration was ~ 40 % shallower in the warmed compared to ambient sediments, the cell-specific methanotroph activity in the slurry incubation might have been under-estimated by sampling the sediment to the same depth and counting inactive methanotrophs in the anoxic sediment layers. If the depth of oxygen penetration serves as a proxy for active methanotroph layer, another 1.37-fold greater CH_4 oxidation capacity accounted for the *ex situ* CH_4 oxidation capacity in the warmed ponds. Combined, the kinetic effect, temperature effect and the effect of sampling the same depths accounted for 1.91-, 1.37- and 1.37- fold, of the increased CH_4 oxidation in the warmed ponds, respectively. Overall, measured *ex situ* CH_4 oxidation capacity is 3.59-fold higher in the warmed compared to ambient sediments. However, this only accounts for ~95% of the extra CH_4 production under warming and not the required 98% that would prevent CH_4 emission from increasing (see *Chapter 5* and further discussion there in).

Methanotrophs utilize CH_4 as their sole carbon and energy source. Thus, their abundance increases with temperature and CH_4 (Bender and Conrad, 1992; Zheng *et al.*, 2012). In our warmed ponds, methanotroph abundance did increase by 2.45-fold over the ambient ponds after 11 years of warming but would need to increase by 2.64-fold to offset the greater warming-induced CH_4 production. As only a portion of the CH_4 oxidized is assimilated into cellular biomass while the remainder being oxidized to carbon dioxide to provide energy for its assimilation (Prior and Dalton, 1985), understanding what the fraction of CH_4 oxidized would be assimilated into biomass, i.e., carbon conversion efficiency, may help to explain the

limited methanotroph abundance under warming. Previous experiments reported that 69 % of CH_4 oxidized was recovered in the bulk organic carbon fraction in land-fill cover soil (Whalen, Reeburgh and Sandbeck, 1990). In oxic water column of lakes, the range of CH_4 assimilated was more extreme (from 6 to 77 %) (Bastviken *et al.*, 2003), whereas in the riverbed, the range was consistent at 50 % (Trimmer *et al.*, 2015). Here the carbon conversion efficiency was shown to be indistinguishable between the warmed and ambient ponds but was suppressed in incubations at both higher CH_4 concentrations and higher temperatures, i.e., the exact conditions induced by warming. Therefore, under warming, methanotrophs grow by oxidizing more CH_4 but assimilating a smaller proportion of this carbon, and thus lacked the potential to reach the required abundance to balance CH_4 production.

Previous experiments have demonstrated a shift of methanotroph community under warming, yet the results appeared to be contradictory. Some experiments have found that rising temperatures increased the relative abundance of type II methanotrophs in tundra soil (Knoblauch *et al.*, 2008) and paddy soils (Ho and Frenzel, 2012), probably due to their higher optimal temperatures compared to type I methanotrophs (Mohanty, Bodelier and Conrad, 2007). In contrast, a study in grassland soil with longer heating treatment (< 2 years) observed a decrease in the relative abundance of type II with temperature (Horz *et al.*, 2005). These contradictory observations suggested that short-term experiments might not be able to capture the shifts of methanotroph community in response to warming. Our experiment demonstrated, for the first time, that the community structure of methanotrophs, after 11 years of warming by moderate warming (+ 4°C above ambient temperatures), was the same in both the warmed and ambient ponds.

Methanotrophs use CH_4 as their sole carbon and energy source and are usually strongly substrate limited *in situ* (Duc, Crill and Bastviken, 2010; Lofton, Whalen and Hershey, 2014;

Trimmer *et al.*, 2015). In contrast to changes seen in the methanogen community composition where hydrogenotrophic methanogens changed their relative abundances because they were energetically favoured at higher temperatures (*see Chapter 3*), the methanotroph community composition stayed the same. While increases in CH_4 availability support larger populations, the abundance of the whole community increases but with no specific selection for a subset of the methanotroph community.

4.6 Conclusion

The net CH_4 emission is regulated by the balance between production and oxidation. In *Chapter 2* and *3*, I demonstrated that long-term warming can continuously increase CH_4 emission driven by a substantial amplification of CH_4 production. Here in this chapter, I demonstrated methanotrophy was able to respond physiologically to higher temperatures and CH_4, though the overall capacity to oxidize CH_4 was limited to 95% of the CH_4 produced and not the required 98% that would prevent CH_4 emission from increasing. The methanotroph abundance did increase by 2.45-fold, but the growth efficiency of methanotrophs was impaired at both higher temperature and CH_4 concentration and thus lacked the potential to reach the needed 2.64-fold increase in abundance to offset the greater CH_4 production induced by warming. These findings provide experimental evidence that methanotrophy will be unable to fully offset the increased CH_4 production induced by warming as their capacity will be limited through impaired growth efficiency.

Chapter 5 Conclusion and suggestions for future work

5.1 Long-term warming increases the efficiency of the methane cycle

Net CH_4 emissions are governed by the difference between CH_4 production (methanogenesis) and oxidation (methanotrophy). Therefore, understanding how these processes respond to warming in freshwaters is fundamental to predicting CH_4 emissions under current warming scenarios. Warming is expected to increase both the activity of methanogenesis and methanotrophy but whether these processes would be balanced and how it might affect the CH_4 emissions remains unknown. Here I show, using a freshwater pond experiment, that while long-term warming (+4 °C for 11 years) not only leads to increasingly greater CH_4 emissions from freshwater ecosystems but makes the CH_4 cycle more efficient at making CH_4 – a strong potential to drive a climate warming positive feedback.

In *Chapter 2*, I first demonstrated that, after 11 years of warming using our year-long, high-frequency (three times daily) measurements, CH_4 and CO_2 emissions have responded to warming in distinct ways – the CH_4 emission capacity, which can be represented by CH_4 emission at 15°C, has been increased in the warmed ponds relative to their ambient controls , but the CO_2 emission stayed the same – leading to an increased CH_4:CO_2 emission ratio and the global warming potential of carbon gases emitted. As the CH_4 emission capacity has increased, there was an ongoing divergence in CH_4 emissions between the warmed and ambient control ponds. Annual CH_4 emissions are now 2.4-fold higher from warmed compared to ambient ponds, far exceeding the predicted 1.61-fold increase due to temperature alone ($e^{\frac{\overline{E_{ME}}}{kT_W}-\frac{\overline{E_{ME}}}{kT_A}}$, where T_W and T_A are the mean annual temperatures of the warmed and ambient ponds (288.15 and 293.15 K, respectively), E_{ME} is the apparent activation energy of CH_4 emission (0.84 eV) and k is the Boltzmann constant (8.62×10^{-5} eV K^{-1})) (Allen, Gillooly

and Brown, 2005; Yvon-Durocher *et al.*, 2014). These observations clearly suggest that the CH_4 cycle has not responded to warming through a simple physiological change, but rather to shifts in the structure and activity of the methanogen community that will affect how changes in CH_4 emissions will be predicted under climate warming scenarios.

In this Chapter, I also demonstrate that the mesocosm ponds, in spite of being isolated and solely reliant on autochthony, are useful tools for understanding and predicting responses in ecosystem-level carbon cycling under current warming scenarios because 1, the sediment characteristics and carbon greenhouse gas emissions were comparable to natural ecosystems and 2, a meta-analysis for global CH_4 and CO_2 emission showed that warmer freshwater have a disproportionately higher capacity to emit CH_4, exactly as the mesocosm ponds predict.

In *Chapter 3*, I rationalized that, using a slurry microcosm experiment, the disproportionate increases in CH_4 emissions were driven by a substantial increase in the CH_4 production capacity of the sediments - the warmed pond sediments now producing 2.53-fold more CH_4 than the ambient ponds. As the methanogen abundance increased by 1.5-fold only in the warmed ponds relative to their ambient controls, the warmed methanogens were ~60% more efficient at making CH_4 and increased the ratio of CH_4 to CO_2 production, strongly indicating a shift in the structure of methanogen community. For example, the two most important pathways for CH_4 production in freshwaters are acetoclastic and hydrogenotrophic methanogenesis. Acetoclastic methanogenesis produces 50 % CH_4 and 50 % CO_2 while hydrogenotrophic methanogenesis produces CH_4 only (acetoclastic: $CH_3COOH \rightarrow CH_4+CO_2$; hydrogenotrophic: $4H_2+CO_2 \rightarrow CH_4+2H_2O$) (Liu and Whitman, 2008). The increases in both methanogen efficiency and CH_4 to CO_2 ratios, therefore, suggested a shift towards a hydrogenotrophic community. To test this hypothesis, the methanogen communities in both warmed and ambient ponds were analysed using molecular techniques, targeting a critical

functional gene for CH_4 production (*mcrA*) (Lever and Teske, 2015). In line with the hypothesis, there were significant shifts in two hydrogenotrophic genera between the warmed and ambient ponds, but no significant changes in any other methanogen group i.e. acetoclastic methanogens. Specifically, the relative abundance of the genus *Methanobacterium* increased significantly from 8.45 % to 13.24 % of the methanogen community, whereas, in contrast, *Methanospirillum* decreased from 31.31 % to 22.69 % between the warmed and ambient ponds, respectively. After 11 years of warming methanogen diversity was conserved, as its richness and evenness remained unchanged, but marginal changes in the relative abundance of *Methanobacterium* and *Methanospirillum* appear to drive changes in the relative contributions of acetoclastic and hydrogenotrophic methanogenesis – increasing CH_4 production and the ratio of CH_4 to CO_2 emitted.

Experiments with a range of methanogenic substrates, including hydrogen, acetate and methanol, were further performed to identify a mechanism for the changes in the methanogen community. All substrates enhanced CH_4 production compared to the controls; however, there was a significant preferential stimulation of CH_4 production by hydrogen in the warmed compared to ambient pond sediments. Short-term temperature manipulations of slurry microcosms were used to show that hydrogenotrophic methanogenesis had a significantly higher temperature sensitivity (apparent activation energy) than other methanogenic substrates (1.40 eV compared to 1.08 eV for acetoclastic methanogenesis). Thus, warming makes hydrogenotrophic methanogenesis more energetically favourable (Conrad, Schütz and Babbel, 1987) and could drive a shift towards a more hydrogenotrophic-based methanogen community.

Short-term (< 3 months) experiments in permafrost soils (Metje and Frenzel, 2007), paddy soils (Fey and Conrad, 2000; Conrad, Klose and Noll, 2009) and lake sediments

(Glissmann *et al.*, 2004; Nozhevnikova *et al.*, 2007) have shown that the relative contribution of hydrogenotrophic methanogenesis decreases at lower temperatures, primarily due to competition with homoacetoclastic bacteria for hydrogen and/or relatively low *in situ* hydrogen concentrations (Schulz, 1996; Nozhevnikova *et al.*, 1997; Kotsyurbenko, 2005). Hydrogenotrophic methanogens have been shown to dominate in tropical lake sediments and a further meta-analysis identified a permanent selection for hydrogenotrophic methanogens in warm environments (Conrad *et al.*, 2011; Wen *et al.*, 2017). Yet the interaction between microbial community ecology and warming gives rise to emergent properties and its effect on net CH_4 emission and CH_4 cycle efficiency is poorly understand. Here, however, I demonstrate for the first time that 11 years of warming of 4°C appears to favour hydrogenotrophic over acetoclastic CH_4 production, permanently altering the methanogen community composition by changing the relative abundances of two hydrogenotrophic genera, *Methanospirillum* and *Methanobacterium* and ultimately leading to a permanent increase in the ratio of produced and emitted CH_4 to CO_2.

Methanotrophy tends to be tightly coupled to CH_4 production, presumably because methanotrophs are often substrate limited in most natural systems (Frenzel, Thebrath and Conrad, 1990; Shelley *et al.*, 2015; Trimmer *et al.*, 2015). The percentage of CH_4 emission oxidized, calculated using the differences between production and emission, did increased from 92.08% in the ambient ponds to 94.68% in the warmed ponds (Table 5.1). However, in order for the CH_4 emission to remain the same under warming, the methanotrophy need to consume 97.85% of the CH_4 produced.

To identify the mechanism limiting the CH_4 oxidation capacity, in *Chapter 4*, I characterised the kinetic and temperature response of CH_4 oxidation. Even though the measured *ex situ* capacity to oxidise CH_4 was the same in both the warmed and ambient ponds,

there was a marked kinetic effect demonstrating a strong physiological response of the methanotroph community to increased CH_4 in the warmed ponds. As warming has increased CH_4 concentrations by 2.1-fold, the *in situ* CH_4 oxidation capacity would be 1.91-fold higher in the warmed ponds. There was a temperature effect too. The temperature sensitivity of CH_4 oxidation was the same in both the warmed and ambient ponds but with the 4 °C difference between the ponds, but an apparent activation energy of 0.57 eV would enable a 1.37-fold greater *in situ* CH_4 oxidation activity in the warmed ponds compared to the ambient controls. Altogether, 4°C warming and warming-induced increases in CH_4 concentrations could account for a 2.62-fold increase in *in situ* CH_4 oxidation capacity in the warmed ponds relative to their ambient controls (Table 5.1).

Methanotrophs are inactive while methane- or oxygen-starved (Roslev and King, 1995; Singh *et al.*, 2010). Oxygen penetrated into sediments for about 1 mm depth only because respiration consumes oxygen very quickly (Frenzel, Thebrath and Conrad, 1990). Therefore, methanotroph activity is confined to a thin, oxic zone at the sediment surface (Reim *et al.*, 2012). Cell-specific, CH_4 oxidation activity (at 15 °C per *pmoA* gene copy) in the warmed ponds was less than half that in the ambient controls and a large fraction, ~60 %, of methanotrophs appeared to be inactive. As oxygen penetration was ~40 % shallower in the warmed compared to ambient sediments, cell-specific methanotroph activity in the laboratory slurry microcosms might have been underestimated by counting inactive methanotrophs in the anoxic sediment layers. Combined, the kinetic effect, temperature effect and the effect of sampling the same depths accounted for 1.91-, 1.37- and 1.37- fold, of the increased CH_4 oxidation in the warmed ponds, respectively. Overall, measured *ex situ* CH_4 oxidation capacity is 3.59-fold higher in the warmed compared to ambient sediments, which agrees well with the field observations of a 3.8-fold increase (*see* Table 5.1 and further discussion there

in). However, this only accounts for 95% of the extra CH_4 production under warming and not the required 98% that would prevent the CH4 emission from increasing.

Whereas the increase in CH_4 production cannot be predicted from a simple physiological response to warming, it is feasible for its consumption through CH_4 oxidation as their community composition responded to warming differently. In contrast to changes seen in the methanogen community composition, the community composition of methanotrophs was the same in both the warmed and ambient ponds (comparison of the key functional gene for CH_4 oxidation (*pmoA*)). I propose that whereas warming makes hydrogenotrophic methanogenesis more energetically favourable, providing a mechanism to drive changes in the methanogen community, there is no such apparent mechanism to alter the methanotroph community. Methanotrophs use CH_4 as their sole carbon and energy source (Hanson and Hanson, 1996) and are usually strongly substrate limited *in situ* (Lofton, Whalen and Hershey, 2014; Shelley *et al.*, 2015). While increases in CH_4 availability support larger populations, the abundance of the whole community increases with no specific selection for a subset of the methanotroph community.

Though the CH_4 oxidizer abundance had increased by 2.45-fold in the warmed ponds over the ambient ponds (qPCR of the *pmoA* gene, t-test, $p<0.001$) but would need to increase by 2.64 to offset the greater warming-induced CH_4 production. To further investigate how warming may affect the growth of methanotrophs, I measured the fraction of CH_4 oxidized assimilated into biomass (carbon conversion efficiency (CCE)) as a proxy for methanotroph-growth-efficiency (Bastviken *et al.*, 2003; Trimmer *et al.*, 2015). I found that their CCE was indistinguishable between the warmed and ambient ponds but was suppressed in incubations at both higher CH_4 concentrations and higher temperatures, i.e., the exact conditions induced by warming. Therefore, under warming, methanotrophs grow by oxidising more CH_4 but

assimilating a smaller proportion of this carbon and therefore lack the potential to reach the required abundance to balance CH_4 production.

Our long-term experiment provides a comprehensive, mechanistic understanding of a potential positive climate warming feedback loop at the molecular microbiology level, up to whole, freshwater ecosystem CH_4 emissions (Figure 5.1). Warming preferentially selects for hydrogenotrophic methanogenesis, permanently increasing the global warming potential of the carbon gases emitted while, at the same time, limiting the capacity of methanotrophs through impaired growth. These apparent emergent properties in the freshwater CH_4 cycle under warming increase CH_4 emissions far beyond a simple physiological increase to rising temperatures alone that will affect how we predict a future CH_4 cycle as Earth continues to warm.

Table 5.5.1 Annual methane budget and sediment characteristics of the experimental ponds.

		Ambient	Warmed	Ratio (W/A)
Production	Methane production capacity at 15 °C[1] (MG_{T15}, μmol CH_4 m^{-2} d^{-1})	2795 (1092)	7086 (2767)	2.5
	Effect of 4 °C warming predicted using the apparent activation energy $\overline{E_{MP}}$ ($Effect_{warming}$)[2]	1	1.5	1.5
	Methane production capacity (totMG)[3]	2795	10274	**3.7**
	mcrA abundance (log_{10}(copy g^{-1}(wet sediments)))	6.59 (0.045)	6.77 (0.034)	1.5
	Cell-specific activity of methanogens (fmol CH_4 *mcrA*$^{-1}h^{-1}$)	0.35	0.59	1.7
Emission and proportion of CH_4 oxidized *in situ*	Annual methane emission (ME, μmol CH_4 m^{-2} d^{-1})	233 (1.0)	562 (1.1)	2.4
	Amount of methane oxidized *in situ*[4] (*in situ* totMO, μmol CH_4 m^{-2} d^{-1})	2563	9713	**3.8**
	Proportion of methane oxidized *in situ*[5] (MO%, %)	92	95	1.03
	Required proportion of CH_4 oxidized ($\%_{pred}$)[6]		**98**	
Oxidation	Kinetic effect of *in situ* methane concentrations ($Effect_{kinetic}$)[7]	1	1.9	1.9
	Effect of 4 °C warming predicted using apparent activation energy $\overline{E_{MO}}$ ($Effect_{warming}$)[2]	1	1.4	1.4
	Effect of sampling depth ($Effect_{sampling}$)[8]	1	1.4	1.4
	Methane oxidation capacity (*ex situ* totMO)[9]			**3.6**
	pmoA abundance (log_{10}(copy g^{-1}(wet sediments)))	3.99 (0.047)	4.38 (0.038)	2.45
	Required *pmoA* abundance to offset warming-induced methane production		2.64	
	Cell-specific activity of methanotrophs (pmol CH_4 *pmoA*$^{-1}h^{-1}$)	25.0	10.2	0.4
Sediment characteristic	Sediment % carbon	0.83 (0.089)	1.23 (0.13)	1.48
	Sediment % nitrogen	0.084 (0.0061)	0.11 (0.0010)	1.31
	Sediment C:N	9.37 (0.41)	10.40 (0.31)	1.11

Numbers given in the brackets are standard errors.

1. Methane production capacity at 15 °C was calculated by taking the exponential of the natural log-transformed methane production rate in equation (2) ($\overline{lnF(T_C)}$) and then converted from nmol g^{-1} h^{-1} to μmol CH_4 m^{-2} d^{-1} based upon sediment density (1,068,000 g m^{-3}) and depth (0.08 m) ($MG_{T15} = \overline{lnF(T_C)} \times 1000000 \times 24 \times$ sediment density × sediment depth).

2. Effect of 4 °C warming on methane production and oxidation was calculated from the apparent activation energies: $\overline{E_{MP}}$ and $\overline{E_{MO}}$ for methane production and oxidation, respectively (*see* equation (3.1), (4.2) and (4.3)). The apparent activation energies for methane production and oxidation in the warmed ponds are 0.68 eV and 0.57 eV, respectively, predicting a 1.5- and 1.4-fold increase in the methane production and oxidation, respectively.

3. In total, warming increased the methane production capacity in the warmed ponds by 3.7-fold ($totMG = MG_{T15} \times Effect_{warming}$).

4. Amount of methane oxidized *in situ* is the difference between the methane production capacity and the annual methane emission (i.e., *in situ* totMO = totMG - ME)

5. Proportion of oxidized methane is the percentage of the annual methane emission to the methane production capacity at annual average temperatures (i.e., MO% = (totMG - ME)/ totMG ×100%).

6. Required proportion of methane oxidation is the required proportion of CH4 oxidation in the warmed ponds that would prevent methane emission form increasing (i.e., $(totMG_{warmed} - ME_{ambient})/ totMG_{warmed} \times 100\%$).

7. Methane oxidation capacities at *in situ* methane concentrations were calculated using Michaelis-Menten model based on the methane concentrations in the pond water (*see* Figure 4.1 and equation 4.1 in *Chapter 4*).

8. Oxygen penetrated 4.86 and 6.67 mm into the warmed and ambient pond sediments, respectively (*see* Figure 4.5 in *Chapter 4*). Oxic depths were used as proxy for the active methanotrophy layer. Therefore, the effect of sampling the same depths in the warmed and ambient ponds for methane oxidation capacity measurements is $\text{Effect}_{\text{sampling}}=\frac{20\ mm}{4.86\ mm}/\frac{20\ mm}{6.67\ mm}$.

9. In total, warming increased the measured methane oxidation capacity in the warmed ponds by 3.59-fold ($\text{Effect}_{\text{kinetic}}\times\text{Effect}_{\text{warming}}\times\text{Effect}_{\text{sampling}}$), accounting for the discrepancy between predicted and measured methane emissions *in situ* (*ex situ* totMG = *in situ* totMO).

In situ methane oxidation is limited by the diffusion of methane and oxygen. I acknowledge that by mixing the sediments and $^{13}C\text{-}CH_4$ in the laboratory slurry measurements, the methane oxidation capacity in the sediments from both the warmed and ambient ponds would have been optimized. Therefore, I represent here, for the *ex situ* methane oxidation capacity, only the ratio between the warmed and ambient pond sediments (ratio W/A) to show that the kinetic effect and temperature effect increased the methane oxidation capacity by 1.9- and 1.4-fold in the warmed ponds relative to their ambient counterparts, respectively. In addition, if the depth of oxygen penetration serves as a proxy for active methanotrophy layer, altogether, the *ex situ* methane oxidation capacity in the warmed ponds would be 3.6-fold higher than in the ambient controls, close to the increase in methane production in the warmed ponds i.e. 3.7-fold, as well as the predicted amount of methane oxidized *in situ* i.e. 3.8-fold.

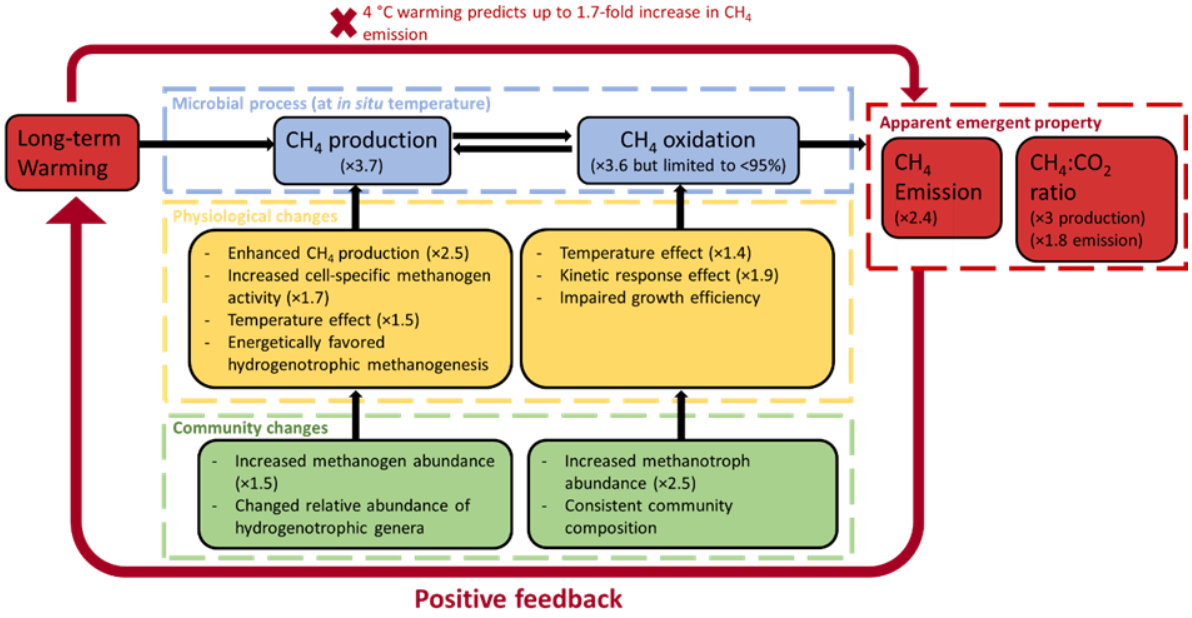

Figure 5.1 Warming enhances methanogenesis over methanotrophy. Despite the consistent temperature sensitivity of CH_4 production, CH_4 emissions cannot be predicted by temperature alone and the ratio CH_4 to CO_2 rises – emergent properties in the overall CH_4 cycle (red arrow). The CH_4 cycle is regulated by microbial CH_4 production and oxidation together (blue rectangle). In order to understand and predict how the CH_4 cycle will respond to warming, it is essential to elucidate any changes in both physiology (yellow rectangle) and community (green rectangle) for both methanogens and methanotrophs under warming scenarios.

5.2 Future directions

This thesis has demonstrated, from microbial community level to ecosystem CH_4 emission, a potential positive feedback mechanism through climate-change. I demonstrated that, 11 years of warming enhanced methanogenesis over methanotrophy, leading to a greater global warming potential of greenhouse gas emitted. The changes have been linked to shifts in methanogenic archaeal community under warming while the methanotrophic bacterial community was conserved. These experimental results strongly indicate that as Earth continues to warm, aquatic ecosystems will emit increasingly more CH_4 to the atmosphere than would be seen in a short-term physiological response to rising temperature alone – serving a positive feedback loop to exacerbate warming.

Previous research mainly focuses on parameterizing biogeochemical processes to develop predictive climate models (Cao and Woodward, 1998; Enquist *et al.*, 2003; Van Groenigen, Osenberg and Hungate, 2011). Microorganisms regulate the biogeochemical processes but are rarely included in predictive climate model because our understanding of their responses to climate change is limited (Lipson *et al.*, 2009; Allison, Wallenstein and Bradford, 2010).

Climate change can affect the biogeochemical processes by either altering their functioning of existing microbial communities or by restructuring the communities by selecting adaptive species (Schimel and Gulledge, 1998; Singh *et al.*, 2010). In this thesis, I demonstrate that methanogen and methanotroph, the two components regulating CH_4 cycle, respond to long-term warming in different ways.

For methanotrophs, their ability to oxidize CH_4 is predictable based on the temperature dependence (Figure 5.2 a). Thus the control mechanism of temperature on CH_4 oxidation rate

remains the same (i.e., the CH_4 oxidation rates would be the same at the same temperature). In line with the constant control mechanism, the methanotroph community stay unchanged. In contrast to the conserved methanotroph community structure, shifts in methanogenic archaeal community under warming have altered the fundamental control mechanism of temperature on CH_4 production rates. Now after 11 years of warming, the shifts in the relative abundances of two hydrogenotrophic methanogen genera, *Methanobacterium* and *Methanospirillum* were observed, suggesting an altered methanogenic function from acetoclastic to hydrogenotrophic methanogenesis. Hydrogenotrophic methanogenesis, which reduces CO_2 to produce CH_4, is more energetically favoured at higher temperatures. Thus, the CH_4 production can no longer be predicted by a simple physiological response by rising temperature alone. Indeed, plotting CH_4 production rates against standardized temperature demonstrated, despite of the consistent slope which represents the apparent activation energy, a clear separation on the intercept – CH_4 production capacity standardized to 15 °C (here at 0) (Figure 5.2 b). Thus, there is a discontinuity in the response of CH_4 production to warming, which can be rationalized by a shift in the methanogen community towards more hydrogenotrophic.

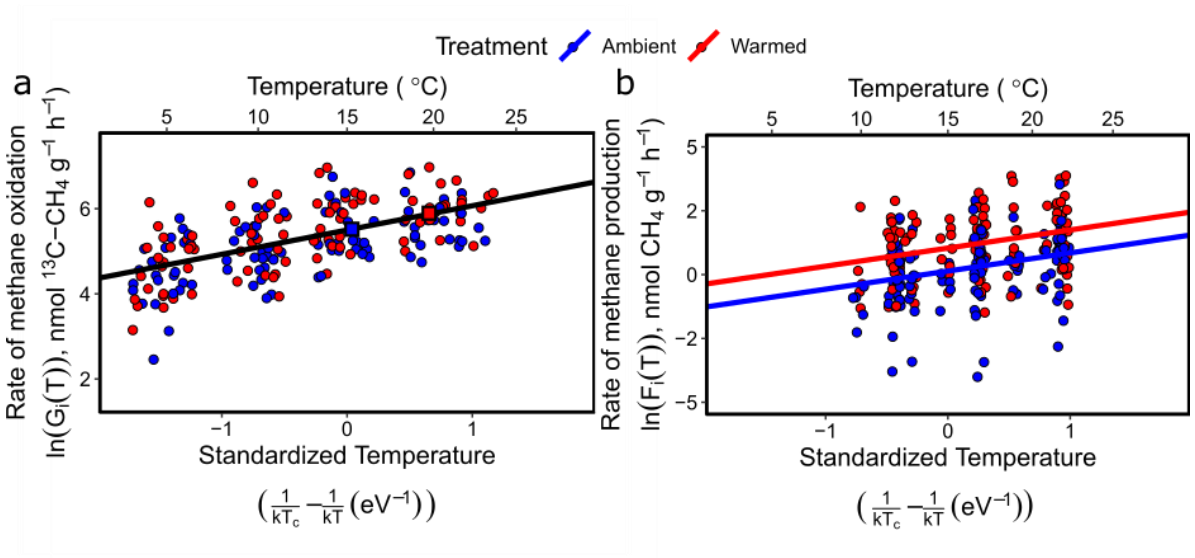

Figure 5.2. The control mechanisms of temperature over the methanotrophy and methanogenesis. a, The control mechanism of temperature over methanotrophy was the same between long-term warmed ponds and their ambient controls. The CH_4 oxidation rates under warming can be predicted by temperature. **b,** The control mechanism of temperature over methanogenesis was different between the long-term warmed ponds and their ambient controls. The CH_4 production rates under warming cannot be predicted by temperature. Squares represent the increase in CH_4 oxidation predicted by temperature alone. No such prediction can be made for CH_4 production as the response to warming is discontinuous.

Recent researches have demonstrated that climate warming may substantially increase the CH_4 emissions from lakes, ponds, permafrost and wetlands (Bridgham *et al.*, 2013; Schuur *et al.*, 2015; Wik *et al.*, 2016). Although warming is expected to increase the metabolic rates of both methanogen and methanotrophs, whether the balance between these two components would be altered and whether the CH_4 emission would be changed remains unknown. Most experiments tested the physiological responses of methanogenesis and methanotrophy to warming (Trimmer *et al.*, 2015), but the results in this thesis suggest that shifts in methanogen community towards more efficient methanogenic pathways at higher temperatures could augment the CH_4 production rates beyond the physiological response predicted by temperature alone. In contrast, there is no mechanism selecting optimal methanotrophs. The

methanotroph community was conserved, therefore lacks the potential to offset the warming induced increase in CH_4 production. The different response of methanogen and methanotroph, in terms of their community structure, lead to a continuous increase in CH_4 emission in excess of prediction by temperature alone, providing a positive-feedback mechanism between CH_4 cycle and climate warming.

This conclusion – that as Earth warms freshwaters will emit increasingly more CH_4 to the atmosphere in a positive feedback warming loop – is further vindicated by a meta-analysis of global CH_4 emissions across a natural gradient of temperature. Natural-logarithm-transformed CH_4 emission at 15 °C for each site, i.e., the CH_4 emission capacity, was positively correlated to average annual temperature (Figure 5.3 a), exactly as the long-term mesocosm ponds predict – naturally warmer freshwaters have a disproportionately higher capacity to make and emit CH_4 (Figure 5.4 a). Indeed, the CH_4 emission capacity in the warmed and ambient ponds maps precisely onto the increased capacity of naturally warmer freshwaters to emit CH_4 (blue and read circles on Figure 5.3 a). In contrast, CO_2 emissions appeared to be conserved – no correlation can be made between the CO_2 emission capacity, i.e., the CO_2 emission at 15 °C, and average annual temperature for each site (Figure 5.3 b). In line with the global CO_2 emission, the CO_2 emission capacity was undistinguishable between the warmed and ambient ponds (Figure 5.4 b) and agrees well with the conserved CO_2 emission across a natural temperature gradient CO_2 (blue and red circles on Figure 5.3 b).

The disproportionate increase in CH_4 emission is driven by the substantial increase in CH_4 production through an alteration to the methanogen community induced by warming, yet the mechanism to constrain CO_2 emission remains unknown. As warming seem to decrease respiration in soils through fungal and bacterial abundance declination and community

structure alteration (Allison and Treseder, 2008), the conserved CO_2 emission may be attributed to a functional redundancy of respiration after long-term warming, i.e., the community structure may be changed but the changed community may function redundantly and result in the same CO_2 emission capacity (Allison and Martiny, 2008). Given that CH_4 is a more potent greenhouse gas than CO_2, the distinct responses of CH_4 and CO_2 to climate warming will increase the global warming potential by emitting disproportionately high CH_4 relative to CO_2.

Overall, microorganisms drive Earth's biogeochemical processes. This thesis reveals that microorganisms can respond to climate warming in two ways: 1) by altering the physiology of existing microbial communities and/or 2) by restructuring the communities through selecting adaptive species. The first scenario predicts biogeochemical processes through physiological responses, e.g., predictable increase in methanotrophy under warming; the second scenario, nevertheless, increases biogeochemical processes beyond a simple prediction by physiology alone, e.g., increased methanogenesis under warming far in excess of prediction by temperature alone. Different responses under climate warming can ultimately disconnect the balance of biogeochemical processes, which could accelerate climate warming in a positive feedback loop. Mechanistic understanding of microorganisms in terms of physiology and community structure is therefore essential to improve our ability to predict feedback between fluxes of potent greenhouse gases and climate warming. The work presented in this thesis I hope to form the basis of my future research.

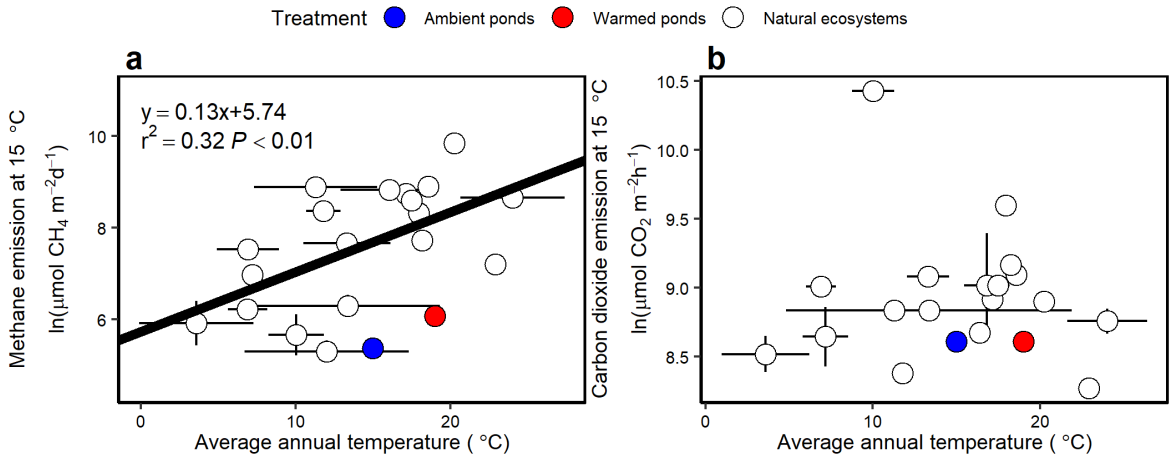

Figure 5.3 Correlations of average annual temperature with carbon gases emissions at 15 °C for globally distributed ecosystems (*n*=19). a, Average annual site temperature is positively correlated with CH_4 emissions at 15 °C (P<0.01). The blue and red symbols mark the average CH_4 emission at 15 °C from our experimental ponds against the average annual temperature in ponds. After 11 years of warming, the CH_4 emission at 15 °C has increased by 2-fold, agreeing with the relationship between global CH_4 emissions and average annual temperatures. **b,** Carbon dioxide emissions at 15 °C is conserved across globally distributed ecosystems (P=0.81), in line with the indistinguishable carbon dioxide emissions at 15 °C from the long-term warmed ponds (red) and their ambient controls (blue).

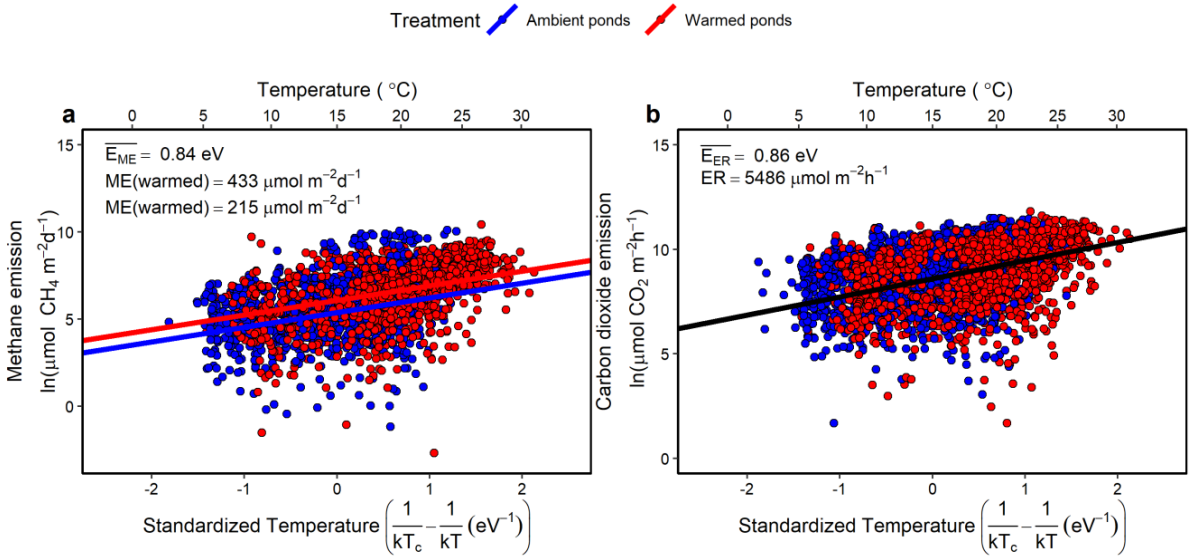

Figure 5.4 Temperature dependence and average rates of carbon gas emissions from experimental ponds after 11 years of warming. a, The temperature dependence of CH_4 emissions, calculated as the apparent activation energy, was the same from both the warmed (red) and ambient (blue) ponds at 0.84 eV (likelihood ratio test, χ^2=0.08, P=0.78) but after 11 years of warming, the average rate of CH_4 emission, at 15 °C (here 0 for standardized temperature), has increased by 2 fold (likelihood ratio test, χ^2=5.53, P<0.05). **b,** The temperature dependence of CO_2 emissions was the same from both the warmed and ambient ponds, with an apparent activation energy at 0.95 eV (likelihood ratio test, χ^2=0.095, P=0.75). In contrast to CH_4 emissions, the average rate of carbon dioxide emission at 15 °C was the same in both the warmed and ambient ponds (likelihood ratio test, χ^2=2.85, P=0.09). The CH_4 and CO_2 emissions were measured three times per day for each pond using high-resolution chambers. Each data point for the CH_4 emission is the integration of the CH_4 fluxes over 24 hours for each pond. Each data point for CO_2 emission is the CO_2 efflux which mainly happened in night.

5.3 Parallel research projects

The role of rivers as important components in global CH_4 budgets is increasingly recognized. Yet the controls, e.g., temperature, organic carbon and their interactions on CH_4 production is poorly understood. Aside from the research presented within this thesis, I explored the effects of organic carbon and temperature on CH_4 production in the sediments

from 8 rivers on two UK dominant geological types (chalk-gravel and sandy). Combined with results from experiments carried out by Dr. Louis Olde in other 6 UK rivers, we find that the temperature sensitivity of CH_4 production was very conserved for an activation energy of around 1.0 eV across geological types (i.e., chalk-gravel or sandy riverbeds) and patch types (i.e., main channel, marginal or vegetated). In contrast to the consistent temperature sensitivity, the CH_4 production in the chalk-gravel were higher than the sandy riverbed, driven by its higher sediment organic carbon content. Organic carbon content had a stronger effect on CH_4 production than temperature: the CH_4 production capacity is projected to increase by 1.7-fold under current 4 °C warming scenario but to increase by 2.6-fold for only 1 % rise in sediment organic carbon content. Furthermore, the river sediments had a very large spare capacity not only to produce CH_4 with immediate methanogenic substrate (i.e., acetate and hydrogen) but also to convert complex organic substance into acetate for further CH_4 production. Our results suggest that increased organic carbon due to human disturbance, would increase the CH_4 production in the riverbed sediments and need to be included in future climate mitigation and land use strategies. We are currently preparing the results for publication.

References

Allen, A. P., Gillooly, J. F. and Brown, J. H. (2005) 'Linking the global carbon cycle to individual metabolism', *Functional Ecology*, 19(2), pp. 202–213. doi: 10.1111/j.1365-2435.2005.00952.x.

Allison, S. D. and Martiny, J. B. H. (2008) 'Resistance, resilience, and redundancy in microbial communities', *Proceedings of the National Academy of Sciences*, 105, pp. 11512–11519. doi: 10.1073/pnas.0801925105.

Allison, S. D. and Treseder, K. K. (2008) 'Warming and drying suppress microbial activity and carbon cycling in boreal forest soils', *Global Change Biology*, 14(12), pp. 2898–2909. doi: 10.1111/j.1365-2486.2008.01716.x.

Allison, S. D., Wallenstein, M. D. and Bradford, M. A. (2010) 'Soil-carbon response to warming dependent on microbial physiology', *Nature Geoscience*, 3(5), pp. 336–340. doi: 10.1038/ngeo846.

Anderson, M. J. (2017) 'Permutational Multivariate Analysis of Variance (PERMANOVA)', in *Wiley StatsRef: Statistics Reference Online*. UK: Wiley, pp. 1–15.

Aselmann, I. and Crutzen, P. J. (1989) 'Global distribution of natural freshwater wetlands and rice paddies, their net primary productivity, seasonality and possible methane emissions', *Journal of Atmospheric Chemistry*, 8(4), pp. 307–358. doi: 10.1007/BF00052709.

Balcombe, P., Speirs, J. F., Brandon, N. P. and Hawkes, A. D. (2018) 'Methane emissions: choosing the right climate metric and time horizon', *Environmental Science: Processes and Impacts*. Royal Society of Chemistry, 20(10), pp. 1323–1339. doi: 10.1039/c8em00414e.

Baldocchi and Dennis (2016a) 'AmeriFlux US-Myb Mayberry Wetland'. doi: 10.17190/AMF/1246139.

Baldocchi and Dennis (2016b) 'AmeriFlux US-Tw1 Twitchell Wetland West Pond'. doi: 10.17190/AMF/1246147.

Baldocchi and Dennis (2016c) 'AmeriFlux US-Tw4 Twitchell East End Wetland'. doi: 10.17190/AMF/1246151.

Baldocchi and Dennis (2016d) 'AmeriFlux US-Twt Twitchell Island'. doi: 10.17190/AMF/1246140.

Baldocchi and Dennis (2018) 'AmeriFlux US-Sne Sherman Island Restored Wetland'. doi: 10.17190/AMF/1418684.

Barton, K. (2018) 'MuMIn: Multi-Model Inference'. Available at: https://cran.r-project.org/package=MuMIn.

Bastviken, D., Cole, J., Pace, M. and Tranvik, L. (2004) 'Methane emissions from lakes: Dependence of lake characteristics, two regional assessments, and a global estimate', *Global Biogeochemical Cycles*, 18(4), pp. 1–12. doi: 10.1029/2004GB002238.

Bastviken, D., Ejlertsson, J., Sundh, I. and Tranvik, L. (2003) 'Methane as a source of carbon and energy for lake pelagic food webs', *Ecology*, 84(4), pp. 969–981.

Bastviken, D., Tranvik, L. J., Downing, J. A., Crill, P. M. and Enrich-Prast, A. (2011) 'Freshwater methane emissions offset the continental carbon sink', *Science*, 331(6013), p. 50. doi: 10.1126/science.1196808.

Bates, D. M., Maechler, M., Bolker, B. and Walker, S. (2015) 'Fitting linear mixed-effects models using lme4', *Journal of Statistical Software*, 67, pp. 1–48. doi: 10.1177/009286150103500418.

Battin, T. J., Luyssaert, S., Kaplan, L. A., Aufdenkampe, A. K., Richter, A. and Tranvik, L. J. (2009) 'The boundless carbon cycle', *Nature Geoscience*, 2(9), pp. 598–600. doi: 10.1038/ngeo618.

Bell, T., Newman, J. A., Silverman, B. W., Turner, S. L. and Lilley, A. K. (2005) 'The contribution of species richness and composition to bacterial services', *Nature*, 436(7054), pp. 1157–1160. doi: 10.1038/nature03891.

Bellisario, L. M., Bubier, J. L., Moore, T. R. and Chanton, J. P. (1999) 'Controls on CH_4 emissions from a northern peatland', *Global Biogeochemical Cycles*, 13(1), pp. 81–91. doi: 10.1029/1998GB900021.

Bender, M. and Conrad, R. (1992) 'Kinetics of CH_4 oxidation in oxic soils exposed to ambient air or high CH_4 mixing ratios', *FEMS Microbiology Letters*, 101(4), pp. 261–270. doi: 10.1111/j.1574-6968.1992.tb05783.x.

Benton, T. G., Solan, M., Travis, J. M. J. and Sait, S. M. (2007) 'Microcosm experiments can inform global ecological problems', *Trends in Ecology & Evolution*, 22(10), pp. 516–521. doi: 10.1016/j.tree.2007.08.003.

Bier, R. L., Bernhardt, E. S., Boot, C. M., Graham, E. B., Hall, E. K., Lennon, J. T., Nemergut, D. R., Osborne, B. B., Ruiz-González, C., Schimel, J. P., Waldrop, M. P. and Wallenstein, M. D. (2015) 'Linking microbial community structure and microbial processes: An empirical and conceptual overview', *FEMS Microbiology Ecology*, 91(10), pp. 1–11. doi: 10.1093/femsec/fiv113.

Bohrer and Gil (2016) 'AmeriFlux US-ORv Olentangy River Wetland Research Park'. doi: 10.17190/AMF/1246135.

Bohrer and Gil (2018) 'AmeriFlux US-OWC Old Woman Creek'. doi: 10.17190/AMF/1418679.

Bourne, D. G., McDonald, I. R. and Murrell, J. C. (2001) 'Comparison of *pmoA* PCR Primer Sets as Tools for Investigating Methanotroph Diversity in Three Danish Soils', *Applied and Environmental Microbiology*, 67(9), pp. 3802–3809. doi: 10.1128/AEM.67.9.3802-3809.2001.

Bradford, M. A. (2013) 'Thermal adaptation of decomposer communities in warming soils', *Frontiers in Microbiology*, 4, pp. 1–16. doi: 10.3389/fmicb.2013.00333.

Bridgham, S. D., Cadillo-Quiroz, H., Keller, J. K. and Zhuang, Q. (2013) 'Methane emissions from wetlands: Biogeochemical, microbial, and modeling perspectives from local to global scales', *Global Change Biology*, 19(5), pp. 1325–1346. doi: 10.1111/gcb.12131.

Brown, J. H., Gillooly, J. F., Allen, A. P., Savage, V. M. and West, G. B. (2004) 'Toward a metabolic theory of ecology', *Ecology*, 85(7), pp. 1771–1789. doi: 10.1890/03-9000.

Burnham, K. P. and Anderson, D. R. (2002) *Model Selection and Multimodel Inference: A Practical Information-Theoretic Approach (2nd ed)*, *Ecological Modelling*. doi: 10.1016/j.ecolmodel.2003.11.004.

Callahan, B. J., McMurdie, P. J. and Holmes, S. P. (2017) 'Exact sequence variants should replace operational taxonomic units in marker-gene data analysis', *ISME Journal*, 11(12), pp. 2639–2643. doi: 10.1038/ismej.2017.119.

Callahan, B. J., McMurdie, P. J., Rosen, M. J., Han, A. W., Johnson, A. J. A. and Holmes, S. P. (2016) 'DADA2: High-resolution sample inference from Illumina amplicon data', *Nature Methods*, 13(7), pp. 581–583. doi: 10.1038/nmeth.3869.

Cao, M. K. and Woodward, F. I. (1998) 'Dynamic responses of terrestrial ecosystem carbon cycling to global climate change', *Nature*, 393(6682), pp. 249–252. doi: Doi 10.1038/30460.

Caporaso, J. G., Kuczynski, J., Stombaugh, J., Bittinger, K., Bushman, F. D., Costello, E. K., Fierer, N., Peña, A. G., Goodrich, J. K., Gordon, J. I., Huttley, G. A., Kelley, S. T., Knights, D., Koenig, J. E., Ley, R. E., Lozupone, C. A., McDonald, D., Muegge, B. D., Pirrung, M., Reeder, J., Sevinsky, J. R., Turnbaugh, P. J., Walters, W. A., Widmann, J., Yatsunenko, T., Zaneveld, J. and Knight, R. (2010) 'QIIME allows analysis of high-throughput community sequencing data', *Nature Methods*, 7(5), pp. 335–336. doi: 10.1038/nmeth.f.303.

Cardinale, B. J., Duffy, J. E., Gonzalez, A., Hooper, D. U., Perrings, C., Venail, P., Narwani, A., Mace, G. M., Tilman, D., Wardle, D. A., Kinzig, A. P., Daily, G. C., Loreau, M., Grace, J. B., Larigauderie, A., Srivastava, D. S. and Naeem, S. (2012) 'Biodiversity loss and its impact on humanity', *Nature*, 486, pp. 59–67. doi: 10.1038/nature11148.

Chen and Jiquan (2016a) 'AmeriFlux US-CRT Curtice Walter-Berger cropland'. doi: 10.17190/AMF/1246156.

Chen and Jiquan (2016b) 'AmeriFlux US-WPT Winous Point North Marsh'. doi: 10.17190/AMF/1246155.

Chin, K. J., Lukow, T. and Conrad, R. (1999) 'Effect of temperature on structure and function of the methanogenic archaeal community in an anoxic rice field soil', *Applied and Environmental Microbiology*, 65(6), pp. 2341–2349.

Ciais, P., Sabine, C., Bala, G., Bopp, L., Brovkin, V., Canadell, J., Chhabra, A., DeFries, R., Galloway, J., Heimann, M. and others (2014) 'Carbon and other biogeochemical cycles', in *Climate change 2013: the physical science basis. Contribution of Working Group I to the Fifth Assessment Report of the Intergovernmental Panel on Climate Change*. Cambridge University Press, pp. 465–570.

Conrad, R. (1999) 'Contribution of hydrogen to methane production and control of hydrogen concentrations in methanogenic soils and sediments', *FEMS Microbiology Ecology*, 28(3), pp. 193–202. doi: 10.1016/S0168-6496(98)00086-5.

Conrad, R., Bak, F., Seitz, H. J., Thebrath, B., Mayer, H. P. and Schütz, H. (1989) 'Hydrogen turnover by psychrotrophic homoacetogenic and mesophilic methanogenic bacteria in anoxic paddy soil and lake sediment', *FEMS Microbiology Letters*, 62(5), pp. 285–293. doi: 10.1016/0378-1097(89)90010-4.

Conrad, R., Klose, M. and Noll, M. (2009) 'Functional and structural response of the methanogenic microbial community in rice field soil to temperature change', *Environmental Microbiology*, 11(7), pp. 1844–1853. doi: 10.1111/j.1462-2920.2009.01909.x.

Conrad, R., Noll, M., Claus, P., Klose, M., Bastos, W. R. and Enrich-Prast, A. (2011) 'Stable carbon isotope discrimination and microbiology of methane formation in tropical anoxic lake sediments', *Biogeosciences*, 8(3), pp. 795–814. doi: 10.5194/bg-8-795-2011.

Conrad, R., Schütz, H. and Babbel, M. (1987) 'Temperature limitation of hydrogen turnover and methanogenesis in anoxic paddy soil', *FEMS Microbiology Letters*, 45(5), pp. 281–289. doi: 10.1016/0378-1097(87)90005-X.

Crawford, J. T. and Stanley, E. H. (2016) 'Controls on methane concentrations and fluxes in streams draining human-dominated landscapes', *Ecological Applications*, 26(5), pp. 1581–1591. doi: 10.1890/15-1330.

Davidson, T. A., Audet, J., Jeppesen, E., Landkildehus, F., Lauridsen, T. L., Søndergaard, M. and Syväranta, J. (2018) 'Synergy between nutrients and warming enhances methane ebullition from experimental lakes', *Nature Climate Change*. Springer US, 8(2), pp. 156–160. doi: 10.1038/s41558-017-0063-z.

Dean, J. F., Middelburg, J. J., Röckmann, T., Aerts, R., Blauw, L. G., Egger, M., Jetten, M. S. M., de Jong, A. E. E., Meisel, O. H., Rasigraf, O., Slomp, C. P., in't Zandt, M. H. and Dolman, A. J. (2018) 'Methane Feedbacks to the Global Climate System in a Warmer World', *Reviews of Geophysics*, 56(1), pp. 207–250. doi: 10.1002/2017RG000559.

Desai and Ankur (2016a) 'AmeriFlux US-Los Lost Creek'. doi: 10.17190/AMF/1246071.

Desai and Ankur (2016b) 'AmeriFlux US-PFa Park Falls/WLEF'. doi: 10.17190/AMF/1246090.

Deutzmann, J. S., Wörner, S. and Schink, B. (2011) 'Activity and Diversity of Methanotrophic Bacteria at Methane Seeps in Eastern Lake Constance Sediments', *Applied and Environmental Microbiology*, 77(8), pp. 2573–2581. doi: 10.1128/AEM.02776-10.

Dinsmore, K. J., Billett, M. F. and Dyson, K. E. (2013) 'Temperature and precipitation drive temporal variability in aquatic carbon and GHG concentrations and fluxes in a peatland catchment', *Global Change Biology*, 19(7), pp. 2133–2148. doi: 10.1111/gcb.12209.

Duc, N. T., Crill, P. and Bastviken, D. (2010) 'Implications of temperature and sediment characteristics on methane formation and oxidation in lake sediments', *Biogeochemistry*, 100(1–3), pp. 185–196. doi: 10.1007/s10533-010-9415-8.

Dunfield, P., knowles, R., Dumont, R. and Moore, T. R. (1993) 'Methane production and consumption in temperate and subarctic peat soils: Response to temperature and pH', *Soil Biology and Biochemistry*, 25(3), pp. 321–326. doi: 10.1016/0038-0717(93)90130-4.

Enquist, B. J., Economo, E. P., Huxman, T. E., Allen, A. P., Ignace, D. D. and Gillooly,

J. F. (2003) ‘Scaling metabolism from organisms to ecosystems’, *Nature*, 423(6940), pp. 639–642. doi: 10.1038/nature01671.

Faust, K. and Raes, J. (2012) ‘Microbial interactions: from networks to models’, *Nature Reviews Microbiology*, 10(8), pp. 538–550. doi: 10.1038/nrmicro2832.

Fey, A. and Conrad, R. (2000) ‘Effect of Temperature on Carbon and Electron Flow and on the Archaeal Community in Methanogenic Rice Field Soil’, *Applied and Environmental Microbiology*, 66(11), pp. 4790–4797. doi: 10.1128/AEM.66.11.4790-4797.2000.

Freitag, T. E., Toet, S., Ineson, P. and Prosser, J. I. (2010) ‘Links between methane flux and transcriptional activities of methanogens and methane oxidizers in a blanket peat bog’, *FEMS Microbiology Ecology*, 73(1), pp. 157–165. doi: 10.1111/j.1574-6941.2010.00871.x.

Frenzel, P., Thebrath, B. and Conrad, R. (1990) ‘Oxidation of methane in the oxic surface layer of a deep lake sediment (Lake Constance)’, *FEMS Microbiology Letters*, 73(2), pp. 149–158. doi: 10.1016/0378-1097(90)90661-9.

Frey, S. D., Drijber, R., Smith, H. and Melillo, J. (2008) ‘Microbial biomass, functional capacity, and community structure after 12 years of soil warming’, *Soil Biology and Biochemistry*, 40(11), pp. 2904–2907. doi: 10.1016/j.soilbio.2008.07.020.

Friborg, T., Soegaard, H., Christensen, T. R., Lloyd, C. R. and Panikov, N. S. (2003) ‘Siberian wetlands: Where a sink is a source’, *Geophysical Research Letters*, 30(21), pp. 1999–2002. doi: 10.1029/2003GL017797.

Frolking, S., Roulet, N. and Fuglestvedt, J. (2006) ‘How northern peatlands influence the Earth’s radiative budget: Sustained methane emission versus sustained carbon sequestration’, *Journal of Geophysical Research: Biogeosciences*, 111(1), pp. 1–10. doi: 10.1029/2005JG000091.

Gamfeldt, L., Hillebrand, H. and Jonsson, P. R. (2008) ‘Multiple functions increase the importance of biodiversity for overall ecosystem functioning’, *Ecology*, 89(5), pp. 1223–1231. doi: 10.1007/978-3-319-30427-4_7.

Gillooly, J. F., Allen, A. P., Savage, V. M., Charnov, E. L., West, G. B. and Brown, J. H. (2006) ‘Response to Clarke and Fraser: Effects of temperature on metabolic rate’, *Functional Ecology*, 20(2), pp. 400–404. doi: 10.1111/j.1365-2435.2006.01110.x.

Gillooly, J. F., Brown, J. H., West, G. B., Savage, V. M. and Charnov, E. L. (2001) ‘Effects of size and temperature on metabolic rate.’, *Science (New York, N.Y.)*, 293(5538), pp. 2248–51. doi: 10.1126/science.1061967.

Girvan, M. S., Campbell, C. D., Killham, K., Prosser, J. I. and Glover, L. A. (2005) ‘Bacterial diversity promotes community stability and functional resilience after perturbation’, *Environmental Microbiology*, 7(3), pp. 301–313. doi: 10.1111/j.1462-2920.2004.00695.x.

Glissmann, K., Chin, K. J., Casper, P. and Conrad, R. (2004) ‘Methanogenic pathway and archaeal community structure in the sediment of eutrophic Lake Dagow: Effect of temperature’, *Microbial Ecology*, 48(3), pp. 389–399. doi: 10.1007/s00248-003-2027-2.

Gómez, P. and Buckling, A. (2013) ‘Real-time microbial adaptive diversification in

soil', *Ecology Letters*, 16(5), pp. 650–655. doi: 10.1111/ele.12093.

Griffiths, B. S., Kuan, H. L., Ritz, K., Glover, L. A., McCaig, A. E. and Fenwick, C. (2004) 'The relationship between microbial community structure and functional stability, tested experimentally in an upland pasture soil', *Microbial Ecology*, 47(1), pp. 104–113. doi: 10.1007/s00248-002-2043-7.

Van Groenigen, K. J., Osenberg, C. W. and Hungate, B. A. (2011) 'Increased soil emissions of potent greenhouse gases under increased atmospheric CO_2', *Nature*, 475(7355), pp. 214–216. doi: 10.1038/nature10176.

Gudasz, C., Bastviken, D., Steger, K., Premke, K., Sobek, S. and Tranvik, L. J. (2010) 'Temperature-controlled organic carbon mineralization in lake sediments', *Nature*, 466(7305), pp. 478–481. doi: 10.1038/nature09186.

Hall, E. K., Bernhardt, E. S., Bier, R. L., Bradford, M. A., Boot, C. M., Cotner, J. B., Giorgio, P. A., Evans, S. E., Graham, E. B., Jones, S. E., Lennon, J. T., Locey, K. J., Nemergut, D., Osborne, B. B., Rocca, J. D., Schimel, J. P., Waldrop, M. P. and Wallenstein, M. D. (2018) 'Understanding how microbiomes influence the systems they inhabit', *Nature Microbiology*, 3, pp. 977–982. doi: 10.1038/s41564-018-0201-z.

Hanson, R. S. and Hanson, T. E. (1996) 'Methanotrophic bacteria', *Microbiological Reviews*, 60(2), pp. 439–471. doi: 10.1002/0471263397.env316.

Hartmann, D. L., Klein Tank, A. M. G., Rusticucci, M., Alexander, L. V., Brönnimann, S., Charabi, Y. A. R., Dentener, F. J., Dlugokencky, E. J., Easterling, D. R., Kaplan, A., Soden, B. J., Thorne, P. W., Wild, M. and Zhai, P. (2013) 'Observations: Atmosphere and Surface', in Intergovernmental Panel on Climate Change (ed.) *Climate Change 2013 - The Physical Science Basis*. Cambridge: Cambridge University Press, pp. 159–254. doi: 10.1017/CBO9781107415324.008.

Hedges, J. I. and Stern, J. H. (1984) 'Carbon and nitrogen determinations of carbonate-containing solids', *Limnology and Oceanography*, 29(3), pp. 657–663. doi: 10.4319/lo.1984.29.3.0657.

Helbig, M., Chasmer, L. E., Kljun, N. C., Quinton, W. L., Treat, C. C. and Sonnentag, O. (2017) 'The positive net radiative greenhouse gas forcing of increasing methane emissions from a thawing boreal forest-wetland landscape', *Global Change Biology*, 23(6), pp. 2413–2427. doi: 10.1111/gcb.13520.

Ho, A. and Frenzel, P. (2012) 'Heat stress and methane-oxidizing bacteria: Effects on activity and population dynamics', *Soil Biology and Biochemistry*, 50, pp. 22–25. doi: 10.1016/j.soilbio.2012.02.023.

Ho, A., Lüke, C. and Frenzel, P. (2011) 'Recovery of methanotrophs from disturbance: Population dynamics, evenness and functioning', *ISME Journal*, 5(4), pp. 750–758. doi: 10.1038/ismej.2010.163.

Hoehler, T. M. and Alperin, M. J. (2014) 'Biogeochemistry: Methane minimalism', *Nature*, 507(7493), pp. 436–437. doi: 10.1038/nature13215.

Høj, L., Olsen, R. A. and Torsvik, V. L. (2008) 'Effects of temperature on the diversity and community structure of known methanogenic groups and other archaea in high Arctic

peat', *ISME Journal*, 2(1), pp. 37–48. doi: 10.1038/ismej.2007.84.

Holgerson, M. A. and Raymond, P. A. (2016) 'Large contribution to inland water CO_2 and CH_4 emissions from very small ponds', *Nature Geoscience*, 9(3), pp. 222–226. doi: 10.1038/ngeo2654.

Horz, H. P., Rich, V., Avrahami, S. and Bohannan, B. J. M. (2005) 'Methane-oxidizing bacteria in a California upland grassland soil: Diversity and response to simulated global change', *Applied and Environmental Microbiology*, 71(5), pp. 2642–2652. doi: 10.1128/AEM.71.5.2642-2652.2005.

Huttunen, J. T., Alm, J., Liikanen, A., Juutinen, S., Larmola, T., Hammar, T., Silvola, J. and Martikainen, P. J. (2003) 'Fluxes of methane, carbon dioxide and nitrous oxide in boreal lakes and potential anthropogenic effects on the aquatic greenhouse gas emissions', *Chemosphere*, 52(3), pp. 609–621. doi: 10.1016/S0045-6535(03)00243-1.

IPCC (2014) *Climate Change 2014: Synthesis Report. Contribution of Working Groups I, II and III to the Fifth Assessment Report of the Intergovernmental Panel on Climate Change*, *Ipcc*. Edited by Core Writing Team, R. K. Pachauri, and L. A. Meyer.

Iwata, H., Ueyama, M. and Harazono, Y. (2016) 'AmeriFlux US-Uaf University of Alaska, Fairbanks'. doi: 10.17190/AMF/1480322.

Jurasinski, G., Koebsch, F. and Hagemann, U. (2012) 'flux: Flux rate calculation from dynamic closed chamber measurements', *https://CRAN.R-project.org/package=flux*. Available at: https://cran.r-project.org/web/packages/flux/index.html (Accessed: 22 May 2018).

King, G. M. (1990) 'Regulation by light of methane emissions from a wetland', *Nature*, 345(6275), pp. 513–515. doi: 10.1038/345513a0.

King, G. M. and Adamsen, A. P. S. (1992) 'Effects of temperature on methane consumption in a forest soil and in pure cultures of the methanotroph *Methylomonas rubra*', *Applied and Environmental Microbiology*, 58(9), pp. 2758–2763.

King, T., Butcher, S. and Zalewski, L. (2017) 'Apocrita - High Performance Computing Cluster for Queen Mary University of London'. doi: 10.5281/ZENODO.438045.

Kip, N., van Winden, J. F., Pan, Y., Bodrossy, L., Reichart, G.-J., Smolders, A. J. P., Jetten, M. S. M., Damsté, J. S. S. and Op den Camp, H. J. M. (2010) 'Global prevalence of methane oxidation by symbiotic bacteria in peat-moss ecosystems', *Nature Geoscience*. Nature Publishing Group, 3(9), pp. 617–621. doi: 10.1038/ngeo939.

Knoblauch, C., Zimmermann, U., Blumenberg, M., Michaelis, W. and Pfeiffer, E. M. (2008) 'Methane turnover and temperature response of methane-oxidizing bacteria in permafrost-affected soils of northeast Siberia', *Soil Biology and Biochemistry*, 40(12), pp. 3004–3013. doi: 10.1016/j.soilbio.2008.08.020.

Konopka, A. (2009) 'What is microbial community ecology', *ISME Journal*, 3(11), pp. 1223–1230. doi: 10.1038/ismej.2009.88.

Kotsyurbenko, O. R. (2005) 'Trophic interactions in the methanogenic microbial community of low-temperature terrestrial ecosystems', in *FEMS Microbiology Ecology*, pp. 3–13. doi: 10.1016/j.femsec.2004.12.009.

Krauss and Ken (2016a) 'AmeriFlux US-LA1 Pointe-aux-Chenes Brackish Marsh'. doi: 10.17190/AMF/1543386.

Krauss and Ken (2016b) 'AmeriFlux US-LA2 Salvador WMA Freshwater Marsh'. doi: 10.17190/AMF/1543387.

Kuivila, K. M., Murray, J. W., Devol, A. H. and Novelli, P. C. (1989) 'Methane production, sulfate reduction and competition for substrates in the sediments of Lake Washington', *Geochimica et Cosmochimica Acta*, 53(2), pp. 409–416. doi: 10.1016/0016-7037(89)90392-X.

Kuznetsova, A., Brockhoff, P. B. and Christensen, R. H. B. (2017) '{lmerTest} Package: Tests in Linear Mixed Effects Models', *Journal of Statistical Software*, 82(13), pp. 1–26. doi: 10.18637/jss.v082.i13.

Lever, M. A. and Teske, A. P. (2015) 'Diversity of methane-cycling archaea in hydrothermal sediment investigated by general and group-specific PCR primers', *Applied and Environmental Microbiology*, 81(4), pp. 1426–1441. doi: 10.1128/AEM.03588-14.

Lipson, D. A., Monson, R. K., Schmidt, S. K. and Weintraub, M. N. (2009) 'The trade-off between growth rate and yield in microbial communities and the consequences for under-snow soil respiration in a high elevation coniferous forest', *Biogeochemistry*, 95(1), pp. 23–35. doi: 10.1007/s10533-008-9252-1.

Liu, Y. and Whitman, W. B. (2008) 'Metabolic, Phylogenetic, and Ecological Diversity of the Methanogenic Archaea', *Annals of the New York Academy of Sciences*, 1125(1), pp. 171–189. doi: 10.1196/annals.1419.019.

Lofton, D. D., Whalen, S. C. and Hershey, A. E. (2014) 'Effect of temperature on methane dynamics and evaluation of methane oxidation kinetics in shallow Arctic Alaskan lakes', *Hydrobiologia*, 721(1), pp. 209–222. doi: 10.1007/s10750-013-1663-x.

Louca, S., Parfrey, L. W. and Doebeli, M. (2016) 'Decoupling function and taxonomy in the global ocean microbiome', *Science*, 353(6305), pp. 1272–1277. doi: 10.1126/science.aaf4507.

Louca, S., Polz, M. F., Mazel, F., Albright, M. B. N., Huber, J. A., O'Connor, M. I., Ackermann, M., Hahn, A. S., Srivastava, D. S., Crowe, S. A., Doebeli, M. and Parfrey, L. W. (2018) 'Function and functional redundancy in microbial systems', *Nature Ecology & Evolution*, 2(6), pp. 936–943. doi: 10.1038/s41559-018-0519-1.

Love, M. I., Huber, W. and Anders, S. (2014) 'Moderated estimation of fold change and dispersion for RNA-seq data with DESeq2', *Genome Biology*, 15(12), p. 550. doi: 10.1186/s13059-014-0550-8.

Luo, Y., Wan, S., Hui, D. and Wallace, L. L. (2001) 'Acclimatization of soil respiration to warming in a tall grass prairie', *Nature*, 413(6856), pp. 622–625. doi: 10.1038/35098065.

Marotta, H., Pinho, L., Gudasz, C., Bastviken, D., Tranvik, L. J. and Enrich-Prast, A. (2014) 'Greenhouse gas production in low-latitude lake sediments responds strongly to warming', *Nature Climate Change*, 4(6), pp. 467–470. doi: 10.1038/nclimate2222.

McDonald, I. R., Bodrossy, L., Chen, Y. and Murrell, J. C. (2008) 'Molecular ecology

techniques for the study of aerobic methanotrophs', *Applied and Environmental Microbiology*, 74(5), pp. 1305–1315. doi: 10.1128/AEM.02233-07.

McGenity, T. J., Timmis, K. N. and Nogales, B. (eds) (2017) *Hydrocarbon and Lipid Microbiology Protocols*, *Springer Protocols Handbooks*. Berlin, Heidelberg: Springer Berlin Heidelberg (Springer Protocols Handbooks). doi: 10.1007/978-3-662-52793-1.

McMurdie, P. J. and Holmes, S. (2013) 'phyloseq: An R Package for Reproducible Interactive Analysis and Graphics of Microbiome Census Data', *PLoS ONE*, 8(4), p. e61217. doi: 10.1371/journal.pone.0061217.

McMurdie, P. J. and Holmes, S. (2014) 'Waste Not, Want Not: Why Rarefying Microbiome Data Is Inadmissible', *PLoS Computational Biology*, 10(4), p. e1003531. doi: 10.1371/journal.pcbi.1003531.

Melillo, J. M. (2002) 'Soil Warming and Carbon-Cycle Feedbacks to the Climate System', *Science*, 298(5601), pp. 2173–2176. doi: 10.1126/science.1074153.

Metje, M. and Frenzel, P. (2007) 'Methanogenesis and methanogenic pathways in a peat from subarctic permafrost', *Environmental Microbiology*, 9(4), pp. 954–964. doi: 10.1111/j.1462-2920.2006.01217.x.

Mohanty, S. R., Bodelier, P. L. E. and Conrad, R. (2007) 'Effect of temperature on composition of the methanotrophic community in rice field and forest soil', *FEMS Microbiology Ecology*, 62(1), pp. 24–31. doi: 10.1111/j.1574-6941.2007.00370.x.

Morgan, J. a (2002) 'ECOLOGY: Looking Beneath the Surface', *Science*, 298(5600), pp. 1903–1904. doi: 10.1126/science.1079808.

Narihiro, T. and Sekiguchi, Y. (2015) 'Primers: Functional Genes and 16S rRNA Genes for Methanogens', in *Hydrocarbon and Lipid Microbiology Protocols - Springer Protocols Handbooks*, pp. 79–139. doi: 10.1007/8623_2015_138.

Nazaries, L., Tate, K. R., Ross, D. J., Singh, J., Dando, J., Saggar, S., Baggs, E. M., Millard, P., Murrell, J. C. and Singh, B. K. (2011) 'Response of methanotrophic communities to afforestation and reforestation in New Zealand', *ISME Journal*, 5(11), pp. 1832–1836. doi: 10.1038/ismej.2011.62.

Neubacher, E. C., Parker, R. E. and Trimmer, M. (2011) 'Short-term hypoxia alters the balance of the nitrogen cycle in coastal sediments', *Limnology and Oceanography*, 56(2), pp. 651–665. doi: 10.4319/lo.2011.56.2.0651.

Nisbet, E. G., Dlugokencky, E. J. and Bousquet, P. (2014) 'Methane on the Rise--Again', *Science (New York, N.Y.)*, 343(6170), pp. 493–495. doi: 10.1126/science.1247828.

Nozhevnikova, A. N., Holliger, C., Ammann, A. and Zehnder, A. J. B. (1997) 'Methanogenesis in sediments from deep lakes at different temperatures (2-70°C)', *Water Science and Technology*, 36(6–7), pp. 57–64. doi: 10.1016/S0273-1223(97)00507-6.

Nozhevnikova, A. N., Nekrasova, V., Ammann, A., Zehnder, A. J. B., Wehrli, B. and Holliger, C. (2007) 'Influence of temperature and high acetate concentrations on methanogenensis in lake sediment slurries', *FEMS Microbiology Ecology*, 62(3), pp. 336–344. doi: 10.1111/j.1574-6941.2007.00389.x.

Oakley, B. B., Carbonero, F., Dowd, S. E., Hawkins, R. J. and Purdy, K. J. (2012) 'Contrasting patterns of niche partitioning between two anaerobic terminal oxidizers of organic matter', *ISME Journal*, 6(5), pp. 905–914. doi: 10.1038/ismej.2011.165.

Oksanen, J., Blanchet, F. G., Friendly, M., Kindt, R., Legendre, P., McGlinn, D., Minchin, P. R., O'Hara, R. B., Simpson, G. L., Solymos, P., Stevens, M. H. H., Szoecs, E. and Wagner, H. (2018) 'vegan: Community Ecology Package'.

Paliy, O. and Shankar, V. (2016) 'Application of multivariate statistical techniques in microbial ecology', *Molecular Ecology*, 25(5), pp. 1032–1057. doi: 10.1111/mec.13536.

Pester, M., Friedrich, M. W., Schink, B. and Brune, A. (2004) '*pmoA*-based analysis of methanotrophs in a littoral lake sediment reveals a diverse and stable community in a dynamic environment', *Applied and Environmental Microbiology*, 70(5), pp. 3138–3142. doi: 10.1128/AEM.70.5.3138-3142.2004.

Peter, H., Beier, S., Bertilsson, S., Lindström, E. S., Langenheder, S. and Tranvik, L. J. (2011) 'Function-specific response to depletion of microbial diversity', *ISME Journal*, 5(2), pp. 351–361. doi: 10.1038/ismej.2010.119.

Petit, R. J., Raynaud, D., Basile, I., Chappellaz, J., Ritz, C., Delmotte, M., Legrand, M., Lorius, C. and Pe, L. (1999) 'Climate and atmospheric history of the past 420,000 years from the Vostok ice core, Antarctica', *Nature*, 399, pp. 429–413. doi: 10.1038/20859.

Pinheiro, J., Bates, D., DebRoy, S., Sarkar, D. and R Core Team (2018) 'nlme: Linear and Nonlinear Mixed Effects Models'. Available at: https://cran.r-project.org/package=nlme.

Pinheiro, J. C. and Bates, D. M. (2000) *Mixed-Effects Models in S and S-PLUS*. doi: 10.1007/b98882.

Pohlman, J. W., Greinert, J., Ruppel, C., Silyakova, A., Vielstädte, L., Casso, M., Mienert, J. and Bünz, S. (2017) 'Enhanced CO_2 uptake at a shallow Arctic Ocean seep field overwhelms the positive warming potential of emitted methane', *Proceedings of the National Academy of Sciences*, 114(21), pp. 5355–5360. doi: 10.1073/pnas.1618926114.

Prior, S. D. and Dalton, H. (1985) 'The Effect of Copper Ions on Membrane Content and Methane Monooxygenase Activity in Methanol-grown Cells of *Methylococcus capsulatus* (Bath)', *Journal of General Microbiology*, 131(1), pp. 155–163. doi: 10.1099/00221287-131-1-155.

Prosser, J. I., Bohannan, B. J. M., Curtis, T. P., Ellis, R. J., Firestone, M. K., Freckleton, R. P., Green, J. L., Green, L. E., Killham, K., Lennon, J. J., Osborn, A. M., Solan, M., van der Gast, C. J. and Young, J. P. W. (2007) 'The role of ecological theory in microbial ecology', *Nature Reviews Microbiology*, 5(5), pp. 384–392. doi: 10.1038/nrmicro1643.

R Core Team (2014) 'R: A Language and Environment for Statistical Computing'. Vienna, Austria.

Raymond, P. A., Hartmann, J., Lauerwald, R., Sobek, S., McDonald, C., Hoover, M., Butman, D., Striegl, R., Mayorga, E., Humborg, C., Kortelainen, P., Dürr, H., Meybeck, M., Ciais, P. and Guth, P. (2013) 'Global carbon dioxide emissions from inland waters', *Nature*, 503(7476), pp. 355–359. doi: 10.1038/nature12760.

Reim, A., Lüke, C., Krause, S., Pratscher, J. and Frenzel, P. (2012) 'One millimetre

makes the difference: High-resolution analysis of methane-oxidizing bacteria and their specific activity at the oxic-anoxic interface in a flooded paddy soil', *ISME Journal*, 6(11), pp. 2128–2139. doi: 10.1038/ismej.2012.57.

Rocca, J. D., Hall, E. K., Lennon, J. T., Evans, S. E., Waldrop, M. P., Cotner, J. B., Nemergut, D. R., Graham, E. B. and Wallenstein, M. D. (2015) 'Relationships between protein-encoding gene abundance and corresponding process are commonly assumed yet rarely observed', *ISME Journal*, 9(8), pp. 1693–1699. doi: 10.1038/ismej.2014.252.

Roslev, P. and King, G. M. (1995) 'Aerobic and anaerobic starvation metabolism in methanotrophic bacteria', *Applied and Environmental Microbiology*, 61(4), pp. 1563–1570. doi: 10.1186/1472-6963-10-248.

Rothfuss, F. and Conrad, R. (1992) 'Vertical profiles of CH_4 concentrations, dissolved substrates and processes involved in CH_4 production in a flooded Italian rice field', *Biogeochemistry*, 18(3), pp. 137–152. doi: 10.1007/BF00003274.

Santoro, A. L., Bastviken, D., Gudasz, C., Tranvik, L. and Enrich-Prast, A. (2013) 'Dark Carbon Fixation: An Important Process in Lake Sediments', *PLoS ONE*, 8(6), pp. 1–7. doi: 10.1371/journal.pone.0065813.

Saunois, M., Bousquet, P., Poulter, B., Peregon, A., Ciais, P., Canadell, J. G., Dlugokencky, E. J., Etiope, G., Bastviken, D., Houweling, S., Janssens-Maenhout, G., Tubiello, F. N., Castaldi, S., Jackson, R. B., Alexe, M., Arora, V. K., Beerling, D. J., Bergamaschi, P., Blake, D. R., Brailsford, G., Brovkin, V., Bruhwiler, L., Crevoisier, C., Crill, P., Covey, K., Curry, C., Frankenberg, C., Gedney, N., Höglund-Isaksson, L., Ishizawa, M., Ito, A., Joos, F., Kim, H.-S., Kleinen, T., Krummel, P., Lamarque, J.-F., Langenfelds, R., Locatelli, R., Machida, T., Maksyutov, S., McDonald, K. C., Marshall, J., Melton, J. R., Morino, I., Naik, V., O'Doherty, S., Parmentier, F.-J. W., Patra, P. K., Peng, C., Peng, S., Peters, G. P., Pison, I., Prigent, C., Prinn, R., Ramonet, M., Riley, W. J., Saito, M., Santini, M., Schroeder, R., Simpson, I. J., Spahni, R., Steele, P., Takizawa, A., Thornton, B. F., Tian, H., Tohjima, Y., Viovy, N., Voulgarakis, A., van Weele, M., van der Werf, G. R., Weiss, R., Wiedinmyer, C., Wilton, D. J., Wiltshire, A., Worthy, D., Wunch, D., Xu, X., Yoshida, Y., Zhang, B., Zhang, Z. and Zhu, Q. (2016) 'The global methane budget 2000–2012', *Earth System Science Data*, 8(2), pp. 697–751. doi: 10.5194/essd-8-697-2016.

Schimel, J. P. and Gulledge, J. (1998) 'Microbial community structure and global trace gases', *Global Change Biology*, 4(7), pp. 745–758. doi: 10.1046/j.1365-2486.1998.00195.x.

Schneider, P. and Hook, S. J. (2010) 'Space observations of inland water bodies show rapid surface warming since 1985', *Geophysical Research Letters*. Wiley-Blackwell, 37(22), p. n/a-n/a. doi: 10.1029/2010GL045059.

Schulz, S. (1996) 'Influence of temperature on pathways to methane production in the permanently cold profundal sediment of Lake Constance', *FEMS Microbiology Ecology*, 20(1), pp. 1–14. doi: 10.1016/0168-6496(96)00009-8.

Schulz, S., Matsuyama, H. and Conrad, R. (1997) 'Temperature dependence of methane production from different precursors in a profundal sediment (Lake Constance)', *FEMS Microbiology Ecology*, 22(3), pp. 207–213. doi: 10.1111/j.1574-6941.1997.tb00372.x.

Schutz, H., Seiler, W. and Conrad, R. (1989) 'Processes involved in formation and emission of methane in rice paddies', *Biogeochemistry*, 7(1), pp. 33–53. doi:

10.1007/BF00000896.

Schuur, E. A. G., McGuire, A. D., Schädel, C., Grosse, G., Harden, J. W., Hayes, D. J., Hugelius, G., Koven, C. D., Kuhry, P., Lawrence, D. M., Natali, S. M., Olefeldt, D., Romanovsky, V. E., Schaefer, K., Turetsky, M. R., Treat, C. C. and Vonk, J. E. (2015) 'Climate change and the permafrost carbon feedback', *Nature*, pp. 171–179. doi: 10.1038/nature14338.

Schuur and Ted (2018) 'AmeriFlux US-EML Eight Mile Lake Permafrost thaw gradient, Healy Alaska.' doi: 10.17190/AMF/1418678.

Shade, A., Gregory Caporaso, J., Handelsman, J., Knight, R. and Fierer, N. (2013) 'A meta-analysis of changes in bacterial and archaeal communities with time', *ISME Journal*. Nature Publishing Group, 7(8), pp. 1493–1506. doi: 10.1038/ismej.2013.54.

Shelley, F., Abdullahi, F., Grey, J. and Trimmer, M. (2015) 'Microbial methane cycling in the bed of a chalk river: oxidation has the potential to match methanogenesis enhanced by warming', *Freshwater Biology*, 60(1), pp. 150–160. doi: 10.1111/fwb.12480.

Singh, B. K., Bardgett, R. D., Smith, P. and Reay, D. S. (2010) 'Microorganisms and climate change: Terrestrial feedbacks and mitigation options', *Nature Reviews Microbiology*, 8(11), pp. 779–790. doi: 10.1038/nrmicro2439.

Sonnentag, O. and Quinton, W. L. (2016) 'AmeriFlux CA-SCB Scotty Creek Bog'. doi: 10.17190/AMF/1498754.

Stanley, E. H., Casson, N. J., Christel, S. T., Crawford, J. T., Loken, L. C. and Oliver, S. K. (2016) 'The ecology of methane in streams and rivers: Patterns, controls, and global significance', *Ecological Monographs*, 86(2), pp. 146–171. doi: 10.1890/15-1027.

Stewart, R. I. A., Dossena, M., Bohan, D. A., Jeppesen, E., Kordas, R. L., Ledger, M. E., Meerhoff, M., Moss, B., Mulder, C., Shurin, J. B., Suttle, B., Thompson, R., Trimmer, M. and Woodward, G. (2013) *Mesocosm Experiments as a Tool for Ecological Climate-Change Research*, *Advances in Ecological Research*. Elsevier Ltd. doi: 10.1016/B978-0-12-417199-2.00002-1.

Thauer, R. K., Kaster, A.-K., Seedorf, H., Buckel, W. and Hedderich, R. (2008) 'Methanogenic archaea: ecologically relevant differences in energy conservation', *Nature Reviews Microbiology*, 6(8), pp. 579–591. doi: 10.1038/nrmicro1931.

Thornley, J. H. M. and Cannell, M. G. R. (2000) 'Dynamics of mineral N availability in grassland ecosystems under increased [CO_2]: Hypotheses evaluated using the Hurley Pasture Model', *Plant and Soil*, 224(1), pp. 153–170. doi: 10.1023/A:1004640327512.

Tranvik, L. J., Downing, J. A., Cotner, J. B., Loiselle, S. A., Striegl, R. G., Ballatore, T. J., Dillon, P., Finlay, K., Fortino, K., Knoll, L. B., Kortelainen, P. L., Kutser, T., Larsen, S., Laurion, I., Leech, D. M., McCallister, S. L., McKnight, D. M., Melack, J. M., Overholt, E., Porter, J. A., Prairie, Y., Renwick, W. H., Roland, F., Sherman, B. S., Schindler, D. W., Sobek, S., Tremblay, A., Vanni, M. J., Verschoor, A. M., von Wachenfeldt, E. and Weyhenmeyer, G. A. (2009) 'Lakes and reservoirs as regulators of carbon cycling and climate', *Limnology and Oceanography*, 54(6), pp. 2298–2314. doi: 10.4319/lo.2009.54.6_part_2.2298.

Trimmer, M., Shelley, F. C., Purdy, K. J., Maanoja, S. T., Chronopoulou, P.-M. and Grey, J. (2015) 'Riverbed methanotrophy sustained by high carbon conversion efficiency', *The ISME Journal*, 9(10), pp. 2304–2314. doi: 10.1038/ismej.2015.98.

Tveit, A. T., Urich, T., Frenzel, P. and Svenning, M. M. (2015) 'Metabolic and trophic interactions modulate methane production by Arctic peat microbiota in response to warming', *Proceedings of the National Academy of Sciences*. National Academy of Sciences, 112(19), pp. E2507–E2516. doi: 10.1073/pnas.1420797112.

Valentini, R., Matteucci, G., Dolman, A. J., Schulze, E. D., Rebmann, C., Moors, E. J., Granier, A., Gross, P., Jensen, N. O., Pilegaard, K., Lindroth, A., Grelle, A., Bernhofer, C., Grünwald, T., Aubinet, M., Ceulemans, R., Kowalski, A. S., Vesala, T., Rannik, Ü., Berbigier, P., Loustau, D., Guomundsson, J., Thorgeirsson, H., Ibrom, A., Morgenstern, K., Clement, R., Moncrieff, J., Montagnani, L., Minerbi, S. and Jarvis, P. G. (2000) 'Respiration as the main determinant of carbon balance in European forests', *Nature*, 404(6780), pp. 861–865. doi: 10.1038/35009084.

Vargas and Rodrigo (2016) 'AmeriFlux US-StJ St Jones Reserve'. doi: 10.17190/AMF/1480316.

Wallin, M. B., Löfgren, S., Erlandsson, M. and Bishop, K. (2014) 'Representative regional sampling of carbon dioxide and methane concentrations in hemiboreal headwater streams reveal underestimates in less systematic approaches', *Global Biogeochemical Cycles*, 28(4), pp. 465–479. doi: 10.1002/2013GB004715.

Wen, X., Yang, S., Horn, F., Winkel, M., Wagner, D. and Liebner, S. (2017) 'Global biogeographic analysis of methanogenic archaea identifies community-shaping environmental factors of natural environments', *Frontiers in Microbiology*, 8(JUL), pp. 1–13. doi: 10.3389/fmicb.2017.01339.

Whalen, S. C., Reeburgh, W. S. and Sandbeck, K. A. (1990) 'Rapid methane oxidation in a landfill cover soil', *Applied and Environmental Microbiology*, 56(11), pp. 3405–3411.

Whiting, G. J. and Chanton, J. P. (1993) 'Primary production control of methane emission from wetlands', *Nature*, 364(6440), pp. 794–795. doi: 10.1038/364794a0.

Whiting, G. J. and Chanton, J. P. (2001) 'Greenhouse carbon balance of wetlands: Methane emission versus carbon sequestration', *Tellus, Series B: Chemical and Physical Meteorology*, 53(5), pp. 521–528. doi: 10.3402/tellusb.v53i5.16628.

Whiting, G. J., Chanton, J. P., Bartlett, D. S. and Happell, J. D. (1991) 'Relationships between CH_4 emission, biomass, and CO_2 exchange in a subtropical grassland', *Journal of Geophysical Research*, 96(D7), p. 13067. doi: 10.1029/91JD01248.

Wiesenburg, D. a. and Guinasso, N. L. (1979) 'Equilibrium solubilities of methane, carbon monoxide, and hydrogen in water and sea water', *Journal of Chemical & Engineering Data*, 24(4), pp. 356–360. doi: 10.1021/je60083a006.

Wik, M., Thornton, B. F., Bastviken, D., MacIntyre, S., Varner, R. K. and Crill, P. M. (2014) 'Energy input is primary controller of methane bubbling in subarctic lakes', *Geophysical Research Letters*, 41(2), pp. 555–560. doi: 10.1002/2013GL058510.

Wik, M., Varner, R. K., Anthony, K. W., MacIntyre, S. and Bastviken, D. (2016)

'Climate-sensitive northern lakes and ponds are critical components of methane release', *Nature Geoscience*, 9(2), pp. 99–105. doi: 10.1038/ngeo2578.

van Winden, J. F., Reichart, G.-J., McNamara, N. P., Benthien, A. and Damsté, J. S. S. (2012) 'Temperature-Induced Increase in Methane Release from Peat Bogs: A Mesocosm Experiment', *PLoS ONE*. Edited by K. Treseder, 7(6), p. e39614. doi: 10.1371/journal.pone.0039614.

Winfree, R., Fox, J. W., Williams, N. M., Reilly, J. R. and Cariveau, D. P. (2015) 'Abundance of common species, not species richness, drives delivery of a real-world ecosystem service', *Ecology Letters*, 18(7), pp. 626–635. doi: 10.1111/ele.12424.

Yver Kwok, C. E., Müller, D., Caldow, C., Lebègue, B., Mønster, J. G., Rella, C. W., Scheutz, C., Schmidt, M., Ramonet, M., Warneke, T., Broquet, G. and Ciais, P. (2015) 'Methane emission estimates using chamber and tracer release experiments for a municipal waste water treatment plant', *Atmospheric Measurement Techniques*, 8(7), pp. 2853–2867. doi: 10.5194/amt-8-2853-2015.

Yvon-Durocher, G. (2010) *On the Community and Ecosystem Level Consequences of Warming*. Ph.D. Thesis, Queen Mary University of London, U.K. Available at: http://qmro.qmul.ac.uk/xmlui/handle/123456789/660.

Yvon-Durocher, G., Allen, A. P., Bastviken, D., Conrad, R., Gudasz, C., St-Pierre, A., Thanh-Duc, N. and del Giorgio, P. a (2014) 'Methane fluxes show consistent temperature dependence across microbial to ecosystem scales.', *Nature*, 507(7493), pp. 488–91. doi: 10.1038/nature13164.

Yvon-Durocher, G., Allen, A. P., Cellamare, M., Dossena, M., Gaston, K. J., Leitao, M., Montoya, J. M., Reuman, D. C., Woodward, G. and Trimmer, M. (2015) 'Five Years of Experimental Warming Increases the Biodiversity and Productivity of Phytoplankton', *PLoS Biology*, 13(12), pp. 1–22. doi: 10.1371/journal.pbio.1002324.

Yvon-Durocher, G., Allen, A. P., Montoya, J. M., Trimmer, M. and Woodward, G. (2010) 'The Temperature dependence of the carbon cycle in aquatic ecosystems', in *Integrative Ecology: From Molecules to Ecosystems*. Oxford : Elsevier. Available at: http://www.researchonline.mq.edu.au/vital/access/manager/Repository/mq:13263 (Accessed: 14 February 2016).

Yvon-Durocher, G., Caffrey, J. M., Cescatti, A., Dossena, M., Giorgio, P. del, Gasol, J. M., Montoya, J. M., Pumpanen, J., Staehr, P. A., Trimmer, M., Woodward, G., Allen, A. P., del Giorgio, P., Gasol, J. M., Montoya, J. M., Pumpanen, J., Staehr, P. A., Trimmer, M., Woodward, G. and Allen, A. P. (2012) 'Reconciling the temperature dependence of respiration across timescales and ecosystem types', *Nature*, 487(7408), pp. 472–476. doi: 10.1038/nature11205.

Yvon-Durocher, G., Hulatt, C. J., Woodward, G. and Trimmer, M. (2017) 'Long-term warming amplifies shifts in the carbon cycle of experimental ponds', *Nature Climate Change*, 7(3), pp. 209–213. doi: 10.1038/nclimate3229.

Yvon-Durocher, G., Montoya, J. M., Trimmer, M. and Woodward, G. (2011) 'Warming alters the size spectrum and shifts the distribution of biomass in freshwater ecosystems', *Global Change Biology*, 17(4), pp. 1681–1694. doi: 10.1111/j.1365-2486.2010.02321.x.

Yvon-Durocher, G., Montoya, J. M., Woodward, G., Jones, J. I. and Trimmer, M. (2011) 'Warming increases the proportion of primary production emitted as methane from freshwater mesocosms', *Global Change Biology*, 17(2), pp. 1225–1234. doi: 10.1111/j.1365-2486.2010.02289.x.

Zheng, Y., Yang, W., Sun, X., Wang, S. P., Rui, Y. C., Luo, C. Y. and Guo, L. D. (2012) 'Methanotrophic community structure and activity under warming and grazing of alpine meadow on the Tibetan Plateau', *Applied Microbiology and Biotechnology*, 93(5), pp. 2193–2203. doi: 10.1007/s00253-011-3535-5.

Zuur, A. F. (2009) *Mixed effects models and extensions in ecology with R*. Springer.